

2013

## **Experimental Investigation And Aspen Plus Simulation Of The Msw Pyrolysis Process**

Emmanuel Ansah

*North Carolina Agricultural and Technical State University*

Follow this and additional works at: <https://digital.library.ncat.edu/theses>

---

### **Recommended Citation**

Ansah, Emmanuel, "Experimental Investigation And Aspen Plus Simulation Of The Msw Pyrolysis Process" (2013). *Theses*. 104.

<https://digital.library.ncat.edu/theses/104>

This Thesis is brought to you for free and open access by the Electronic Theses and Dissertations at Aggie Digital Collections and Scholarship. It has been accepted for inclusion in Theses by an authorized administrator of Aggie Digital Collections and Scholarship. For more information, please contact [iyanna@ncat.edu](mailto:iyanna@ncat.edu).

Experimental Investigation and APSEN Plus Simulation of the MSW Pyrolysis Process

Emmanuel Ansah

North Carolina Agricultural & Technical State University

A thesis submitted to the graduate faculty  
in partial fulfillment of the requirements for the degree of

MASTER OF SCIENCE

Department: Chemical, Biological and Bioengineering

Major: Chemical Engineering

Major Professor: Dr. Lijun Wang

Greensboro, North Carolina

2013

The Graduate School  
North Carolina Agricultural and Technical State University  
This is to certify that the Master's Thesis

Emmanuel Ansah

has met the thesis requirements of  
North Carolina Agricultural and Technical State University

Greensboro, North Carolina  
2013

Approved by:

---

Dr. Lijun Wang  
Major Professor

---

Dr. Abolghasem Shahbazi  
Committee Member

---

Dr. G.B. Reddy  
Committee Member

---

Dr. Stephen Knisley  
Department Chair

---

Dr. Sanjiv Sarin  
Dean, The Graduate School



### **Biographical Sketch**

Emmanuel Ansah was born on May 12, 1982 in Accra, Ghana. He started his tertiary education at Kwame Nkrumah University of Science and Technology in Kumasi, Ghana where he received his bachelor of science in Chemical Engineering in May 2006. In the year 2011 during the Fall semester, he enrolled at the North Carolina Agricultural and Technical State University, Greensboro North Carolina to pursue a Master of science program in Chemical Engineering. Mr. Ansah has been involved in the research of Municipal Solid Waste (MSW) pyrolysis to produce transportation fuels and has presented on the technical and economic assessment of MSW pyrolysis at the national conference on Advances in Environmental Science and Technology held in Greensboro on September 12, 2013. He is a student member of American Institute of Chemical Engineers (AIChE) and also a member of International Association for Exchanging Students for Technical Experience (IAESTE) and pursued an internship from October 2006 to December 2006 in Germany under the auspices of IAESTE, Germany. He is currently a candidate for the Master of Science degree in Chemical Engineering

## **Dedication**

With gratitude and appreciation, this thesis is dedicated to my family and my best friend Ms Phyllis Opare and all those who contributed positively in my life. Their love, support and understanding helped make this project possible.

## Acknowledgements

This thesis would not have been made possible without the unflinching support and guidance of my major advisor, Dr. Lijun Wang. He motivated me and taught me the rudiments of research and I am most grateful to him for imparting such knowledge and skills in me.

I would like to also thank Dr. Abolghasem Shahbazi and Dr. G.B Reddy for being in my thesis committee. I am grateful especially to Dr. Shahbazi for assisting me with resources and logistics.

This project was partially supported by funds provided by Biofuels Center of North Carolina (Award number: 2011-121) and by USDA-National Institute of Food and Agriculture (Grant number: USDA NIFA USDA NIFA 2010-38821-21512). The contents of this publication are solely the responsibility of the authors and do not necessarily represent the official views of the National Institute of Food and Agriculture.

The authors would like to thank Mr. John Eshun at North Carolina A&T State University for the measurement of the properties of MSW samples, Ms Mitchele Mims at North Carolina A & T State University for making all my laboratory needs accessible to me and Mr. Matthew Todd at the North Carolina A&T State University for the construction of the pyrolysis reactor

## Table of Contents

List of Figures .....	xi
List of Tables .....	xv
Abstract .....	2
CHAPTER 1 Introduction.....	3
1.1 Scope and Objectives.....	5
CHAPTER 2 Literature Review .....	7
2.1 Introduction.....	7
2.1.1 Wood. ....	7
2.1.2 Paper/card board. ....	7
2.1.3 Textiles. ....	7
2.1.4 Plastics. ....	8
2.2 Residual Derived Fuels used as Combustibles of MSW .....	10
2.3 Waste to Energy Technologies .....	11
2.4 MSW Pretreatment Methods .....	12
2.4.1 Torrefaction. ....	12
2.4.2 Pelletizing. ....	13
2.5 Thermochemical Conversion.....	14
2.5.1 Pyrolysis. ....	14
2.5.2 Gasification.....	15
2.5.3 Incineration or combustion.....	15
2.6 Pyrolysis Principles .....	17
2.6.1 Products of pyrolysis of Municipal Solid Waste.....	19

2.6.1.1 Biochar. ....	19
2.6.1.2 Bio-oil or tar. ....	19
2.6.1.3 Non condensable gas ( NCG). ....	20
2.7 Types of Pyrolysis .....	20
2.7.1 Conventional or slow pyrolysis. ....	20
2.7.2 Fast pyrolysis. ....	21
2.8 Reactor Types and Configuration used in Slow or Conventional Pyrolysis .....	22
2.8.1 Fixed Bed.....	22
2.9 Reactor Types and Configuration used in Fast Pyrolysis .....	23
2.9.1 Bubbling Fluidized Bed.....	24
2.9.2 Circulating fluidized bed. ....	25
2.9.3 Ablative pyrolyzer .....	26
2.9.4 Screw auger pyrolyzer. ....	27
2.9.5 Rotating cone pyrolyzer .....	28
2.10 Relative Merits of Fast Pyrolysis Reactors.....	30
2.11 Biomass Pyrolysis using Screw Auger Reactor by Past Research Works.....	30
2.12 Past Research Work in Pyrolysis of MSW using Fixed Bed Reactor .....	32
2.13 Pyrolysis Process Operating Conditions.....	33
2.13.1 Temperature.....	33
2.13.2 Residence time.....	34
2.13.3 Size of feed particles. ....	35
2.13.4 Heating rate .....	36
2.14 Thermogravimetric Analysis (TGA) of Pyrolysis of MSW .....	38
2.15 Thermal Properties of Biomass during Pyrolysis .....	40
2.15.1 Heating Value (HV). ....	40

2.15.2 Specific heat.....	40
2.15.3 Thermal conductivity.....	41
CHAPTER 3 Experimental Methods and Materials.....	42
3.1 Introduction.....	42
3.2 Preparation of MSW Samples .....	42
3.3 Pyrolytic Experiments .....	44
3.3.1 Pyrolytic reaction unit.....	44
3.3.2 Statistical experimental design.....	45
3.3.3 Pyrolysis procedure.....	45
3.4 Analysis of the Physical and Chemical Properties of MSW samples and Pyrolysis Products .....	46
3.4.1 Particle size analysis.....	46
3.4.2 Bulk density.....	47
3.4.3 Heating value.....	47
3.5 TGA-DSC- MS Experiments.....	49
3.5.1 Sample preparation.....	50
CHAPTER 4 Aspen Plus Simulation of Pyrolysis Process .....	53
4.1 Introduction.....	53
4.2 Model Development .....	55
4.3 Physical Property Method.....	55
4.4 Aspen Simulation Flowsheet .....	55
4.5 Simulation Procedure.....	57
CHAPTER 5 Economic Assessment of MSW Pyrolysis .....	60
5.1 Methodology.....	60
5.1.1 Operating cost.....	60

5.1.1.1 MSW preparation.....	60
5.1.1.2 Size reduction.....	61
5.1.1.3 Drying.....	61
5.1.1.4 Pyrolysis.....	62
5.1.1.5 Volatile gas cleaning.....	64
5.1.1.6 Bio-oil collection.....	64
5.1.1.7 Storage.....	64
5.1.2 The Capital cost.....	65
5.1.3 Other operating costs.....	67
CHAPTER 6 Results and Discussion.....	68
6.1 Introduction.....	68
6.2 Particle Size Distribution of MSW Components used for the Pyrolysis Process.....	68
6.3 Product Distribution.....	69
6.3.1 Effect of temperature.....	70
6.4 Product Analysis.....	72
6.4.1 High Heating Value (HHV).....	74
6.4.2 Moisture content.....	75
6.4.3 Volatile matter (VM).....	75
6.5 Elemental Composition of Biochar and Bio-oil from MSW Pyrolysis at different temperatures.....	77
6.5.1 Biochar.....	77
6.6 Kinetic Studies of MSW Components Pyrolysis from TGA Experiments.....	82
6.6.1 Pyrolysis in nitrogen atmosphere.....	83
6.6.1.1 Reaction kinetics parameters for pyrolysis in nitrogen atmosphere.....	87
6.6.1.2 Effect of heating rate.....	88

6.6.2 Pyrolysis in CO <sub>2</sub> atmosphere.....	91
6.6.2.1 Parameters of reaction kinetics for pyrolysis in CO <sub>2</sub> atmosphere.....	91
6.7 Differential Scanning Calorimetry (DSC) of the Pyrolysis of MSW Components.....	95
6.8 Mass Spectrometry of the gas evolved from the Pyrolysis of MSW Components .....	101
6.8.1 Gas analysis from the pyrolysis of MSW in nitrogen atmosphere.....	101
6.9 Aspen Simulation Results.....	106
6.10 Results of Economic Assessment of MSW Pyrolysis .....	110
CHAPTER 7 Conclusions and Recommendations .....	115
7.1 Conclusion .....	115
7.2 Recommendations for Future Work .....	117
References.....	118

## List of Figures

Figure 1. MSW generation in the US.....	3
Figure 2. Thermochemical conversion processes and their products[35].....	16
Figure 3. Schematic representation of a continuous down flow fixed bed reactor[51] .....	23
Figure 4. A schematic representation of a laboratory scale fluidized bed reactor adapted from[58] .....	25
Figure 5. A schematic representation of Circulating fluidized bed reactor .....	26
Figure 6. A schematic diagram of ablative pyrolysis reactor by Ashton university[28] .....	27
Figure 7. Schematic representation of a continuous screw auger pyrolyzer[1].....	28
Figure 8. Principle of rotating cone [62].....	29
Figure 9. Characterized MSW samples dried in the sun.....	43
Figure 10. Thomas Wiley Mill for grinding MSW samples.....	43
Figure 11. A simple schematic representation of the fixed bed pyrolysis process.....	44
Figure 12. Sieve size arrangement and shaker for particle size analysis .....	47
Figure 13. Measuring balance for weighing MSW samples and products .....	47
Figure 14. Oxygen Bomb calorimeter for heating value determination .....	48
Figure 15. Mettler Toledo T50 for moisture content determination .....	49
Figure 16. PE 2400 Elemental Analyzer (Perkin Elmer).....	52
Figure 17. Thermo gravimetric- Differential Scanning Calorimetric- Mass spectrometry (TGA- DSC-MS) analyzer (TA Instrument) .....	52
Figure 18. Process flow diagram of MSW pyrolysis process in Aspen plus.....	59
Figure 19. Pyrolysis plant cost (pyrolysis and oil recovery system) [90].....	66
Figure 20. Particle size distribution of wood biomass.....	69

Figure 21. Particle size distribution of paper .....	69
Figure 22. Effect of temperature on oil yield for three MSW components .....	71
Figure 23. Effect of temperature on biochar yield for MSW samples.....	72
Figure 24. Samples of bio-oil obtained at different temperatures .....	73
Figure 25. Samples of biochar of MSW at different temperatures .....	74
Figure 26. Heating value of biochar from MSW components from fixed bed pyrolysis at different temperatures .....	75
Figure 27. Elemental composition of biochar fraction of paper pyrolysis .....	80
Figure 28. Elemental composition of biochar fraction from textile pyrolysis.....	80
Figure 29. Elemental composition of biochar fraction from wood pyrolysis .....	81
Figure 30. Thermal degradation profile of different MSW with increasing temperature.....	84
Figure 31. DTG curve for different MSW components at increasing temperature .....	84
Figure 32. TG and DTG curve for cellulose, hemicelluloses and lignin standard components ...	85
Figure 33. Temperature dependency of the rate constant of MSW pyrolysis at a heating rate of 40 oC/min for plastic, wood, paper and textile.....	87
Figure 34. Temperature dependency of the reaction rate of the pyrolysis of plastic (PE) at different heating rate .....	89
Figure 35. Temperature dependency of the reaction rate of the pyrolysis of wood at different heating rate.....	89
Figure 36. Temperature dependency of the reaction rate of the pyrolysis of paper at different heating rate.....	90
Figure 37. Temperature dependency of the reaction rate of the pyrolysis of textile at different heating rate.....	90

Figure 38. TGA profile of MSW in CO <sub>2</sub> atmosphere .....	91
Figure 39. Temperature dependency of the reaction rate of the pyrolysis of paper at different heating rate.....	93
Figure 40. Temperature dependency of the reaction rate of the pyrolysis of plastic (PE) at different heating rate .....	93
Figure 41. Temperature dependency of the reaction rate of the pyrolysis of wood at different heating rate.....	94
Figure 42. Temperature dependency of the reaction rate of the pyrolysis of textile at different heating rate.....	94
Figure 43. DSC profile of different MSW components with increasing temperature in nitrogen atmosphere at heating rate of 20°C/min.....	97
Figure 44. DSC curve and caloric requirement by integrating DSC curve of wood .....	99
Figure 45. DSC curve and caloric requirement by integrating DSC curve of paper .....	99
Figure 46. DSC curve and caloric requirement by integrating DSC curve of textile .....	100
Figure 47. DSC curve and caloric requirement by integrating DSC curve of plastic.....	100
Figure 48. Mass spectra corresponding to the pyrolysis of textile .....	102
Figure 49. Mass spectra corresponding to the pyrolysis of wood.....	103
Figure 50. Mass spectra corresponding to the pyrolysis of plastic (PE).....	104
Figure 51. Mass spectra corresponding to the pyrolysis of paper.....	104
Figure 52. Mass spectra of hemicellulose pyrolysis .....	105
Figure 53. Mass spectra of lignin pyrolysis .....	105
Figure 54. Mass spectra of cellulose pyrolysis .....	106
Figure 55. Effect of temperature of pyrolyser on the yields of pyrolysis products .....	109

Figure 56. Composition of components in non condensable gas varying with pyrolyser

temperature ..... 109

## List of Tables

Table 1 Comparison of different types of fast pyrolysis reactors .....	30
Table 2 Phase composition of bio-oil and water content .....	73
Table 3 Proximate analysis of MSW biochar from fixed bed pyrolysis at different temperatures .....	76
Table 4 Proximate and Ultimate analysis of raw MSW components before pyrolysis .....	77
Table 5 Elemental composition of biochar from paper pyrolysis at different temperatures .....	78
Table 6 Elemental composition of biochar from wood pyrolysis at different temperatures .....	79
Table 7 Elemental composition of biochar from textile pyrolysis at different temperatures .....	79
Table 8 Elemental composition of bio-oil from textile pyrolysis at different temperatures.....	81
Table 9 Elemental composition of bio-oil from paper pyrolysis at different temperatures.....	82
Table 10 Elemental composition of bio-oil from wood pyrolysis at different temperatures.....	82
Table 11 Temperature range and weight loss of MSW components at different heating rates in nitrogen atmosphere.....	86
Table 12 Comparison of activation energy and pre-exponential factors for MSW components in nitrogen atmosphere.....	88
Table 13 Comparison of activation energy and pre-exponential factors for MSW components in CO <sub>2</sub> atmosphere .....	92
Table 14 Relationship of calorific value and mass residue of plastic with temperature.....	97
Table 15 Relationship of calorific value and mass residue of textile with temperature .....	98
Table 16 Relationship of calorific value and mass residue of paper with temperature .....	98
Table 17 Relationship of calorific value and mass residue of wood with temperature .....	98
Table 18 Yield of pyrolysis product at varying reactor temperature .....	107

Table 19 Composition of pyrolysis products at pyrolysis temperature (400oC to 500°C).....	107
Table 20 Composition of pyrolysis products at pyrolysis temperature (525°C to 700°C) .....	108
Table 21 Composition of pyrolysis products at pyrolysis temperature (625°C to 700°C) .....	108
Table 22 Economic assessment results of MSW pyrolysis process plant at a loading capacity of 100 MT MSW/day .....	111
Table 23 Economic assessment results of MSW pyrolysis process plant .....	112
Table 24 Economic assessment results of MSW pyrolysis process plant (continuation).....	113
Table 25 Cost of MSW pyrolysis plant at different scales .....	114

## Abstract

Municipal solid waste (MSW) is a potential feedstock for producing transportation fuels because it is readily available using an existing collection/transportation infrastructure and fees are provided by the suppliers or government agencies to treat MSW. North Carolina with a population of 9.4 millions generates 3.629 million metric tons of MSW each year, which contains about 113,396,356 TJs of energy. The average moisture content of MSW samples is 44.3% on a wet basis. About 77% of the dry MSW mass is combustible components including paper, organics, textile and plastics. The average heating values of MSW were 9.7, 17.5, and 22.7 MJ/kg on a wet basis, dry basis and dry combustible basis, respectively. The MSW generated in North Carolina can produce 7.619 million barrels of crude bio-oil or around 4% of total petroleum consumption in North Carolina. MSW can be thermally pyrolyzed into bio-oil in the absence of oxygen or air at a temperature of 500°C or above. As bio-oil can be easily stored and transported, compared to bulky MSW, landfill gas and electricity, pyrolysis offers significant logistical and economic advantages over landfilling and other thermal conversion processes such as combustion and gasification. Crude bio-oils produced from the pyrolysis of MSW can be further refined to transportation fuels in existing petroleum refinery facilities.

The objective of this research is to analyze the technical and economic feasibility of pyrolyzing MSW into liquid transportation fuels. A combined thermogravimetric analyzer (TGA) and differential scanning calorimeter (DSC) instrument, which can serve as a micro-scale pyrolysis reactor, was used to simultaneously determine the degradation characteristics of MSW during pyrolysis. An ASPEN Plus-based mathematical model was further developed to analyze the technical and economic feasibility of pyrolyzing of MSW into liquid transportation fuels in fixed bed reactors at varying operating conditions.

## CHAPTER 1

### Introduction

Municipal solid waste (MSW) is commonly called “trash” or “garbage” which includes waste such as tires, furniture, newspapers, plastics, wood waste, textile residues, grass clippings, food and yard waste. This category of waste is generally referred to as common household, office and retail waste and sometimes includes commercial waste. In general, MSW does not include hazardous and industrial waste. According to the U.S Environmental Protection Agency, the annual MSW generation in the U.S has increased by 65% since 1980 to the current level of about 250 million tons per year. There was an increase of more than 20% of per capita generation since 1980.

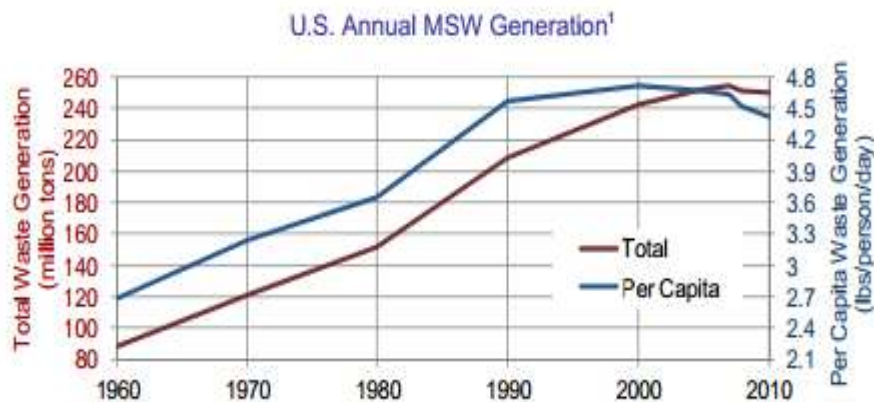


*Figure 1.* MSW generation in the US

As shown in Figure 1, MSW is considered as a very useful energy resource. MSW-to-energy technology can be a competitive solution not only to produce energy with negligible costs but also to decrease the volume for the storage in landfill which has associated environmental problems of gas emissions and leachate production. The 1991 National energy strategy encourages the conversion of MSW to energy and as a result extensive research has been done

on viable mechanisms of generating energy from MSW. One of these mechanisms that were studied in this research for converting MSW to energy is **pyrolysis**.

Pyrolysis is an ancient thermochemical process for converting biomass to energy. It is a thermochemical process in which biomass feedstock is heated at temperatures around 400°C to 500°C in the absence of oxygen to produce char (bio-char), gases (synthesis gas) and vapors or aerosols to be rapidly condensed to form bio-oil which is a mixture of organic chemicals with water. Basically, there are three products obtained from the conversion process and the relative yield and properties of each product stated above depends on the operating conditions of the pyrolysis process. Numerous studies have been conducted to investigate a pyrolysis process for the conversion of different biomass feedstocks to bio-oil that can be further upgraded and improved into marketable products [1]. In these past studies, several different types of equipment such as semi-batch reactor [2, 3] and fixed bed reactor [4] were employed for the pyrolysis. This research is to investigate the dynamic chemical and physical changes in MSW pyrolysis to produce bio-oil and bio-char in a fixed bed reactor. The study aims at characterizing the bio-oil and bio-char generated at different pyrolysis temperatures. The pyrolysis process is conducted in a tubular reactor and a rapid cooling of the reactor in cold water is provided to ensure the biochar is analyzed at the specified pyrolysis temperature. In the study, MSW combustibles used as feedstock is placed in the tubular reactor of 100 ml volume and heated in an electric tube furnace with a purging gas (nitrogen) connected to the reactor to provide inert conditions in the reactor and push pyrolysis product into condenser unit for bio-oil recovery. In this study, Aspen plus simulation was performed on pyrolysis of MSW to yield liquid (fuel oil), non-condensable gas (NCG) and residue char (and ash). The liquid fuel oil can be used as a substitute or blending

agent for transport fuels. The char and the NCG are by-products which can be burnt on-site to provide the energy required for the process and possibly for auxiliary electric power generation.

### **1.1 Scope and Objectives**

During pyrolysis, temperature plays a critical role in the physical and chemical characteristics of the three pyrolysis products since it supplies the heat to breakdown the bonds in the biomass resource. It is expected that thermal properties such as heating value, thermal conductivity and specific heat of the pyrolysis products will vary with pyrolysis temperatures. Therefore, it is critical to determine the properties of the products during pyrolysis. A major setback in this type of experimental set up is the slow cooling of the reactor to ambient temperature after reaching a pyrolysis temperature to determine the properties of the biochar. In this experimental set up, the tubular reactor after it reached the set pyrolysis temperature was rapidly cooled in a cooling water bath instantaneously. The biochar remaining in the reactor was then collected and its properties were determined. The main goal of this research was to determine the effect of temperature, type of MSW components and other process operating parameters on the physical and chemical properties of biochar and bio-oil generated.

The specific objectives for the research are as follows:

1. Analyze the yields, and physical and chemical properties of bio-oil and biochar affected by the pyrolysis temperature and the type of organic MSW components including paper, woody biomass, plastics and textile during fast pyrolysis
- 2 Analyze the thermal degradation characteristics, kinetics, reaction heat and evolved gas profiles during the pyrolysis of MSW components at different conditions using a combination of thermogravimetric (TGA), differential scanning calorimetry (DSC) and mass spectrometry (MS) (TGA-DSC-MS).

3 Develop an ASPEN Plus model to analyze the technical and economic feasibility of the pyrolysis of MSW.

## CHAPTER 2

### Literature Review

#### 2.1 Introduction

Municipal solid waste (MSW) basically refers to materials discarded in urban areas, including predominantly household waste with sometimes the addition of commercial wastes, collected and disposed by the municipalities [5]. These wastes are generated and accumulated as a result of human activities [6]. MSW is heterogeneous in composition and is made up of materials with widely variation in sizes and shapes [7]. MSW contains a significant fraction of paper, food waste, wood and yard trimmings, cotton, and leather, and is a source of biomass [5]. Zheng et al. (2009) described the major combustible components of MSW which includes six renewable materials: paper, wood, food residue, plastic, rubber and fabrics [8]. Materials derived from fossil fuels, such as plastics, rubber, and fabrics, are also found in MSW [5].

**2.1.1 Wood.** consists of three major components: cellulose (40-45 wt%), the skeletal polysaccharide; hemicelluloses (27-39 wt%) which form the matrix; and lignin (21-30 wt%), the encrusting substance that binds the cells together [9].

**2.1.2 Paper/card board.** It is produced from the paper pulp which is produced mechanically or chemically from wood. During the production process, certain chemicals such as sulfite, chlorine and soda are used to reduce the hemicelluloses and lignin content. Paper or cardboard may also contain inorganic additives (such as pigment), binder and chemical additives (such as lubricant, foam reducer of coating melt) which is as a result of the coating process [9].

**2.1.3 Textiles.** Textile is one of the main components in MSW which is diverted from landfill for material and energy recovery [10]. The textile waste is a mixture of natural and synthetic fibers such as cotton, wool, silk, nylon, olefin and polyester. Cotton and polyester are

the most commonly used [10]. Textile residues found in MSW that exhibit particular combustion behavior are mostly of cotton origin [11]. It is important to note that some of these textile materials are treated with flame retardant. Flame retardants can be inorganic, halogen-containing or phosphorus-containing that are physically mixed or chemically bonded to the polymer in order to meet fire safety regulations for certain textiles including toys, nightwear and upholstery. In the final analysis, flame retardants effectively reduce the heat transfer to the polymer once ignition starts [10]

**2.1.4 Plastics.** It forms a major component in MSW are mainly PS (polystyrene), PP (polypropylene), LDPE(low-density polyethylene), HDPE (high-density polyethylene), PVC (poly(vinylchloride)) [9]. Polyethylene (PE) in general, is cheap and easy to process, and its applications include heavy duty sacks, refuse sacks, carrier bags, toys, electric cable insulation and general packaging. The polymeric structure of both LDPE and HDPE is essentially a long chain of aliphatic hydrocarbons [9]. PP has a methyl group in the repeating unit. PP is often used as textile and ‘fast turnover food’ packaging such as margarine tubs. PS is made from the styrene monomer and the repeating unit contains a benzene ring ( $C_6H_6$ ) and it is often used in products such as storage containers, toys and electrical equipment. PVC, has the methyl group of PP substituted with chlorine (Cl) and has wide application from rigid piping and window frames to soft flexible foams [9]. PVC has high content of chlorine and generates corrosive gases when being burned [12]. Renewable sources of energy are those that can be replenished by nature, examples are hydropower, wind power, solar power, and biomass.

On the average, these four components of paper, plastic, textile and wood account for, 31%, 13%, 4.6%, and 7.0% of all the discarded (after recovery) wastes in the MSW stream in the United States, respectively, and constitute 94% of all the combustibles in MSW [12].

Large tonnages of MSW are generated throughout the world each year. For example, about 246 million tons of MSW was generated in the USA in 2006 according to US Environmental Protection Agency (EPA) [13]. The U.S. EPA considers MSW as a renewable energy resource because the waste would otherwise be sent to landfills (U.S. Environmental Protection Agency, 2006) [5]. The U.S. Department of Energy includes MSW in renewable energy only to the extent that the energy content of the MSW source stream is biogenic. The non-renewable portion of MSW has to be either separated or accepted as part of the fuel, and practically all the wastes in MSW after material recovery and recycling are treated as renewable [5]. Paolo Baggio et al. (2008) describes MSW used for energy recovery typically contains 60 wt% cellulosic fraction (paper, cardboard, wood), 20 wt% plastics (high-density polyethylene (HDPE), low density polyethylene (LDPE), polypropylene (PP), polystyrene (PS), polyvinyl-chloride (PVC)) and 20 wt% moisture [14].

MSW has played a significant role as a source for energy by means of waste-to-energy technologies (pyrolysis, gasification and combustion) and residual derived fuels at very high conversion efficiencies in many countries [6]. The development of innovative technologies for energy recovery from MSW could contribute to the reduction of both environmental pollution and dependence on fossil fuels[14]

From an energy perspective, MSW can be grouped into three fractions:

- mixed high calorific waste materials suitable for SRF (solid residual fuel) production,
- organic waste materials suitable for biological treatment, and
- mixed waste materials not fitting into the former two fractions.[15]

MSW used 'as received' as input to waste-to-energy processes, can lead to variable (and even unstable) operating conditions, resulting in quality fluctuations in the end product(s). In addition,

the more advanced thermochemical treatment technologies require an input feed with a sufficiently high calorific value in order to obtain high process efficiencies [7]

## **2.2 Residual Derived Fuels used as Combustibles of MSW**

The quality of municipal solid waste is more regionally dependent and can vary over a wider range. Nearly 45–50% by mass of household waste is combustible, and certain sources can reach as high as 85–90% [3]. Residual derived fuel (RDF) represents a fraction of MSW stream where the recyclable components, such as glass and metals have been removed [13]. It is also explained by Cozzani et al. (1995), as the material produced converting the combustible fraction of MSW into a fuel [16]. A RDF involves a process where the main end product is the production of a fuel in the form of the combustible fraction of MSW[13]. Processing of MSW to remove low calorific materials such as putrescibles and very fine material increase the calorific value of the residual product which consists of paper, plastics, textiles and other combustible material [13]. It is obtained following mechanical sorting and processing to improve the physical and combustion characteristics of the starting refuse material. Currently, the most common densification process to manufacture d-RDF commercially is pelletizing [12]. Pelletized or densified RDFs undergo further processing to ensure uniform size and weight, and increased energy density so that they are suitable to be used as a feedstock for conventional boilers and processes of pyrolysis and gasification to recover its energy [16]. RDF has an advantage of relatively constant composition, prolonged life span, ease with transportation and storage as compared to original MSW. However, it is important to note that pelletizing usually requires heating of the waste materials and accurate control of moisture, making the process energy-intensive, costly and complicated [12].

The major steps involved in producing RDF pellets are preliminary liberation where bags of waste are mechanically opened and size screening, magnetic separation and coarse shredding, a refining separation stage and finally a series of processes to control the physical characteristics of the fuel for ease of combustion [13].

### **2.3 Waste to Energy Technologies**

Waste-to-Energy is the process of recovering energy, in the form of electricity and/or heat, from waste[7]. Waste incineration has in the past been a technology to reduce the volume and destroy harmful substances in order to prevent threats to human health [7]. Nowadays, waste incineration is always combined with energy recovery. The importance of the energy recovery part has increased over time [7]. Waste-to-energy (WTE) processes recover the energy from the waste through either direct thermochemical conversion (e.g., incineration, pyrolysis, and gasification) or production of combustible fuels in the forms of methane, hydrogen, and other synthetic fuels (e.g., anaerobic digestion, mechanical biological treatment, and refuse-derived fuel).

Compared to the option of landfilling, WTE can curb the contribution of MSW on GHG emissions through avoiding the release of methane from landfills and offsetting emissions from fossil fuel power plants. Comparative studies of WTE and landfilling have shown that WTE can reduce up to 1.4 tons of carbon equivalent per ton of MSW through avoiding the release of methane from landfills and offsetting emissions from fossil fuel power plants [5]

Psomopoulos, et al [17] concluded based on several independent studies that WTE reduces greenhouse gas emissions by an estimated 1 ton of carbon dioxide per ton of trash combusted rather than landfilled. Therefore, in addition to the energy benefits, the combustion of MSW in WTE facilities reduces US greenhouse gas emissions by about 28.6 million tons of

carbon dioxide [17]. Waste-to-energy power plants are in operation in 25 US states. They are fuelled by 28.9 million tons of MSW and have a generating capacity of 2700 MW of electricity [17]. When selecting between these technologies on a strategic level for implementation or further development of waste-to-energy technologies, a solid basis for comparing the environmental benefits and drawbacks of the technologies is required. An optimal choice for a waste processing technology is a subject not only to economic requirements but it is especially limited by environmental regulation compliance requirements [18]. Life cycle assessment (LCA) has been proven to be a suitable decision tool for the selection of waste-to-energy technologies.

Past research work on MSW has been focused on which technology should be preferred for energy production, now and in the future. Biomass and MSW can be converted into liquid by thermal, biological and physical methods. Thermal conversion methods include combustion, gasification, liquefaction, pyrolysis and carbonization [19]. Direct combustion generates heat for power, gasification breakdowns biomass into gases and pyrolysis produces gas, char and liquid [20].

## **2.4 MSW Pretreatment Methods**

MSW differs in physical, chemical and morphological characteristics and due to the heterogenous nature of MSW, a pretreatment process is essential to improve process efficiency prior to the main thermal conversion process. Torrefaction and densification (also known as pelletizing) are pretreatment methods that are applied to MSW to increase the energy density on mass basis and improve water resistivity of biomass[21]

**2.4.1 Torrefaction.** It is a thermal technology performed at an atmospheric pressure in the absence of oxygen and relatively low temperatures between 200 and 300°C , which produces a solid uniform product with very low moisture content and a high calorific value compared to

fresh biomass [22, 23]. The process decomposes the hemicellulose fraction thereby increasing the energy density of the biomass, enhancing the hydrophobicity and friability which is preferred in further thermal processing [24]. An important factor during torrefaction is the composition of the biomass resource since the content of cellulose, hemicellulose and lignin changes and therefore influences the product distribution. The physical and chemical properties of biomass before and after torrefaction are analyzed for yield, energy content, elemental composition, change in major components, hydrophobicity, and ease of comminution [23]. In the case of energy density, a typical example is explained in the mass and energy balance of woody biomass where 70% of the mass is retained as a solid product, containing 90% of the initial energy content. The torrefaction gas from the process was reported to contain the remaining 30% of the initial mass which contains only 10% of the initial energy content [24]. It is important to note that torrefaction is considered as a biomass resource pretreatment process.

**2.4.2 Pelletizing.** It is a process of producing fuel pellets by placing ground biomass under high pressure and forcing it through a round opening “die”. It is an extrusion process. The biomass comes out as pellets when exposed to the right condition during the process. Depending on the type of biomass, some will require some binding agents to enhance the pellets formation. The entire process of pelletization involves feedstock grinding, moisture control, extrusion, cooling and packaging. Wood and plant materials have in general low densities due to their porous structure with densities ranging from 40 to 150 kg/m<sup>3</sup> for grass type biomass and 320–720 kg/m<sup>3</sup> for most types of dried hard- and softwoods. Typical unit densities of pelletized biomass can be as high as 1000-1400 kg/m<sup>3</sup> and bulk densities are about 700 kg/m<sup>3</sup>[25]. Biomass pellets are generally a superior fuel when compared to their raw feedstock. A high-quality pellet is dry, hard, and durable, with low amounts of ash remaining after combustion. It is interesting to

note that the pellets are not only more energy dense, but also easier to handle and use in automated feed systems. These advantages, when combined with the sustainable and ecologically sound properties of the fuel, make the pellets very attractive for use.

## **2.5 Thermochemical Conversion**

Thermochemical conversion as applied to MSW is basically a process of altering the chemical and physical structure of the MSW resource by applying heat with the aim of obtaining maximum fuel and chemical yields from the MSW resource. These processes are mainly pyrolysis, gasification, liquefaction and supercritical fluid extraction. They encompass a wide range of operating conditions [26].

**2.5.1 Pyrolysis.** It is the basis of almost all available thermochemical processes [8]. Buah et al, (2007) describes pyrolysis as a process of thermal degradation of organic materials in the absence of oxygen to produce recyclable products of char, oil/ wax and combustible gases [13]. In this thermal process, three different products are produced: a solid fraction (charcoal), a liquid fraction (bio-oils or tars) and non-condensable gases [27]. Depending on the pyrolysis (temperature and residence time) conditions the individual fractions of three products can be maximized [28]. Lower process temperatures and longer vapor residence times favor the production of charcoal (673 K). High temperatures and longer residence times increase biomass conversion to gas (1023–1173 K), and moderate temperatures (773 K) and short vapor residence times are the optimum conditions to produce liquids (bio-oil) [27]. The liquid product obtained from a pyrolysis process is considered as a very valuable biofuel which can be easily transported, directly burnt in power stations and gas turbines and upgraded to obtain transport fuel although it is highly oxygenated, viscous, corrosive, thermally unstable and chemically very complex [29]. The bio-oil has a high energy density and is easy to store and transport [20]. The char may be

used as solid fuels for barbeque or activated carbon. The gas product may be used for the energy requirement of the pyrolysis plant since it has a high calorific value [28] Currently, pyrolysis of biomass is getting more attention because it can produce liquid yield up to 75% wt on a dry-feed [19]. There are a number of factors that affect the performance of pyrolysis. The factors include temperature, particle sizes, sweeping gas flow rate and reactor types [29]

**2.5.2 Gasification.** In a gasification process, waste is subjected to chemical treatments through partial oxidation by an oxidant such as air and steam to produce a synthesis gas, called “syngas” which is principally composed of hydrogen and carbon monoxide [30]. It is worth noting that a gasifier can use air, oxygen, steam, carbon dioxide or a mixture of these as gasification agents [7]. The syngas is required to be cooled and cleaned since it contains contaminants such as higher hydrocarbon such as ethane and propane, inert gases originating from gasification agents [7]. Syngas can be used as a fuel in different kind of power plant such as gas turbine cycle, steam cycle, combined cycle, internal and external combustion engine and Solid Oxide Fuel Cell (SOFC) [30]. One of the major issues in biomass gasification of MSW is to deal with the tar formation during the process [31]. Catalytic cracking is recognized as the most efficient method to diminish the tar formation in the gas mixture [32]. In gasification, the heavy compounds are further broken down into gases by thermal and catalytic cracking. Char is also converted into gases such as CO, CO<sub>2</sub>, CH<sub>4</sub> and H<sub>2</sub> by reactions with gasifying agents [33]. It is worth noting that syngas may have poor heating value when the content of N<sub>2</sub> and CO<sub>2</sub> is high [14].

**2.5.3 Incineration or combustion.** It is a destructive process in which the hydrocarbon content of MSW is converted into flue gases at a high temperature [14]. It can be applied to different types of wastes and it takes place when there is a surplus of oxygen (complete

oxidation) [34]. The main stages of the incineration process are: drying and degassing, pyrolysis and gasification, oxidation [7]. These individual stages generally overlap, meaning that spatial and temporal separation of these stages during waste incineration may only be possible to a limited extent [7]. Waste incineration can be an environmentally friendly method if it is combined with energy recovery, control of emissions and an appropriate disposal method for the ultimate waste [7]. In spite of the advantages derived from the incineration of MSW, such as heat recovery, reduction of volume by 90% [34], there are numerous disadvantages of incineration including production of large flue gas volumes, hazardous waste streams associated with the fly ash and a poor public image [13]. The figure below shows the three main thermochemical conversion processes and their product utilization [35]

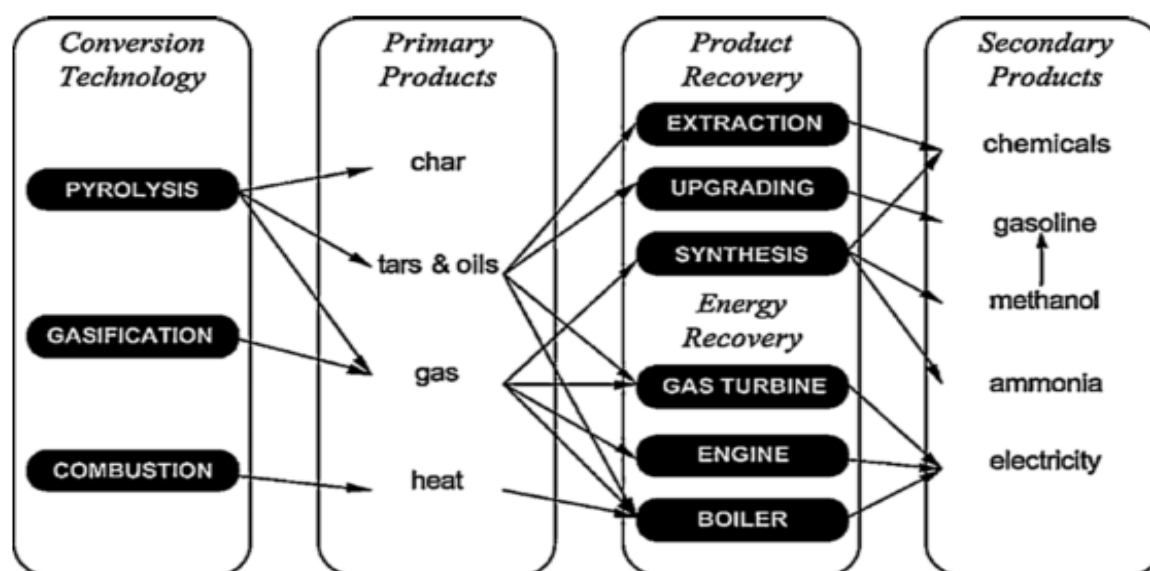


*Figure 2.* Thermochemical conversion processes and their products[35]

Both pyrolysis and gasification differ from combustion in that they may be used for recovering the chemical value of the waste, rather than its energetic value [7]. In recent years, pyrolysis and gasification technologies have emerged to address these issues and improve the energy output [31]. MSW pyrolysis and gasification technology is an attractive way to treat MSW with less

pollution emissions than other methods of treatment [31]. The two processes offer a potential for higher energy efficiency[31].

It is estimated that about 130 million tons of MSW are combusted annually in over 600 WTE facilities worldwide, producing electricity and steam for district heating after recovering metals from the MSW [5]. In very recent times, owing to the number of research in that area, pyrolysis technique of biomass has become a priority since it can produce liquid yield up to 75% wt on a dry feed. Conversion of biomass to liquid provides comparative benefit of transport, storage, combustion, and flexibility in production and marketing [19]. Discarded MSW is a viable energy source for electricity generation in a carbon-constrained world, thus a MSW management technology with the benefits of recovering energy from the waste is a promising alternative in solving the MSW disposal problem [5]

## **2.6 Pyrolysis Principles**

Pyrolysis is the thermal decomposition of materials in the absence of oxygen or when significantly less oxygen is present than required for complete combustion. Pyrolysis processes are mainly classified into carbonization (very slow), conventional (slow), fast and flash depending on the operating conditions that are used [36]. The vapor residence times are days, 5–30 min, 0.5–5 s, and <1 s in carbonization, conventional, fast and flash, respectively [36]. Pyrolysis process conditions can be optimized to produce either a solid char, gas or liquid/oil product [13]. Pyrolysis must well be differentiated from gasification. Gasification decomposes biomass to syngas by carefully controlling the amount of oxygen present, but pyrolysis on the other hand is not explicitly defined. Gas, liquid and char are the three major products of a pyrolysis process. Pyrolysis, based on various independent research is seen as an

environmentally attractive alternative for the recovery of hydrocarbon materials from a wide range of polymeric waste streams such as plastic waste [9, 37]

The general changes that occur during pyrolysis are enumerated below as explained by Bridgewater (2012):

- Heat transfer from a heat source to increase the temperature inside the fuel;
- The initiation of primary pyrolysis reactions at the high temperature to release volatiles and form char;
- The flow of hot volatiles toward colder solids to cause heat transfer between hot volatiles and colder unpyrolyzed fuel;
- Condensation of some of the volatiles in the colder parts of the fuel, followed by secondary reactions to produce tar or bio-oil.
- Autocatalytic secondary pyrolysis reactions proceed while primary pyrolytic reactions (item 2, above) simultaneously occur in competition; and
- Further thermal decomposition, reforming, water gas shift reactions, radicals recombination, and dehydrations can also occur, which are a function of the process's residence time/temperature/pressure profile [11]

Low process temperatures and long vapor residence times favor the production of charcoal. High temperatures and long residence times increase biomass conversion to gas, and moderate temperatures and short vapor residence time are optimum for producing liquids [28]. Aho et al (2008) summarized that during biomass pyrolysis, high liquid yields require high heating rates, short vapor residence times, and rapid cooling of the pyrolysis gases. Pyrolysis occurring in this range of process parameters is termed "fast pyrolysis" [38].

**2.6.1 Products of pyrolysis of Municipal Solid Waste.** As most of combustible materials in MSW are lignocellulosic, they have similar pyrolysis properties to biomass [33]. According to most published research, there are three main products of pyrolysis which are the char (Bio-char), the condensable vapors (Bio-oil) and the non-condensable gases (syngas).

**2.6.1.1 Biochar.** Any organic material, such as wood, straw or manure and generally solid waste that is heated in an oxygen limited or zero oxygen environment yields a solid product (Biochar) among other products as non condensable gases(syngas) and liquid (bio-oil) [39]. Biochar is normally intended for use as soil amendment. Biochar has high content of stable carbon, typically 50–85% of which resists decay and remains in soils for long periods of time, and is thus removed from the atmospheric carbon cycle [39, 40]. Bio-char is also regarded as a suitable feedstock for direct gasification. The obtained gas from direct gasification of raw biomass was usually rich in tar, because of the high volatile matter content. In the case of char gasification, gas products with lower content of tar can be obtained, since the volatile matter content was eliminated during the pyrolysis [41].

**2.6.1.2 Bio-oil or tar.** Bio-oil is a liquid mixture of oxygenated compounds containing carbonyl, carboxyl and phenolic functional groups and it consists of 20-25% water, 25-30% water insoluble pyrolytic lignin, 5-12% organic acids, 5-10% non-polar hydrocarbons, 5-10% anhydrosugars, and 10-25% other oxygenated compounds [42]. The kinematic viscosity of bio-oil varies from as low as 11 mm<sup>2</sup>/s to as high as 115 mm<sup>2</sup>/s at 313 K depending on nature of the feedstock, temperature of pyrolysis process, thermal degradation degree and catalytic cracking, the water content of the bio-oil, the amount of light ends that have collected, and the pyrolysis process used. The bio-oil has a density between 1150-1300 kg/m<sup>3</sup> and a pH in the range of 2.5-3.0 [42]. Pyrolysis of waste produces a liquid rich in oxygenated hydrocarbon which is of major

interest for biofuel application. Maximum liquid yield is achieved by fast (or flash) pyrolysis at around 500°C, atmospheric pressure, high heating rates and very short residence times [42, 43]. The liquid obtained after condensation and filtering (char removal) is called bio-oil, which is a dark brown viscous liquid with high density and moderate heating value. Baggio et al. (2008) defines bio-oil as a complex liquid mixture containing resins, acids, alcohols, intermediate carbohydrates, phenols, aromatics, and aldehydes which has a heating value comparable with those of oxygenated fuels (CH<sub>3</sub>OH, C<sub>2</sub>H<sub>5</sub>OH) [14]. The complex composition of bio-oil causes difficulties in its further processing or upgrading (e.g., coking, abrasion and slag deposition). Bio-oil is upgraded by hydrotreating and hydrocracking. These are seen as the most promising approaches for processing bio-oil into transportation fuels as they are at their engineering development stage or have been demonstrated at a laboratory scale [43]

**2.6.1.3 Non condensable gas (NCG).** Gas obtained from pyrolysis of solid waste remains the most interesting of the three products from the energetic point of view [40]. Syngas is mainly composed of H<sub>2</sub>, CO, CO<sub>2</sub>, and CH<sub>4</sub>. Syngas may be sufficient to be used to meet the energy requirement of a biomass waste pyrolysis plant and might also be employed in internal combustion engines, gas turbines and other operating devices [40]

## **2.7 Types of Pyrolysis**

**2.7.1 Conventional or slow pyrolysis.** Conventional pyrolysis is defined as the pyrolysis, which occurs under a slow heating rate [42]. Slow pyrolysis is characterized by a 2 h process and a slow heating rate of 4°C/min up to 550°C [2]. It is an ancient process with continuous removal of vapors and the process is mainly for charcoal production [35]. Owing to the long residence time, gas phase products have sufficient chance of continuously reacting with each other to form charcoal [44].

**2.7.2 Fast pyrolysis.** of biomass is gaining recognition as a viable thermochemical process to convert lignocellulosic biomass resources into a renewable fuel, energy and other bioproducts. Biomass fast pyrolysis has a more recent history of development (1980s) than gasification [45].

Fast pyrolysis is currently a widely accepted technique for biomass liquefaction in which decomposition of biomass occurs at a high temperature for a short residence time-purposely to avoid any re-polymerization of decomposed products. As fast pyrolysis occurs in a few seconds or less, heat and mass transfer processes and phase transition phenomena, as well as chemical reaction kinetics, play important roles [28]. The critical issue is to bring the reacting biomass particles to the optimum process temperature and minimize their exposure to the lower temperatures that favor formation of charcoal [28].

Fast pyrolysis usually requires dried feedstock (10% moisture contents), crushed biomass particles usually in size range of ~2–3mm to expose particles for necessary heat transfer, rapid heating of biomass and quenching of hot pyrolysis vapor (Bridgewater, et al. 2012). Fast pyrolysis requires drying the feed to typically less than 10% water in order to minimize the water in the product liquid oil, grinding the feed to give sufficiently small particles to ensure rapid reaction, fast pyrolysis, rapid and efficient separation of solids (char), and rapid quenching and collection of the liquid product (often referred to as bio-oil). According to literature, the yield of pyrolysis oils ranges from 40% to 75% of dried biomass, which is dependent on operating parameters. In fast pyrolysis, product yields are sensitive to pyrolysis temperature, biomass types, heat transfer mechanism, size of feed particles, and residence times [46]. One of the main advantages of fast pyrolysis lies in the fact that it is an effective method for densification of voluminous biomass for decentralised densification/centralised conversion platform models [45].

As previously noted, fast pyrolysis is a rapid heating process in the absence of oxygen to decompose biomass into a liquid fuel, with solid and gaseous by-products. It is generally accepted that there are four main process characteristics for fast pyrolysis [46].

- Very high heating rates and very high heat transfer rates at the biomass particle reaction interface usually require a finely ground biomass feed of typically less than 3 mm as biomass generally has a low thermal conductivity [28, 46]
- Controlled reaction temperature around 500°C to maximize the liquid yield for most biomass [28]
- Short vapor residence times, typically less than 2s to minimize secondary reactions [28, 46]
- Rapid separation and cooling of reaction products [46]

The yields of each product during pyrolysis depend upon operating parameters, properties of biomass and type of pyrolysis process.

## **2.8 Reactor Types and Configuration used in Slow or Conventional Pyrolysis**

Slow pyrolysis of MSW is favored when there is relatively low process temperature and longer vapor residence time which results in biochar [47]. The formation of products and its composition is affected by operating parameters which will be discussed in subsequent sections and also largely depend on the type and configuration of the pyrolysis reactor.

**2.8.1 Fixed Bed.** The configuration of fixed bed reactor comes in different forms [48]. The supply of heat to a fixed bed reactor can be done by external or internal heating. In the case of internal heating, the reactor chamber is heated internally by fire-tubes containing insulated electric coil [49] and in the case of external heating, the reactor chamber is externally heated by electric tube furnace [50].

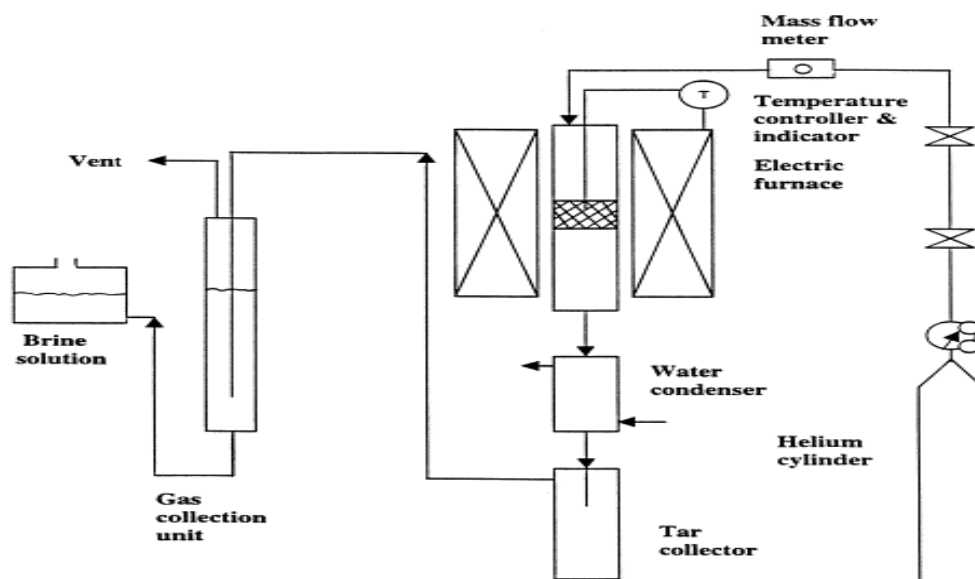


Figure 3. Schematic representation of a continuous down flow fixed bed reactor[51]

## 2.9 Reactor Types and Configuration used in Fast Pyrolysis

During fast pyrolysis, organic and other solid waste are rapidly heated to 400-600°C in absence of oxygen to produce vapors, aerosols, permanent gases and char. The vapors and aerosols are condensed to a liquid called pyrolysis oil [52]. Pyrolysis oil obtained from the process contains a mixture of water and hundreds of (oxygenated) organic compounds [53]. The composition of the pyrolysis oil depends on various operating factors discussed in different articles [28, 52, 54]. Most research and development has been focused on developing and testing different reactor configurations on a variety of feedstocks, although increasing attention is now being paid to control and improvement of liquid quality and improvement of liquid collection systems [28]. These reactors differ with respect to heating rate, vapor residence time and temperature [52]. There has been a lot of research effort in the last few years in exploring innovations in the types of reactor.

A reactor forms a very vital part of the entire pyrolysis process and in most cases termed as the heart of the fast pyrolysis process. Research has been focused largely on designing and

development of different reactor types and configurations which take into account of the type and nature of feedstock, the quality of bio-oil produced and the suitable collection system for pyrolysis products. Bridgwater et al (2012) reviewed different fast pyrolysis reactor configurations, historical background, heating requirements and source and the general operation.

**2.9.1 Bubbling Fluidized Bed.** Bubbling fluidized beds are the most widely used type of reactor for fast pyrolysis and a well understood technology. They are simple in construction and operation, good temperature control and very efficient heat transfer to biomass particles arising from the high solids density and the bubbling bed is “self-cleaning” in principle, which means that char as a byproduct is carried out of the reactor with the product gases and vapors [28, 55, 56]. Fluidized bed is a well-developed technology, which can provide a heating rate of more than 103 K/s [57]. In its operation and referring to the figure below, a feeding system is used to mechanically convey biomass into the vertical vessel filled with hot sand bed. The fluidizing gas is injected at the base of the reactor through a perforated steel distributor plate to provide a well mixed volume with good heat transfer. In this particular schematic representation, adapted from the pyrolysis of MBM (meat bone meal), the total reactor volume is  $2.71 \times 10^{-3} \text{ m}^3$ , which results in a vapor residence time of 2 s for all experiments [58]. A hot-gas filter is placed at the gas exit of the reactor to prevent the entrainment of solids (both sand and char). The reaction is carried out at temperatures ranging from 450°C to 600°C with nitrogen gas used as a fluidizing and feeding system gas [58].

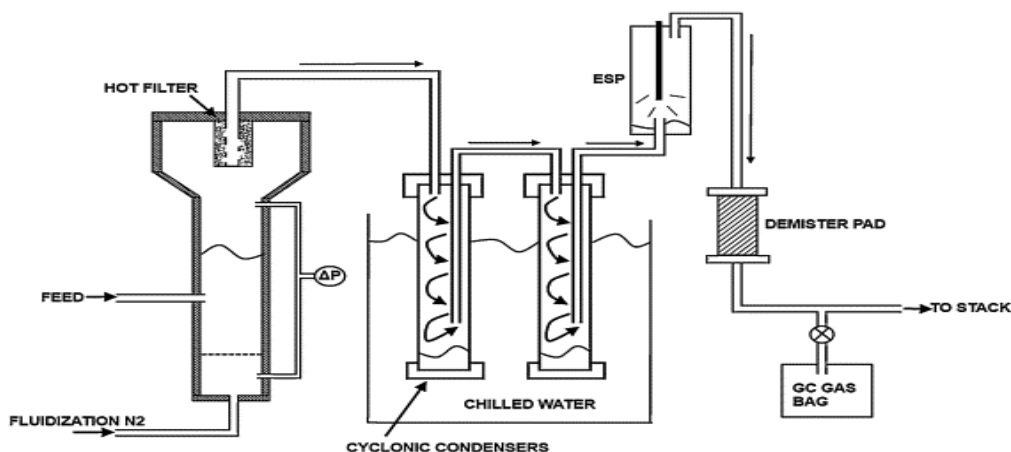


Figure 4. A schematic representation of a laboratory scale fluidized bed reactor adapted from [58]

**2.9.2 Circulating fluidized bed.** Circulating fluidized bed (CFB) and transported bed reactor systems have many of the features of bubbling beds described above, except that the residence time of the char is almost the same as those of vapors and gas, and the char is more attrited due to the higher gas velocities and movement of the sand and biomass particles at the elbows and bends where there is more forceful interaction between the particle and sand [28, 45, 56]. An added advantage is that CFBs are potentially suitable for larger throughputs even though the hydrodynamics is more complex as this technology is widely used at very high throughputs in the petroleum and petrochemical industry [28]. The operation of CFB is similar to the Bubbling Fluidized bed except that the heat supply is usually from recirculation of heated sand from a secondary char combustor, which can be either a bubbling or circulating fluid bed [28]. The incompletely pyrolyzed larger particles will end up in the char combustor where they will simply be burned [56].

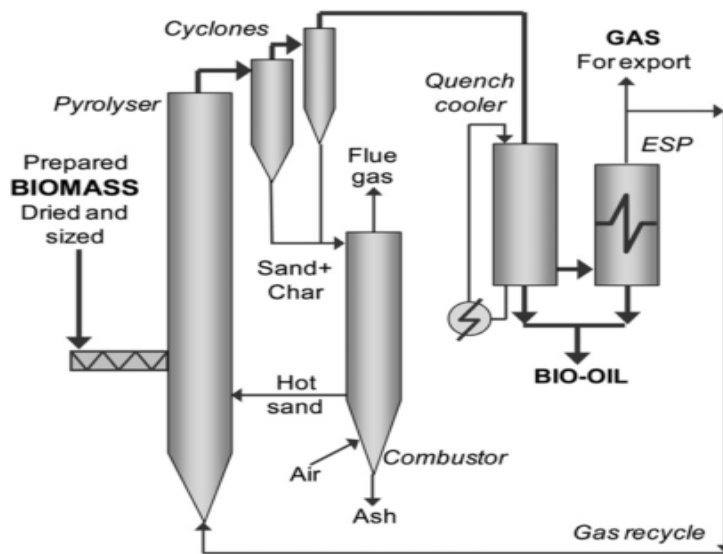


Figure 5. A schematic representation of Circulating fluidized bed reactor

**2.9.3 Ablative pyrolyzer.** Ablative pyrolysis is one of fast or flash pyrolysis technologies for the production of liquids in high yields which offers the potential for high reactor specific throughputs with reduced equipment size, costs and improved controllability [59]. Ablation depicts the phenomena occurring when a solid material, subjected to a high external heat flux density undergoes superficial melting and/or sublimation reactions, with rapid elimination of the products [60]. Ablation is observed if the rate of physical and chemical transformations of the solid and of the external heat transfer is much faster than heat conduction through the solid [60]. A consequence is that the reactions occur inside a superficial layer close to the surface and inside which very steep temperature gradients exist [60]. The biomass feedstock is pressed by a piston on the hot moving surface of a heated rotating disk. Heat transfer and the pyrolysis reaction take place in the contact zone between biomass and the hot surface, where biomass is converted into a liquid that evaporates immediately [43]. The pyrolysis rate increases with the applied pressure and the relative velocity between the hot surface and the biomass (the reaction is possible with a fixed surface, but the rate of ablation is smaller) [60]. Ablative pyrolysis process reduces the cost

of feedstock size reduction since larger sizes of biomass can be used. Jacques (2003) concludes that there were two main techniques of ablative pyrolysis namely contact ablative pyrolysis and radiant ablative pyrolysis. In the contact ablative pyrolysis, the influence of pressure and relative velocity of the hot surface and biomass source results in the flow and rapid elimination of intermediate liquids at the sides of the interface. The result is the existence of a very thin liquid layer through which high heat fluxes may be transferred (heat transfer coefficients may be higher than  $10^4 \text{ Wm}^{-2} \text{ K}^{-1}$ ) [60]. In the case of radiant ablative pyrolysis, specifically designed mirrors are used to concentrate radiation from the sun or high power lamps to very high flux density (above  $10^6 \text{ Wm}^{-2}$ ) onto the surface of a piece of biomass to produce intermediate liquid compounds.

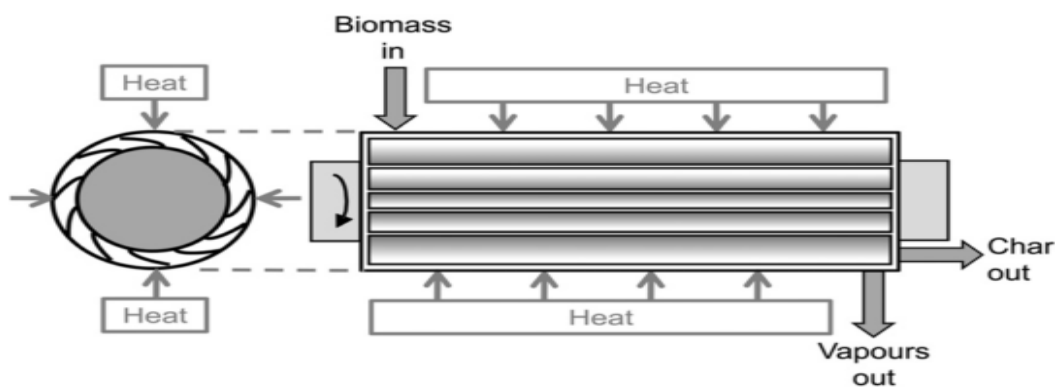


Figure 6. A schematic diagram of ablative pyrolysis reactor by Ashton university[28]

**2.9.4 Screw auger pyrolyzer.** According to Butler, (2011), screw auger reactors were dated back to at least 1927 when Laucks (1927) described the decomposition of coal to produce a smokeless fuel in a screw auger reactor. Considerable experience has been gained over the past 50 years in auger conversion technology [45]. Liaw et al, (2012) summarized that screw type reactors are robust, do not require large volumes of carrier gases and the reactor can use a wide range of biomass particles and appear to be promising for processing capacities between 50 and

100 tons/day [61]. In screw auger reactor, the feedstock is mechanically moved through the reactor by an auger or augers compared to the fluidized system where the movement is by fluid. Heating can be done internally (with a recycled hot heat carrier such as hot sand, steel or ceramic balls [28]) or externally (by electrical heating which is split into three individual heating zones where the temperature is adjusted separately [27]). The twin-screw concept utilizes hot and recirculated sand as a heat carrier, accounting for the nickname ‘‘sand cracker’’ [46]

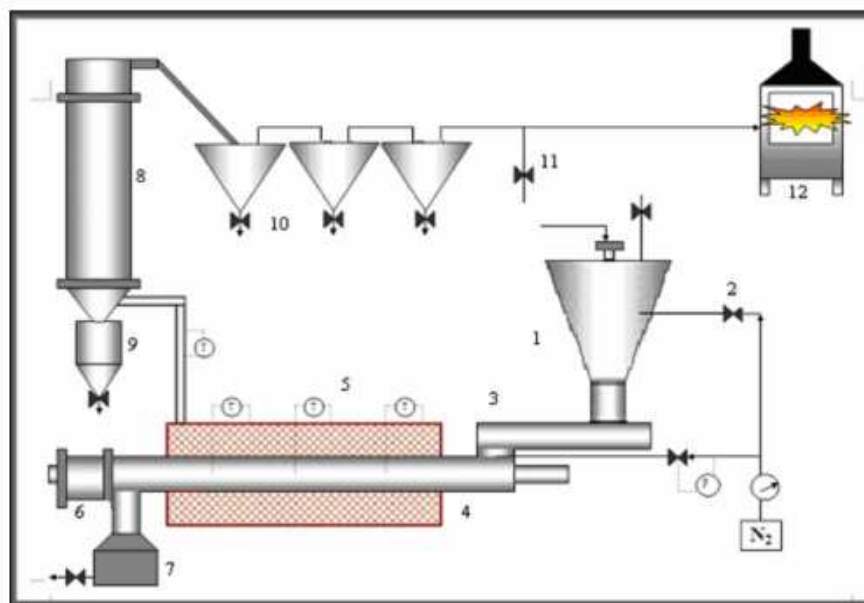
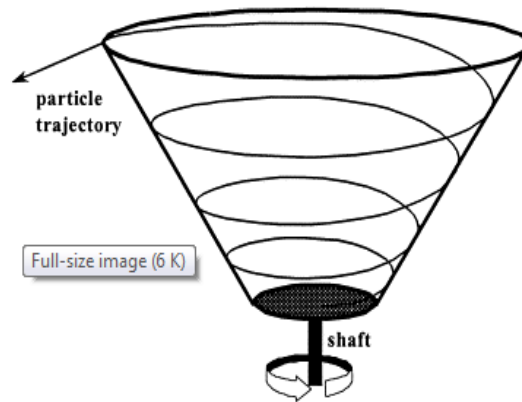


Figure 7. Schematic representation of a continuous screw auger pyrolyzer[1]

**2.9.5 Rotating cone pyrolyzer.** It is a type of fast pyrolysis reactor in which the feedstock particles are transported together with a heat carrier in a mechanical way, thus bypassing the need for carrier gas. The rotating cone is driven from underneath by a shaft connected to the closed bottom with holes near the bottom acting as the sand inlet [62]. By partly submerging the rotating cone into a fluid bed of sand particles, a flow of sand through the reactor is induced, entering through the apertures near the bottom and leaving the reactor over the top edge [62]. During operation of the Rotating Cone Reactor (RCR), the biomass particles are

heated very rapidly and have a very short residence time (usually within several seconds) [63]. The thermal degradation process starts immediately after the biomass particle enters the reactor. The RCR has an advantage of compactness, operation at atmospheric conditions and has high biomass capacity [62]



*Figure 8.* Principle of rotating cone [62]

## 2.10 Relative Merits of Fast Pyrolysis Reactors

Table 1

*Comparison of different types of fast pyrolysis reactors*

Property	Status (Throughput)	Bio-oil wt%	Complexity	Feed size	Inert gas need	Specific size	Scale up
Fluid bed	Demo	75	Medium			Medium	Easy
CFB	Pilot	75		Medium			Easy
Entrained	None	65					Easy
Rotating Cone	Pilot	65			Low	Small	
Ablative	Lab	75		Large	Low	Small	
Auger	Lab	65	Low		Low	Medium	Easy
Vacuum	Demo			Large	Low		
Lab: 1-20 kg h <sup>-1</sup> Pilot: 20-200 kg h <sup>-1</sup> Demo: 200-2000 kg h <sup>-1</sup>							
The darker the cell the less desirable the process							

Source: PYNE IEA Bioenergy <http://www.pyne.co.uk>

## 2.11 Biomass Pyrolysis using Screw Auger Reactor by Past Research Works

Most of the work in the area of biomass pyrolysis using a screw auger pyrolyzer has concentrated on homogenous biomass source as feedstock and an external heat supply. However, it is important to note that some research has been done on heterogeneous feedstock in biomass pyrolysis and in terms of the heat carrier; earlier work was done using sand as an internal heat carrier in fossil fuel processing by pyrolysis. Heterogeneous feedstock pyrolysis was carried out

by Day et al. (1999) [37], in which an experimental study of pyrolysis of auto-shredder residue at temperatures ranging from 500°C to 750°C, with a pyrolysis residence time of 3.2 min was performed. Automobile shredder residue (ASR) is a particularly heterogeneous polymeric waste stream for which pyrolysis may represent a viable resource recovery process. This material was a mixture of plastics, rubber, foam, textiles, glass and dirt, which are the waste produced by shredding operations during the recycling of automobiles [37]. Part of their work was to examine the pyrolysis of the heterogeneous feedstock by fast pyrolysis also known as “ultra-pyrolysis” and to study the process by commercial screw kiln and to analyze the similarities in terms of pyro-oil yield. In their conclusion, ‘Ultrapyrolysis’ produced no pyro-oil at 700–850°C whereas the commercial screw kiln process produced 21% pyro-oil at 500°C [37]. Brown et al. (2011) [46] optimized the process operating parameters of pyrolysis of red oak wood biomass which is a homogenous feedstock in a laboratory scale screw auger reactor (1 kg/h capacity) using steel shot as internal heat carrier. The authors used response surface methodology to develop a regression model to predict the interaction between heat carrier flow rate and auger speed. It was concluded in the experiment for conditions of maximum oil yield and minimum char yield at sweep gas flow rate of 3.5 standard L/min, high heat carrier temperature (~600 °C), high auger speeds (63 RPM) and high heat carrier mass flow rates (18 kg/h).

In a more recent research by Sirijanusorn et al. (2013) [64], the behavior of a counter screw auger was investigated in a pyrolysis process using sand as a heat carrier. It was found that pyrolysis temperature at 550°C, biomass particle size of 0.250-0.425 mm, nitrogen flow rate and pressure of 4 l/min and 2 bar respectively could maximize the oil yield to about 50 wt%. They noted that water content of bio-oil obtained was relatively lower in the counter screw configuration compared to other configuration [64]. The effect of temperature on the yield of oil

was also studied by Liaw et al. (2012) [61] and Puy et al. (2011) [1] under similar conditions in a twin screw auger pyrolysis at comparable process parameters. The yield of bio-oil was 59 wt% which was close to reported yields in fluidized bed reactor.

## **2.12 Past Research Work in Pyrolysis of MSW using Fixed Bed Reactor**

Buah et al. (2007) pyrolyzed MSW in a fixed bed reactor. It was concluded that the yield and composition of the products recovered depended on temperature. The yield of char fell as the pyrolysis temperature was raised from 400°C to 700°C, whereas that of oil/wax and gaseous products increased. The properties of the biochars recovered depended on the size fractions. The total 1.00 mm char sample (0.000–1.000 mm) and also the fractions of the sieved sample sizes of 0.000–0.063 mm, 0.063–0.500 mm and 0.500–1.000 mm were analysed for surface area by the nitrogen adsorption technique using a Quantachrome Corp. Quantasorb instrument [13].

Luo et al. (2009), studied the effect of particle size of individual component of municipal solid waste on the yield of pyrolysis products in a laboratory-scale fixed bed reactor [65]. The hearth of the reactor was made of quartz tube with an externally heated electrical ring furnace covered with insulation layer outside. For a fixed bed temperature of 800°C (the hearth temperature was assumed as the pyrolysis temperature due to difficulties in measuring actual temperature of material), they observed that smaller particle size results in higher gas yield with less tar and char; the decrease of particle size can increase H<sub>2</sub> and CO contents of gas, as well as the ash and carbon element contents in the char. The pyrolysis behavior among others such as devolatilization rate, heat transfer properties, char properties, swelling/shrinkage properties of especially the plastic components was performed in a similar experiment by Zhou et al. (2013) [3] under similar conditions in a fixed bed reactor.

## 2.13 Pyrolysis Process Operating Conditions

There are heat and mass transfer processes that characterize solid waste (biomass) pyrolysis leading to primary and secondary reaction mechanisms [54]. Primary reactions include the decomposition of cellulose, hemicellulose and lignin present in biomass, which leads to the formation of primary products and intermediates [54]. These intermediate species further undergo secondary cracking. Secondary cracking proceeds in two categories. The pathway for the two categories includes:

- dehydration and charring reactions
- decomposition and volatilization of intermediates.

Due to the competitiveness of the reaction, and the molecular structure of biomass composition, the products obtained are sensitive to operational conditions.

**2.13.1 Temperature.** It plays a fundamental role of supplying the heat of decomposition to break down the biomass bonds. At a low temperature ( $< 300^{\circ}\text{C}$ ), the decomposition mainly occurs at heteroatom sites within biomass structure which results in the production of heavy tars [54]. While at a high temperature ( $> 550^{\circ}\text{C}$ ), massive fragmentation of biomass species causes the extremely high molecular disordering which results in the production of numerous types of compounds [54]. For example, Ayhan (2007) conducted experiments on the pyrolysis of wood and found that hemicelluloses would break down first, at temperatures of 470 to 530 K. Cellulose follows in the temperature range 510 to 620 K, with lignin being the last component to pyrolyze at temperatures of 550 to 770 K [36]. This results in a wide spectrum of organic compounds in the pyrolytic liquid fraction[36]

Biomass conversion efficiency increases with the increase in temperature, which is mainly due to extra energy inputs available to break the biomass bonds [54]. From literature by

(Akhtaret al, 2012), 80-90% of total conversion usually occurs in the temperature range of 300 – 400°C. The products of biomass conversion are mainly composed of gas, tar and the char. The relative yield of each varies to different extents with increase in temperature. The gas fraction is mainly made up of carbon dioxide and carbon monoxide, whose yields increase with temperature, due to the enhancement of decarboxylation and decarbonylation reactions [66]. Amutio et al. (2012) found that CO<sub>2</sub> concentration in the gaseous fraction sharply decreases as temperature is increased, whereas that of CO increases during the pyrolysis of pinewood. This is mainly because most of the CO<sub>2</sub> is produced by the release of carboxyl group at relatively low temperatures, but CO and CH<sub>4</sub> are produced at higher temperatures than CO<sub>2</sub> due to the secondary cracking of volatiles [66]. The yield of C<sub>1</sub>–C<sub>4</sub> hydrocarbons increases with temperature. The amount of hydrogen is negligible at low temperatures, but almost 10 vol% is obtained at 600°C [66]. Also they found that bio-oil is the main fraction in the 400–600°C range, with a maximum yield obtained at a reaction temperature around 500°C. This maximum yield of bio-oil is characteristic to woody biomass flash pyrolysis processes. At temperatures above 500°C, secondary cracking reactions reduce the bio-oil yield, and below 400°C the reduction in the liquid yield is caused by the condensation reactions at gas/vapor product temperatures [66].

**2.13.2 Residence time.** At pyrolysis conditions, vapors are prone to secondary cracking or repolymerization. To obtain optimum yields of bio-oil through pyrolysis, it is recommended to maintain vapor residence times of few seconds to few minutes. It is important to note that high temperatures and relatively long residence times favor the production of oxygen free bio-oil. However, it is difficult to achieve complete conversion of biomass due to heat transfer limitations at particle surface. Owing to the above, it is recommended to optimize residence times of pyrolysis process to achieve high yield and better quality of oil.

The pyrolysis time is defined as the period between the introduction of the biomass to the hot end of the reactor and the approximate time at which no more white smoke (aerosols) can be seen at the entrance of the cartridge. This pyrolysis time is a consequence of the heat source temperature value [67]. Pyrolysis time for decomposition of biomass particles must be longer than the vapor residence times to obtain higher yields and biomass conversion [54]. Fassinou et al. (2009) reports lots of complex phenomena (thermal and chemical reactions) happen during a pyrolysis process when residence time increases. And so to that extent it is logical to think that increasing temperature and residence time promote liquid or tar cracking, which increases gas percentage and thus decrease the bio-oil yield [68]. High residence time improves heat exchanges and the transfers of heat in biomass during the pyrolysis process; thus VM and other molecules are easily cracked [68].

**2.13.3 Size of feed particles.** The size of feed particles plays a very significant role on the yield and properties of liquid oil and also impacts on the heat transfer limitations. In general, small particle sizes are preferred in rapid pyrolysis systems. Haykiri –Acmar (2009) explained that decreasing particle size resulted in the decrease of the char yields as small particles have enough surface area to interact with the pyrolysis medium to form volatile products that leaves the biomass matrix without undergoing secondary reactions [69]. Shen et al. (2009) found that when small particles were fed into a fluidized bed with sand, they would be heated up rapidly and almost instantly. However, the heating rates for larger particles would be much slower [70]. This may be the reason that smaller particles heat up uniformly. On the other hand, for larger particles, poor heat transfer to the inner surfaces will lead to low average particle temperatures and hence the yield of liquids may decrease [54]. During pyrolysis, the tar concentration in the pyrolysing biomass/char matrix increases with increasing particle size and the high tar

concentration implies intensive recombination of tarry compounds on the internal surface of the pyrolysing biomass/char particle, thus resulting in reduced weight loss [71]. General feed particle size for different pyrolysis system has been reported in published articles. However, specific data for feed sizes of different biomass types to be used in a pyrolysis system is missing from literature. Akhtar et al. (2012) reviewed that different particle sizes and reactor system was reported by several researchers. These conflicting information on biomass feed sizes make it difficult to generalize the size of feed particles for a specific pyrolysis system. However, Fassinou et al. (2009) found that reduced particle size below 5 mm did not exert any influence on the pyrolysis process and the yield of its products during pyrolysis of pinus pinaster biomass in a screw reactor [68]

**2.13.4 Heating rate.** Various research has shown that heating rate greatly affects the yield of bio-oil (or tar) from biomass. For small particles, the effects of heating rate are mainly because, among many other possible considerations, the fast heating rate may favor the simultaneous bond scission (formation of volatiles) over the recombination (charring) reactions [70]. The relative importance of heating rate is different for each of the bio-polymers forming the biomass (cellulose, hemicelluloses and lignin). While charring reactions are very intense for lignin with yields of char typically close to 50% at slow heating rates (around  $10 \text{ K min}^{-1}$ ), the yields of char resulting from cellulose can be as low as 5% for the same heating rates [70].

The influence of heating rate on gas yield is shown in a comparison of rice straw and sawdust in a pyrolysis reaction in a fluidized bed reactor by Chen et al, 2003. In the research paper, a comparison between gas yield was seen to be conspicuous at low and high heating rates (rice straw saw a relative change of gas yield at 34.1%(+) and sawdust recorded 28.8%(+) when the heating rate was high [72]

**2.13.5 Sweeping gas flow rate.** From literature, the sweeping gas removes products from the hot zone to minimize secondary reactions such as thermal cracking, repolymerization and recondensation, which occur as a result of interaction between escaping pyrolysis vapors with surrounding solid environment [54, 73]. In fast pyrolysis, this results in further maximization of the liquid yield and it is important to note an assumption is made that sweeping gas do not influence the yield of pyrolysis liquid. However, it is considered that a secondary parameter for production of liquid oil from fast pyrolysis [19, 54, 73]. Rapid purging of hot pyrolysis vapor requires the use of inert gases such as N<sub>2</sub>, Ar and water vapor. Nitrogen gas remains the most common sweeping gas in most research apparently because of its cheapness [54]. The nitrogen flow affects the residence time of the vapor phase produced by pyrolysis so that higher flow rates cause rapid removal of products from the reaction medium and minimize secondary reactions such as char formation [73]. Putun et al, [73] accounted for 3% more liquid oils when nitrogen flow was increased from 50 ml/min to 200 ml/min. In the same experiment by Putun et al it was noted that pyrolysis vapors are removed instantly by high sweeping gas flow rates, and if they are quenched sufficiently, the liquid yield should be high. They observed the oil yield reached its maximum of 35.77% with a sweeping gas velocity of 100 cm<sup>3</sup> min<sup>-1</sup> at experimental conditions which were insufficient for quenching. Alina et al (2013) [74] observed that a much low yield of oil of average 0.3% increment when nitrogen gas flow rate was increased from 150 ml/min to 200 ml/min and a decline in yield of 5.5% when nitrogen gas flow was further increased to 500 ml/min during the pyrolysis of EFB from Palm fruit in Malaysia. It is important to note that water vapor has higher effect on liquid yield than sweeping nitrogen gas. Özbay et al (2006) [75] compared the yield of bio-oil using steam and nitrogen as purging gases. They observed that the yield of the liquid product in steam pyrolysis was 27.2% which was

higher than that of the static condition at 22.4% and inert gas atmospheres at 23.2%. They concluded that steam flow dramatically increased the yield of oil at the expense of gaseous and solid products and it was explained that water vapor is not only a vehicle for volatiles but also a reactive agent, which reacts with the pyrolysis product and thereby stabilizing the radicals in the thermal decomposition of the fuel and hence an increase in the yield [75].

#### 2.14 Thermogravimetric Analysis (TGA) of Pyrolysis of MSW

Pyrolysis is an extremely complex process, where numerous reactions take place, practically making it impossible to develop a kinetic model that takes into account all these reactions [76]. Studies are mostly based on pseudo-mechanistic model. Sanshev-Silva et al (2012) reported three main types of kinetic models employed in biomass decomposition studies, which were single-step global reaction models, multiple step reaction models and semi global models [76]. One of the most frequently used models employs independent parallel reactions, assuming that the total reaction rate of pyrolysis process of a biomass equals the sum of the partial contributions of its main components [77]. The temperature-dependant partial contribution of each component is determined by its own reaction rate, multiplied by its initial content in biomass. The reaction for each component is taken as the  $n$ th order and is approximated by an Arrhenius equation [77].

$$\frac{d\alpha}{dt} = k_{i0} \cdot e^{-\frac{E_{ia}}{RT}} \cdot (1 - \alpha_i) \quad \text{for } i = 1, 2, 3 \dots \quad (1)$$

where  $k_i$ ,  $k_{i0}$ , and  $E_{ia}$  are rate constant, pre-exponential factor, and activation energy for the individual component, respectively;  $R$  is the gas constant;  $T$  is the pyrolysis absolute temperature.

The pyrolysis kinetic study by TGA is based on the dynamic mass change of the measured sample due to thermal decomposition. The produced products include gases, volatiles, and charcoal. At any time  $t$ , the measured total mass by TGA is assumed to be a sum of the pyrolyzable biochemicals (cellulose, hemicelluloses, lignin, and wax/protein), the produced charcoal, and ash if the moisture and extractives of the biomass has been removed at a temperature above  $150^{\circ}\text{C}$  [77]. TGA measures the decrease in substrate mass caused by the release of volatiles, or devolatilization, during thermal decomposition. In TGA, the mass of a substrate being heated or cooled at a specific rate is monitored as a function of temperature and time. The first derivative of such thermogravimetric curves (i.e.,  $-dm/dt$ ) curves, known as derivative thermogravimetry (DTG) can be used to determine the maximum reaction rate [78].

Due to the heterogeneity of MSW, the pyrolysis characteristics by TGA and the interactions between different components are of interest and reported by several authors [2]. Pyrolysis of MSW may take place through a reaction network of competitive and parallel reactions [9]. Sorum et al. (2001), summarizes based on the experimental plots that DTG curves observed for pyrolysis of MSW are quite simple and can be described by relatively simple mathematical models. Curves obtained for plastics in the categories of polystyrene (PS), polypropene (PP), low density polyethylene (LDPE), high density polyethylene (HDPE) exhibit a sharp single DTG curve, which can be well described by a single reaction model. However, DTG curves of cellulosic components of MSW exhibit double peaks indicating that more than one reaction are involved, in which case the overall decomposition can be described by a model of independent parallel reactions [9]. In the kinetic study of the decomposition of MSW samples and the major components, an assumption is made to consider experimental data lower than

600°C since above this value limits the weight loss to decomposition of  $\text{CaCO}_3$  present in the ash [79]

## **2.15 Thermal Properties of Biomass during Pyrolysis**

MSW as biomass resource in the context of energy, can have different composition and different properties depending on the origin of the biomass resource. Generally, biomass is made up of cellulose, hemicellulose, lignin, lipids, simple sugars, water, starch, hydrocarbon, ash and other component. In terms of elemental composition, biomass resources are made of carbon (C), hydrogen (H), oxygen (O) and small amount of nitrogen (N), sulfur (S) and chlorine (Cl). In general, the C content makes up around 30–60%, H at 5–6%, and O at 30–45% (wt% on dry basis) and less than 1% of sulfur(S) and chlorine(Cl) [80].

**2.15.1 Heating Value (HV).** It refers to standardized energy content of a fuel and it is often expressed as the higher heating value (HHV) or lower heating value (LHV). Higher heating value or gross heating value refers to the heat released by the complete combustion of a unit volume of fuel leading to the production of water vapor and its eventual condensation. On the other hand, lower heating value or net heating value does not take into account the latent heat of the water and all the water of reaction products remain as water [81]. These values are normally expressed on dry weight or dry ash-free weight basis since they can vary widely depending on the moisture content [80]. Heating value can be determined from mathematical equations derived based on data from physical composition, proximate and elemental analysis from biomass; and can also be determined experimentally by using the bomb calorimeter [81].

**2.15.2 Specific heat.** Specific heat is the amount of kilojoules needed to raise the temperature of 1 kg of fuel by 1 °C. There is very little information about the evolution of biomass heat capacity during conversion. These heat capacity measurements were generally

performed either with adiabatic calorimeter or with Differential Scanning Calorimetry (DSC) [82]. Many studies on food biomass were carried out by the method of calorimetry by mixtures but this technique is not accurate. DSC seems to be a very accurate tool between the two methods. However, low density of biomasses, small volumes of solid, and therefore small masses of biomass, typically of a few milligrams, makes the resulting heat flow very low [82], hence the calorimeter, which requires higher masses of solid, typically of a few grams, seems to be the reference tool for biomass heat capacity measurement. Biomass heat capacity is known to be influenced by both temperature and biomass moisture. There is a general agreement on the linear increase of biomass heat capacity with temperature that goes from 5 K to 423 K depending on the studies. It is interesting to note that biomass heat capacity can be measured only up to temperatures of about 423 K, as biomass begins to decompose when temperature is higher than 423 K.

**2.15.3 Thermal conductivity.** Thermal conductivity of MSW as explained by Eric et al (2012) is a complex thermal property which depends on many factors such as the geometry of porous medium (porosity, size and shape of the pores, pore curvature radius, percentage of closed pores etc.), thermal conductivity of gas and solid-phase, hydrodynamic properties of gas-phase (velocity, pressure and temperature), flow characteristics (laminar or turbulent flow) [83]. Thermal conductivity together with specific heat of biomass are important parameters controlling the rate of heat dissipation within the bulk material.

## CHAPTER 3

### Experimental Methods and Materials

#### 3.1 Introduction

Experiments were conducted to study the effect of pyrolysis temperature on the yield and composition of bio-oil and biochar from different MSW organic components. Additionally, the effect of the pyrolysis temperature on thermophysical properties of bio-oil and biochar including heating value, specific heat capacity were also analyzed. It is important to note that during the pyrolysis of biomass samples under inert conditions, both physical and chemical changes occur in the feedstock. These changes can be analyzed at a specified pyrolysis temperature when the process is stopped at the specified temperature and the reactor immediately cooled. Physical and chemical properties including elemental composition, higher heating value, moisture content and specific heat were conducted on the cooled and dried samples collected at different pyrolysis temperatures to examine the thermal and chemical changes during the pyrolysis.

#### 3.2 Preparation of MSW Samples

MSW was selected as feedstock for this experiment. Three MSW samples (paper, wood and textile residue) were selected and characterized from the MSW collected in the Greensboro MSW transportation Station. These components were selected because data and statistics from the city of Greensboro council, NC indicated that they are the major component of MSW. The paper component in the waste consisted of different varieties ranging from news papers, paper towel, cardboard to label papers. They were in different proportions. The characterized samples were dried in the sun to remove all moisture content as shown in Figure 10.

The paper with different varieties after drying was milled together in a Thomas Wiley Mill with a 1 mm screen as shown in Figure 11 (Thomas Scientific, Swedesboro, NJ). The woody biomass component consisted mainly of wood chips from the hard wood species and saw dust with homogeneous sizes of 5 mm to 10 mm. The wood chips and saw dust were milled together to an uniform size in a Thomas Wiley Mill with a 1 mm screen (Thomas Scientific, Swedesboro, NJ). The particle size at 1 mm was used to minimize the limitation of heat transfer during pyrolysis. The ground MSW samples were not further pretreated after milling and were stored in 10 Litre transparent containers.



*Figure 9.* Characterized MSW samples dried in the sun



*Figure 10.* Thomas Wiley Mill for grinding MSW samples

### 3.3 Pyrolytic Experiments

**3.3.1 Pyrolytic reaction unit.** An experimental unit as shown in Figure 9 is set up to investigate the pyrolysis of MSW. Pyrolysis was conducted in a horizontal stainless steel (#316) fixed bed reactor of 300 mm in length and 30 mm in internal diameter. An electric furnace was used to maintain the pyrolysis temperatures. The temperature of the electric furnace was controlled by an inbuilt controller with a K-type thermocouple. Nitrogen gas was used to purge the air out of the reaction unit. One end of the tubular reactor was connected to the nitrogen gas cylinder by a 1/8 in (0.3175 cm) stainless steel pipe of 100 mm length. The volumetric flow rate of the purging gas was manually controlled by a rotameter. A K-type thermocouple (1/16 inch sheath) was inserted into the reactor that was filled with the feedstock to measure the actual pyrolysis temperature. The gas outlet of the reactor was connected to three 25 ml vials connected in two- stage condensation in cooling water stream.

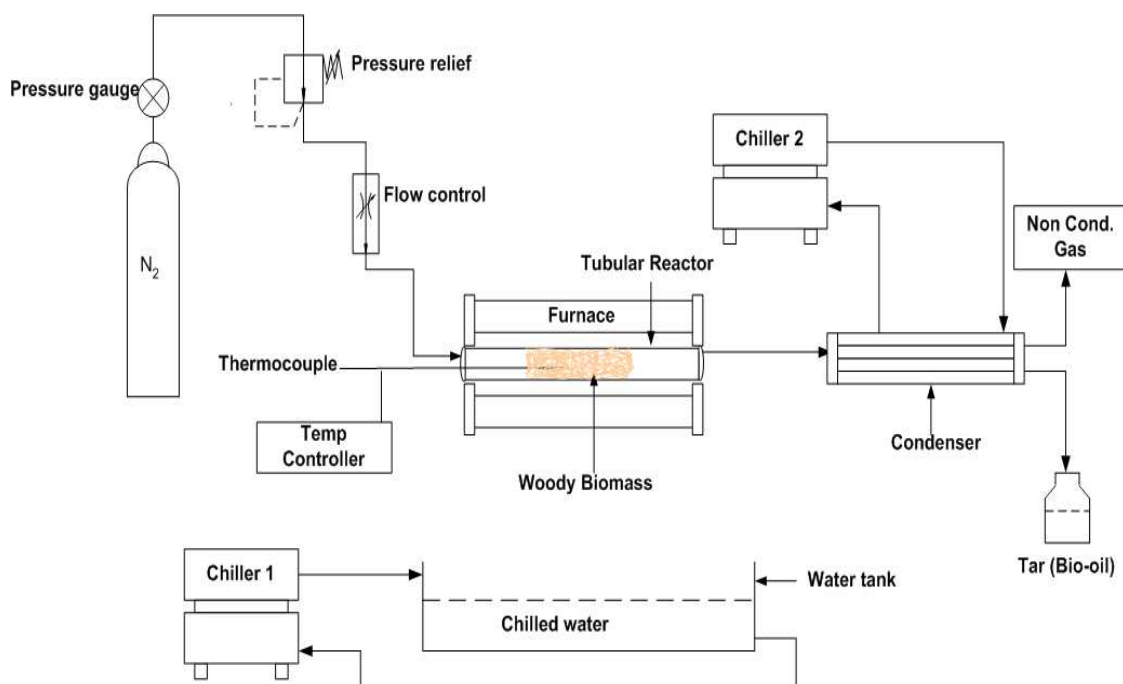


Figure 11. A simple schematic representation of the fixed bed pyrolysis process

**3.3.2 Statistical experimental design.** The design of experiments was based on the measurable and controllable parameters that affect the pyrolysis process. The yield and properties of products from the pyrolysis of MSW depend on several factors. Some of the factors that are considered generally in pyrolysis include temperature, type of sweeping gas and its flow rate, heating rate, residence time, biomass type and biomass feed rate. Depending on the type of pyrolysis and the configuration of the reactor, some of these factors are known to have minimal effect on the process.

In this research, MSW feedstock and temperatures were considered as two controllable factors during the experiment. The simulated MSW which constituted of paper and cardboard, woody biomass and textile were charged to a tubular reactor with a 100 ml working volume. There were three levels of MSW component and eight levels of temperature considered in the experimental design. Each experiment was performed three times to ensure reproducibility.

**3.3.3 Pyrolysis procedure.** In this study, 5 to 10 g of MSW components (paper, wood and textile) were used for each pyrolysis run. After sample preparation, a given mass of each sample was placed in the reactor and it was tightly sealed at both ends using reactor caps. The exact mass of the feedstock was determined by the difference of the mass of the reactor before and after it was filled with the sample. The reactor was heated externally by a thermolyne electric tube furnace placed in a horizontal position. The heating rate of the electric furnace is controlled by a Ni-Cr-Ni thermocouple. Bio-oil and reaction water derived during the pyrolysis were collected in a weighed and labeled 25 ml vials located in the cooling bath. The noncondensable gases were vented through the condenser and the mass was estimated as difference from the initial mass of feedstock and the total mass of biochar and condensable bio-oil.

After the pyrolysis temperature reached the set value, the reactor was rapidly cooled down to stop the reaction and the biochar sample was then collected. During the experiment, the reactor was lowered in a chilled water bath after each run to rapidly cool down the biochar to the ambient temperature. The biochar collected was weighed. The thermal and physical properties of the biochar after pyrolysis was analyzed. The experiment for each pyrolysis was repeated three times. After cooling, biochar samples were collected from the reactor and stored in sealed plastic containers and labelled.

The bio-oil and biochar samples were kept in dark, refrigerated conditions at 5°C. Prior to testing the samples, all bio-oil and biochar samples were removed from the refrigerator and homogenized by vigorously shaking the sample bottle by hand for a minimum of one- minute.

### **3.4 Analysis of the Physical and Chemical Properties of MSW samples and Pyrolysis**

#### **Products**

The physical and chemical properties of MSW, Bio-char and Bio-oil were characterized.

**3.4.1 Particle size analysis.** The particle size distribution of MSW organic compounds is considered an important physical parameter since it influences the flow properties during storage and transport. In pyrolysis process, it affects the heat and mass transfer. In this experiment, a set of sieve with sizes decreasing from top to down mounted on a shaker was employed to determine the particle size. The time for each analysis was set at 5 min to ensure all particle sizes were sufficiently distributed over the sieve size arrangement. The U.S sieve sizes used in the order of decreasing sizes consisted of sieve No.18 ( 1000  $\mu\text{m}$ ), No. 20 ( 850  $\mu\text{m}$ ), No. 30 (600  $\mu\text{m}$ ), No. 50 (300  $\mu\text{m}$ ), No. 60 (250  $\mu\text{m}$ ), No. 100 (150  $\mu\text{m}$ ), No. 200 (75  $\mu\text{m}$ ). After shaking for the set time, the accumulated samples in each sieves was weighed and calculated as a percentage of the total sample weight.



*Figure 12.* Sieve size arrangement and shaker for particle size analysis

**3.4.2 Bulk density.** Bulk density of the MSW samples was determined by measuring the mass of the sample filled in a 100 ml of graduated cylinder. The mass of MSW, biochar and bio-oil samples were measured by an electronic balance as shown in Figure 13



*Figure 13.* Measuring balance for weighing MSW samples and products

**3.4.3 Heating value.** A 1341 oxygen bomb calorimeter (Parr Instrument) was used to determine the calorific value of raw MSW samples, bio-oil and the bio-char from each pyrolysis process. It measures the energy released when the sample undergoes complete combustion in the presence of oxygen under a standard condition. Oxygen was connected to the unit to pressurize the bomb. Measurements were executed in dynamic mode and the calibration of the system was

performed with benzoic acid with a higher heating value (HHV) of 26 460 J/g (relative standard deviation of 0.01%).



*Figure 14.* Oxygen Bomb calorimeter for heating value determination

**3.4.4 Moisture content.** Moisture content is considered an important fuel property since it affects the combustion behavior of the fuel and also its stability. Moisture content of solid MSW and biochar was determined using the standards ASTM E 871 by measuring the weight difference after heating in oven. The moisture contents of biochar and raw feed were determined in an oven by weighing a known mass of samples in an aluminium container and placing the samples in the oven at a set temperature of 105°C for 24 hours. The difference in weight was recorded and calculated as a percentage of sample weight. These were done for all three runs of pyrolysis temperature and the average calculated. Moisture content of bio-oil was determined by the Karl-Fischer Titration method. This was accomplished by a METTLER TOLEDO T50 moisture titrator as shown in Figure following ASTM E203-96 method. In the determination, 3 drops of bio-oil sample from syringe (weighed before and after to determine the mass) was injected in the instrument and dissolved in solvent of methanol: dichloromethane at a 1: 1 ratio and a component reagent (combititrant 5) to react with the water in the bio-oil. Prior to testing, a

drift run was conducted to remove any trapped moisture in the instrument. Moisture content was reported on a percent weight of the wet bio-oil.

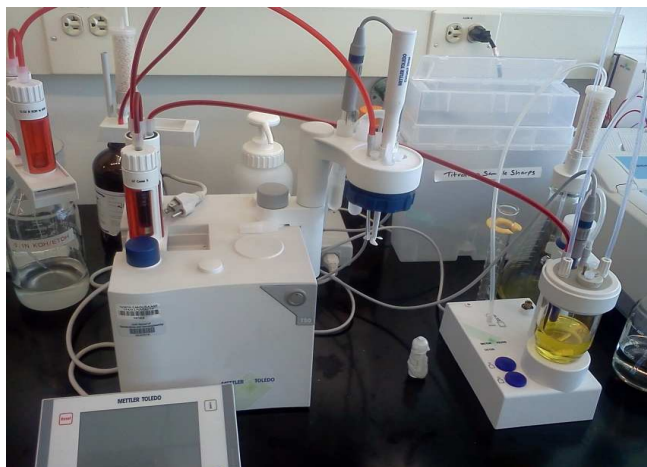


*Figure 15.* Mettler Toledo T50 for moisture content determination

### **3.5 TGA-DSC- MS Experiments**

The combination of thermogravimetric and differential scanning calorimetry analysis (SDT Q 600) coupled with mass spectrometry (DMS - Discovery mass spectrometer) (TGA–DSC-MS) can give a detailed insight of the pyrolysis process and it is reported that one of the most attractive advantage of the combination is its ability to provide real-time and sensitive detection of evolved gases [76, 84]. TGA-DSC-MS analysis of MSW samples can provide the information on thermal degradation kinetics, reaction heat and evolving gas composition. The SDT Q600 provides simultaneous measurement of weight change (TGA) and true differential heat flow (DSC) on the same sample from ambient to 1,500 °C. The TGA analysis was used to characterize MSW samples by weight loss and phase changes as a result of decomposition, dehydration, and oxidation. In this research, TGA and DSC analysis were done to achieve three objectives. In the first experiment, a TGA-DSC analysis of MSW components including paper, wood, plastics and textile were performed in nitrogen (N<sub>2</sub>) and carbon dioxide

(CO<sub>2</sub>) atmosphere to determine the caloric requirement and corresponding mass changes and the relationship of the caloric requirement with temperature using measurement results from TGA-DSC pyrolysis. The second objective was to determine the effect of heating rate on pyrolysis of MSW components in nitrogen and carbon dioxide atmosphere and also use the measurement results to determine the kinetic parameters. In the third objective, a TGA-MS (thermogravimetric- mass spectrometry) was used to study the real time analysis of evolved gases from MSW pyrolysis at different purging gas flows. Two purging gases, nitrogen (N<sub>2</sub>) and carbon dioxide (CO<sub>2</sub>) were used as sweeping gases and MS profiles were analyzed.

**3.5.1 Sample preparation.** The samples were prepared based on the constituent components of MSW obtained from household trash. MSW components were ground into maximum 1 mm particle size in a Thomas - Willey Mill. After being sieved on a vibrator for 10 min, the milled powder was collected and stored in plastic containers and labeled to be used for all TGA-DSC-MS experiments.

**3.5.2 Methodology.** In the first experimental procedure, prepared MSW samples of sizes between 0.25 mm and 1 mm were put in an alumina crucible. The furnace was initially purged to reduce the air absorbed by the powder sample. The experiment was performed from ambient temperature up to maximum temperature of 700°C at a constant heating rate of 20°C/min, 40°C/min and 60°C/min in the analyzer and the product gases were swept by a carrier gas of nitrogen or carbon dioxide at 50 ml/min. After each run, the residue char was burned in air to a final temperature of 900°C.

The second experiment was performed in TGA- MS analyzer to measure the profiles of gases evolved during pyrolysis of MSW samples. Sample sizes of MSW components with maximum weight of 3 mg for each sequence were filled in alumina crucibles of the TGA

instrument and ramped from ambient temperature to 800°C purged with nitrogen and carbon dioxide at 50 ml/min. The Discovery Mass Spectrometer (DMS) can be operated in two modes of recipe preparation; bar chart mode (which scan through all ions from 1 to 50 m/z) and peak jump mode (scan only specified ions). In this experiment, the MS recipes were prepared in a peak jump mode thereby making the scan time shorter and the confidence level of accuracy greater. Prior to performing run for each sample, a preliminary broad scan was performed at a heating rate of 20°C/min. The identified signals relates to the mass spectra of 1, 2, 12, 14,15,16,17,18, 28,32 and 44 a.m.u which corresponds to atomic hydrogen (H), hydrogen gas (H<sub>2</sub>), carbon (C), CH<sub>2</sub> group, methyl group( CH<sub>3</sub>), methane (CH<sub>4</sub>), hydroxyl (OH<sup>-</sup>), water (H<sub>2</sub>O), nitrogen (N<sub>2</sub>), oxygen (O<sub>2</sub>) and carbon dioxide (CO<sub>2</sub>), respectively.

Proximate analysis was performed on MSW components and the products obtained from pyrolysis to determine moisture content (MC), volatile matter (VM), fixed carbon (FC) and ash content. These parameters were determined in TGA shown in Figure 19 according to ASTM standards and the results are provided in Table 3 and 4 in the results section. Sample sizes for the analysis were in the range of 5- 15 mg and nitrogen gas at flow rate of 100 ml/min was used as a purge gas. During the proximate analysis, air was used to combust the remaining char in the solid residue and the mass of final ash after combustion was determined.

Elemental analysis or ultimate analysis of MSW component samples (paper, wood, plastics (PE) and textile residue) and standard samples of cellulose, hemicellulose and lignin were determined by a Perkin Elmer CHNS analyzer as shown in Figure 18. The ultimate analysis determines the weight fractions of non-mineral major elements (i.e., carbon, hydrogen, nitrogen, oxygen, and sulfur) of organic sample[85]

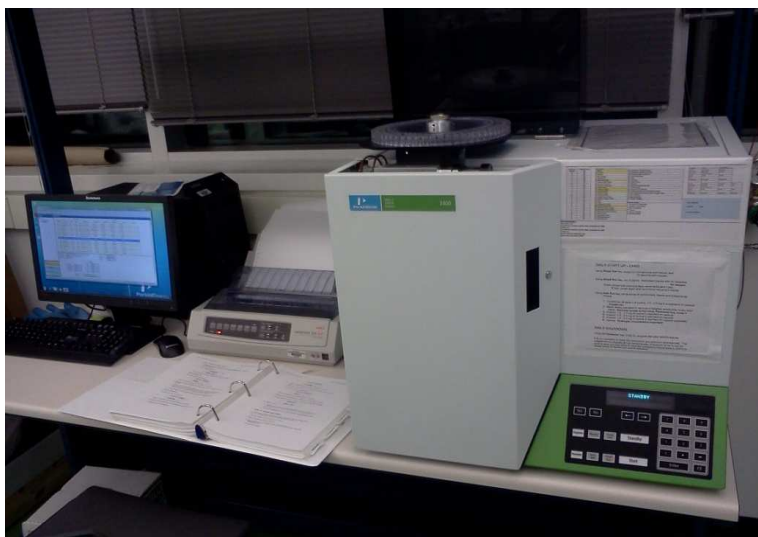


*Figure 16.* PE 2400 Elemental Analyzer (Perkin Elmer)



*Figure 17.* Thermo gravimetric- Differential Scanning Calorimetric- Mass spectrometry (TGA-DSC-MS) analyzer (TA Instrument)

## CHAPTER 4

### Aspen Plus Simulation of Pyrolysis Process

#### 4.1 Introduction

MSW contains several combustibles including biomass, paper, textile and plastics. Due to the various combustibles in MSW, MSW is a heterogeneous feedstock. The biomass mainly consist of the three types of carbohydrate polymers: lignin, cellulose and hemicellulose. The complexity of the structure of the combustibles in MSW and their reaction pathway during pyrolysis makes it somewhat difficult in determining the composition and yield of the bio-oil produced. The process is influenced by factors such as sweeping gas flow rate, heat carrier temperature, reactor temperature, vapor residence time.

The commercial software, ASPEN Plus from AspenTech, Inc., is a widely used simulation platform to analyze the mass and energy balance in a chemical engineering process. ASPEN Plus can be used to develop equilibrium process models. The equilibrium models are important to predict the highest conversion or thermal efficiency that can be possibly obtained by a given process. ASPEN Plus has abundant library models for different unit operations such as reactions, separation and heat exchange. It is also possible for users to develop their own models using FORTRAN codes nested with the ASPEN Plus input file. Another advantage of ASPEN Plus is that it has a large database for the properties of different common chemicals such as water and ethanol. Many key components such as biomass, cellulose, xylan and lignin in a biorefinery are specified as non-conventional components in ASPEN Plus. National Renewable Energy Lab (NREL), USA has defined the properties of those biomass-related components in simulation model.

Most of the work in Aspen plus simulation for the thermochemical conversion of biomass to bio-fuels have largely focused on gasification processes. Aspen plus has been used to simulate biomass gasification in fluidized bed reactor [86], optimize waste plastics gasification[87], Aspen Plus simulation of biomass integrated gasification combined cycle systems at corn ethanol plants[88] .

Pyrolysis involves the decomposition of biomass into bio-oil, biochar and gases at a temperature between 450°C to 500°C in the absence of an oxidizing agent such as air and oxygen. Factors influencing a pyrolysis process include characteristics of biomass and operating conditions of the pyrolysis process. The characteristics of biomass include its proximate and ultimate analyses, heating value, particle size distribution and bulk density. In overall thermochemical conversion processes, different stages are considered in Aspen plus simulation and these stages occur in the order as follows [86];

- Decomposition of the feedstock
- Volatile reactions
- Char combustion
- Condensable gas-noncondensable gas separation
- Gas-solid separation

Decomposition of MSW feedstock is a thermochemical degradation process. When this process occurs in the absence of an oxidizing agent, it is termed as pyrolysis. Pyrolysis or devolatilization involves a series of complex physical and chemical processes [89]. Pyrolysis is initiated at about 230 °C when thermally unstable components and volatiles in a feedstock are broken down and evaporated with other volatile components. Pyrolysis yields char, tar and light

gases like  $H_2$ ,  $CO$ ,  $CH_4$ . The yield and composition of the products evolved is a function of the temperature, pressure and gas composition during the devolatilization [89].

## 4.2 Model Development

The model used to investigate the simulation of pyrolysis of MSW to bio-oil is based on a model previously developed by Philips et al (2007) (NREL) and Yan et al (1999). The modification to this process involved the following three main assumptions:

1. The yield of bio-oil and char from the pyrolysis reactor are based on the experimental data on the fixed bed pyrolysis of the MSW combustibles (paper, wood and textile). The primary component of the gas were assumed to consist of  $CO$ ,  $CO_2$ ,  $CH_4$  and  $H_2$
2. The pyrolysis process was modeled by Ryield reactor and the bio-oil was represented by a mixture of  $C_{10}H_{12}O_4$  and  $C_6H_6$  and
3. The condensation of the hot volatile gases from the pyrolysis was first assumed to be cooled in a heat exchanger and then separated into two outlet streams (non condensable gas and bio-oil) in a separator modeled as FLASH

## 4.3 Physical Property Method

The thermo-physical properties of all conventional components such as  $CO$ ,  $CO_2$  and  $C_6H_6$  in the pyrolysis process were estimated by the Peng Robinson (PENG-ROB) and Redlick Kwong Suave (RKS) equation of state with Boston-Mathias alpha function (PR-BM, RKS-BM). The enthalpy and density models used for non conventional components such as paper, wood and textile are HCOALGEN and DCOALIGT.

## 4.4 Aspen Simulation Flowsheet

In this simulation, the MSW feedstock was assumed to consist of a mixture of paper, wood, textile. It was assumed to be predried from an initial moisture of 50% and controlled at a

moisture content of 10 % before conveyed to the decomposers modeled as three Ryield reactors ( RYLD 1 – 4) with operating temperature varied between 400°C to 700°C. Since MSW is a heterogeneous feedstock, the three main combustibles used in the experiment including paper, wood and textile were decomposed separately in three (RYLD) library model blocks in ASPEN to represent each combustible component of MSW. In the yield calculation for oil, non condensable gases and char, four fortran sub-routines were used to determine the yield of products for each MSW component using polynomial equations (Equations 2 to 9) obtained by correlating the experimental data from the tubular reactor pyrolysis experiment to calculate the temperature-dependent ( $400^{\circ}\text{C} \leq T \leq 700^{\circ}\text{C}$ ) yields of oil and char. The correlation for the plastic was obtained from pyrolysis in TGA in nitrogen atmosphere at each temperatures from 300oC to 700oC to determine the yield of volatiles and char. The equations for the noncondensable gases were correlated from data for CO, CO<sub>2</sub>, CH<sub>4</sub>, C<sub>2</sub>H<sub>2</sub>, C<sub>2</sub>H<sub>4</sub>, C<sub>2</sub>H<sub>6</sub> and H<sub>2</sub> provided in (Equations 8 to 14) and were assumed to be the major components of the noncondensable gaseous stream for the pyrolysis of each MSW component.

Wood:

$$Y_{oil,w} = -46.650 + 0.2820 T - 1.01 \times 10^{-5} T^2 \quad (2)$$

$$Y_{char,w} = 175.03 - 0.4490 T + 1.17 \times 10^{-5} T^2 \quad (3)$$

Paper

$$Y_{oil,p} = -71.090 + 0.4010 T - 1.51 \times 10^{-5} T^2 \quad (4)$$

$$Y_{char,p} = 154.62 - 0.3830 T + 1.70 \times 10^{-5} T^2 \quad (5)$$

Textile

$$Y_{oil,T} = -71.150 + 0.3870 T - 1.20 \times 10^{-5} T^2 \quad (6)$$

$$Y_{char,T} = 189.31 - 0.5110 T + 1.06 \times 10^{-5} T^2 \quad (7)$$

$$Y_{oil,plastic} = -255 + 1.014 T - 1.91 \times 10^{-5} T^2 \quad (8)$$

$$Y_{char,plastic} = -255 + 1.014 T - 1.91 \times 10^{-5} T^2 \quad (9)$$

Non condensable gases

$$CO : Y_{CO} = 133.46 - 0.1029T + 2.08 \times 10^{-5} T^2 \quad (10)$$

$$CO_2 : Y_{CO_2} = -9.5251 + 0.0378 T - 1.49 \times 10^{-5} T^2 \quad (11)$$

$$CH_4 : Y_{CH_4} = -13.82 + 0.0442 T - 1.61 \times 10^{-5} T^2 \quad (12)$$

$$H_2 : Y_{H_2} = -17.99 + 0.0264 T - 1.89 \times 10^{-5} T^2 \quad (13)$$

$$C_2H_2 : Y_{C_2H_2} = -4.3114 + 5.4499 \times 10^{-3} T - 1.56 \times 10^{-6} T^2 \quad (14)$$

$$C_2H_4 : Y_{C_2H_4} = -38.25 + 0.058435 \times 10^{-3} T - 1.98 \times 10^{-5} T^2 \quad (15)$$

$$C_2H_6 : Y_{C_2H_6} = 11.11 - 0.01166 \times 10^{-3} T - 3.06 \times 10^{-6} T^2 \quad (16)$$

where  $Y_i$  is the yields of pyrolysis products (kg/kg MSW component) and T is in °C. From the experiments the maximum yield of oil was at 600°C for the pyrolysis of MSW components. The oil yield declines with the increase in temperature due to the secondary decomposition of the tar vapors at high temperatures.

#### 4.5 Simulation Procedure

The simulation was started with the MSW with an initial 50% of moisture fed into a DRYER in which the operating temperature was maintained at 200°C. The energy required in the dryer is supplied by the hot flue gas from a combustor. From the drier, the exiting stream was assumed to be split into four components of MSW namely paper, wood, textile and plastic and fed into PYROLYZERS (RYLD1 -4) modeled as Ryield reactors. From the four Ryield reactors the volatile stream from each MSW component decomposition were combined in a MIXER . The char component were removed from the volatile stream in an aspen SEPARATOR block and

sent to char combustor simulated in RSTOIC reactor block. The yields of oil, major components in the pyrolysis gas and char in the pyrolyser were temperature-dependent. The pyrolysis product from the pyrolyzer is a mixture of char, and gas that consists of light noncondensable gases and heavy condensable hydrocarbons. The pyrolysis product went through the solid-gas separator to separate the char from the gas. The gas was further separated into two streams through a condensation process: condensable bio-oil and noncondensable syngas. The gas-gas separation was modelled by a heat exchanger to cool down the hot gas and a flasher (FLASH) to obtain the final oil product (BIO-OIL) and the non-condensable gas (NCG).

The separated char went to a combustor (CHARCOMB) modeled as an equilibrium reactor in which all the combustible components were assumed to be burned out. The process flow of the simulation is shown in Figure 18.

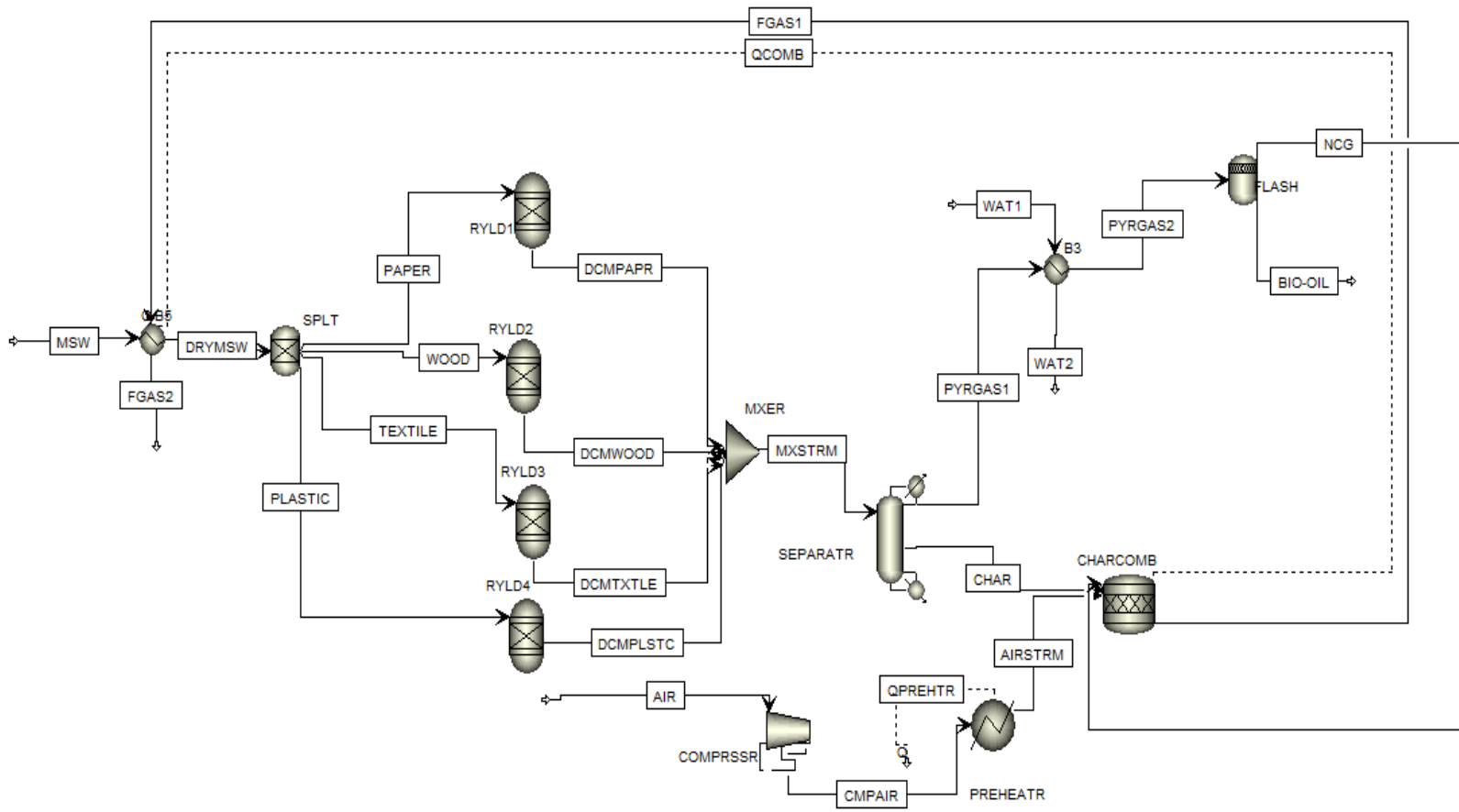


Figure 18. Process flow diagram of MSW pyrolysis process in Aspen plus

## CHAPTER 5

### Economic Assessment of MSW Pyrolysis

#### 5.1 Methodology

Economic feasibility of pyrolysis of MSW to bio-oil and bio-char is essential in order to utilize the technology on a commercial basis. In the techno-economic analysis of the process, a technical aspect is coupled with an economic aspect of the process to analyze its economic viability. Firstly, the theoretical underpinning of the process was developed into a process configuration and a material and energy balance was performed. The second step was the cost estimation based on the capital investment and production cost of biofuel products from the pyrolysis process.

Process modeling is accomplished by employing Aspen plus software to conduct mass and energy calculations. Assumptions and operating conditions were taken from literature and experimental data available. In this study, major assumptions were made from experimental and literature sources for MSW pyrolysis and gasification studies [2, 90, 91].

**5.1.1 Operating cost.** It includes raw material cost and the variable operating cost of production of pyrolysis products.

**5.1.1.1 MSW preparation.** MSW is a heterogeneous mixture of household waste, industrial/trade waste, sewage sludge and biomass waste. These sometimes contain large quantities of components which are considered as not having calorific value and therefore must be segregated and removed from the hydrocarbon sources. These “non-energy” components include metals, glass, stones and sand which form part of the MSW resource.

Refuse derived fuel or process engineered fuel covers a wide range of waste materials which have been processed to fulfill guideline, regulatory or industry specifications mainly to

achieve a high calorific value. The preparation of the MSW is assumed to consist of a number of processes to pretreat the MSW before feeding it to a pyrolyzer and they include separation at source, sorting or mechanical separation, size reduction (shredding, chipping and milling), separation and screening, blending, drying and pelletizing and storage. The quantity of RDF produced per ton of MSW varies depending on the type of collection, treatment process and the quality requirement and it is estimated that the yield ranged between 55% to 85%.

**5.1.1.2 Size reduction.** Grinding and milling is an energy intensive and expensive process and it is estimated to add about \$11/MT of biomass and this depends on the specific energy requirement which varies with the type of equipment and feedstock condition [92]. In some instances, a common assumption is that 50 kWh of energy is required per ton of ground biomass. Research showed that different equipment employed in size reduction presents a number of advantages and disadvantages in their use. For example, hammer mill is reported to employ various screen sizes and work well with friable materials like fiber, and they require minimal maintenance cost. On the other hand, it has a disadvantage of generating excessive noise and pollution and is less efficient compared to roller mill and other grinders.

**5.1.1.3 Drying.** MSW is generated from various household sources and may vary widely in moisture content. Moisture in the MSW consumes process heat and contributes to lower process yield. Drying is therefore considered an important stage in the production process. The average moisture content of MSW sample is reported at 44.3 wt % on wet basis. The recommended moisture content for optimum pyrolysis yield should be less than 7 wt.% [28].

Dryers can be generally classified as direct or indirect based on the mode of application of the heat. Direct drying involves contact between the heating medium and the feed; the

medium can be air or superheated steam. In most commercial dryers, heated air or process gas is employed to dry the feed.

The energy consumption for drying ( $Q_{\text{drying}}$ ) of MSW was calculated using Equation 20:

$$Q_{\text{drying}} = M_{\text{msw}} \times W \times [(C_{p_{\text{water}}} \times \Delta T) + \Delta H_{\text{vap}}] + [M_{\text{msw}} \times (1 - W)] \times C_{p_{\text{msw}}} \times \Delta T \quad (20)$$

where,  $M_{\text{msw}}$  is unit mass of MSW on wet basis, kg,  $W$  is moisture content of MSW,  $H_{\text{vap}}$  is latent heat of vaporization for water (2090 kJ/kg),  $C_{p_{\text{water}}}$  is heat capacity of water (4.2 kJ/kg°C),  $C_{p_{\text{msw}}}$  is heat capacity of MSW combustibles,  $\Delta T$  is the temperature difference between initial and 105°C.

It is important to note that the heat capacities of MSW components may vary due to the chemical composition of the components. Since MSW is mixture of combustible organic fractions, the total heat capacity is estimated by accounting for the weight percentage in the MSW. Heat capacities increase with increasing temperature and therefore the value at 500°C will be about 15% higher than the experimental value at 25°C [93]. DSC curves for the MSW components are shown in Figure 40. It indicates that the heating process is in the endothermic domain of heat requirement

**5.1.1.4 Pyrolysis.** Fast pyrolysis is a thermal process that requires temperatures near 500°C, rapid heat transfer and low residence time. As previously discussed in the literature review section, various reactor design and configurations have been proposed for the process. Most of the research on MSW pyrolysis have been done on a laboratory scale and there are no sufficient data on the commercial viability of the process [2, 13]. However, it is important to highlight the commercial studies on biomass pyrolysis currently being pursued by different researchers [90]. The scalability of these reactor designs have been reported as the major

concerns in the commercialization and therefore in this study an assumption of smaller scales in parallel are employed. Commercial units as large as 200MT/day are currently in operation. Pyrolysis product distribution is adapted from simulation results obtained from Aspen plus software for bio-oil and noncondensable. Bio-oil compounds are selected based on available Aspen plus software compounds and may not share the same properties of actual experimental compound data published in literatures.

There were two components considered in the calculation of energy consumption for pyrolysis. The first component is the heating of the dried MSW components to temperature at which pyrolysis occurs and the second component is the energy consumed during pyrolysis reaction. The first component can be calculated by using Equation 21.

$$Q_{target} = M_{dmsw} \times C_{p\ msw} \times \Delta T \quad (21)$$

where,  $Q_{target}$  is the energy consumption to heat the dried MSW to the temperature at which pyrolysis occurs,  $M_{dmsw}$  is mass of dried MSW sample,  $C_{p\ msw}$  is the average heat capacity for dried MSW and  $\Delta T$  is temperature difference between pyrolysis starting temperature and 105°C.

The second component was the heat of reaction which is clearly in the domain of heat requirement. From the DSC curves, integration of these heat fluxes over time gives the total heat requirement as a function of temperature (Equation 22). With the first term of the equation being the heat required to reach pyrolysis temperature and the second term being the devolatilization heat. It is important to note that the precise measurement of heat of reaction for each MSW component requires rigorous experimental work.

$$\frac{dC}{dt} = C_p \frac{dT}{dt} + \Delta H_r \rightarrow C = \int_0^t \left( C_p \frac{dT}{dt} + \Delta H_r \right) dt \quad (22)$$

The total energy consumption ( $Q_{total}$ ) for the pyrolysis is calculated by Equation 23

$$Q_{total} = Q_{drying} + Q_{target} + Q_{pyrolysis} \quad (23)$$

**5.1.1.5 Volatile gas cleaning.** Hot pyrolysis gases from process reactor contain entrained particles of char of various sizes and in some cases fine sand particles when it is used as heat carrier in the reactor. The particle sizes of these entrained solids are very important because it affects the design and performance of the cleaning equipment such as cyclones and filters. It is assumed that a set of parallel cyclones are employed to remove 90% of entrained char particles. The char collected is sent to the combustion section where it is employed to provide process heat.

**5.1.1.6 Bio-oil collection.** The bio-oil collection system is an important part of the entire process since it affects the quality and yield of the oil. In order to collect high quality and increased yield of oil, the vapors must be condensed within fractions of a second after exiting the reactor. Longer residence time allows secondary reaction to take place in the gas phase and reduces the quantity of the oil collected. To achieve this, an indirect heat exchanger is employed to transfer heat from the vapors to water stream. It has been reported that staged condensation of bio-oil allows for the collection of oil fractions with good quality and in this process, the condensation of most of the water is done in one condenser and oil fractions are allowed to condense in a different condenser [28]. After most of the oil is condensed, an electrostatic precipitator (ESP) unit collects remaining droplets using high voltage charges [46]. It is assumed that any remaining char entrained in the vapor is collected in the ESP unit.

Non condensable gases including methane and hydrogen are sent to the combustor to provide heat for drying the MSW feedstock.

**5.1.1.7 Storage.** Bio-oil and char are collected in the storage section, which must store up products in reasonable time. Bio-oil storage equipment must be made of stainless steel material to prevent corrosion from bio-oil acids. Char contains volatile material and when handled

improperly can pose a fire hazard. Furthermore, the small size of char particles poses an inhalation hazard for people handling the material. Biochar was used as fuel in combustion to recover energy for the drying and pyrolysis process.

Biochar contains carbon from the waste biomass and it is permanently sequestered in the soil when applied as soil conditioner thereby effectively removing that carbon in the atmosphere. It has been shown that carbon in a ton of biochar is equivalent to 3 to 3.5 tons of CO<sub>2</sub>. Another significant economic value of biochar is its use as effective soil conditioner thereby increasing productivity and yield [39].

**5.1.2 The Capital cost.** The capital cost of a plant is expressed as the Total Plant Cost (TPC); that is all the costs that an owner would pay to have the plant designed, built and commissioned excluding site purchase, ground clearance, site access and consenting costs [90]. These exclusions are considered to be functions of the specific site rather than the technology employed.

The equipment cost can be estimated by employing Aspen Icarus software or by referencing from equipment suppliers. Some equipment cost estimate are available from surveys of potential suppliers of equipment which have been used to produce a sizing curve for pyrolysis plant which consist of the pyrolysis system and oil recovery unit. This curve have been updated to 2009 prices and a number of researches have proved its validity [66].

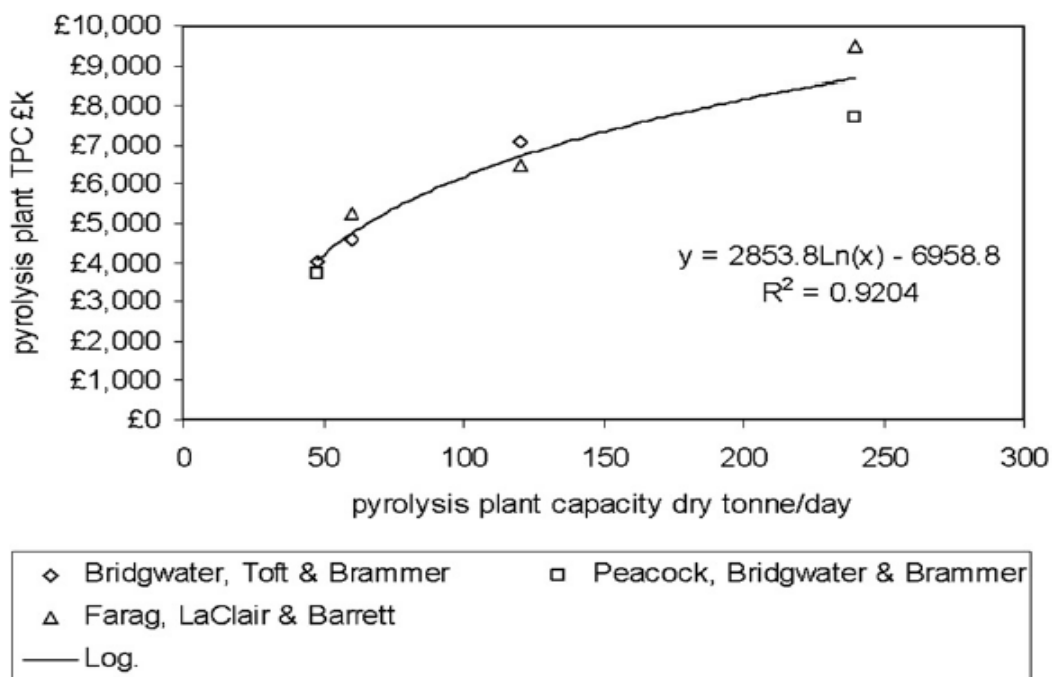


Figure 19. Pyrolysis plant cost (pyrolysis and oil recovery system) [90]

The investment cost of a pyrolysis reactor can be calculated on the basis of the hourly mass flow rate in oven dry ton of MSW per hour ( $\emptyset$  in our case considering  $1.0 \text{ odth}^{-1}$ ) of dried and grinded MSW fed into the reactor given that the reactor is operational during 80% or seven thousand hours (7000 h) per year.

The investment includes a feeding system, the pyrolysis reactor, a liquids recovery system and a storage unit for the pyrolysis oil. The costs concern basic equipment and buildings plus costs for construction and commissioning. A regression model (Equation 24) developed by Bridgewater et al., 2002)[94] is useful in estimating the investment cost of pyrolysis system

$$I_{pyrolysis} = 4.0804 \times 10^4 \times (\emptyset \times 10^3)^{0.6194} + 1.19 \times 10^5 \times (0.7\emptyset)^{0.4045} \quad (24)$$

Following the model proposed by Bridgewater et al, 2002, a more rigorous model (Equation 25) [95] which reflects the results of regression analysis of 13 data points found in literature with an R squared value of 0.957 ( perfectly linear relation) was employed.

$$I_{pyrolysis} = (1.906 + 0.598 \times \phi)^1 \times 10^6 \quad (25)$$

The total initial investment of the pyrolysis reactor system ( including biomass feeding system , product recovery and flue gas treatment) amounts to about 4.5M USD for a 1 odth<sup>-1</sup> of biomass.

The annual capital cost was determine by

$$A = P \times \frac{i(1+i)^n}{(1+i)^n - 1} \quad (26)$$

where P is the total initial capital investment, A is annual capital cost, I is the interest of the capital money, n is the life of the plant.

**5.1.3 Other operating costs.** Other operating costs include the personnel costs and maintenance costs. The annual maintenance cost is usually calculated as a given percentage of capital investment (e.g., 1.5%). It is assumed that the plant requires 3 staffs to operate the facility.

## CHAPTER 6

### Results and Discussion

#### 6.1 Introduction

This chapter presents and discusses results obtained from the fixed bed pyrolysis, the results of pyrolysis conducted in the TGA-DSC-MS instrument for the selected MSW components and finally discussed the simulation results from Aspen plus. In the fixed bed pyrolysis, the discussion includes product distribution variations for all the pyrolysis temperature investigated in the experiment. Additionally, thermo- physical and thermo-chemical analysis of products for all pyrolysis temperatures was presented and correlations between temperature and the thermal and physical properties were drawn using regression analysis. Another part of the discussion was the TGA-DSC profiles of MSW components.

#### 6.2 Particle Size Distribution of MSW Components used for the Pyrolysis Process

The wood component sieve analysis accumulated a median size diameter between 0.3 mm to 0.6 mm corresponding to 56 wt.% and paper fraction in the MSW component also recorded a median particle diameter between 0.3 mm to 0.6 mm at cumulative amount of 38 wt %. The textile fraction was not analyzed through the sieves due to its linty texture but was however assumed to be less than 0.1 mm average

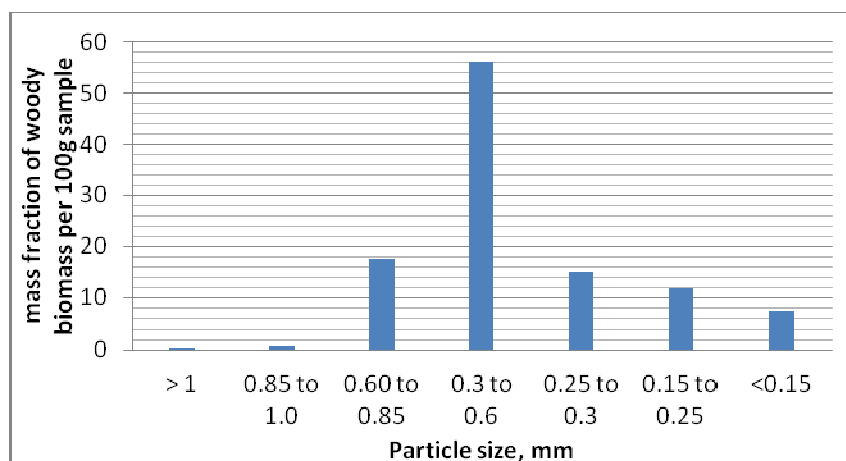


Figure 20. Particle size distribution of wood biomass

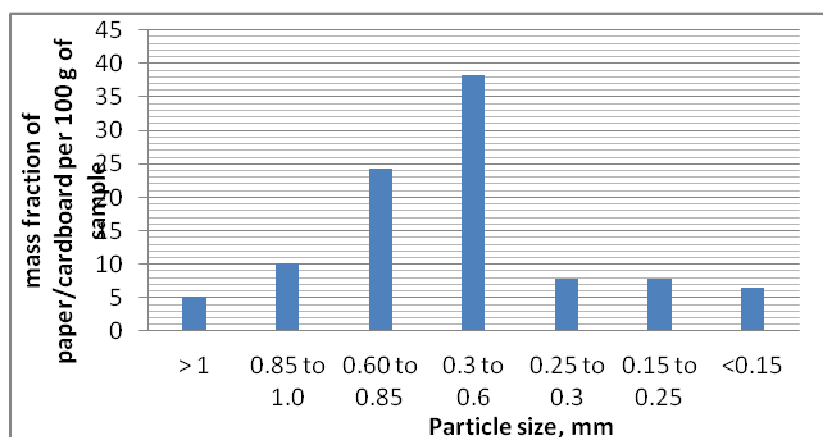


Figure 21. Particle size distribution of paper

### 6.3 Product Distribution

As explained in the objective of this research, physical and chemical properties of biochar and bio-oil vary with pyrolysis temperature. However, before discussing how temperature affects these properties, it is important to study the yield spectrum within this broad temperature range. The study was conducted in the fixed bed reactor at a temperature from 100°C to 800°C and nitrogen gas at a flow rate of 50 ml/min was used to purge the products out of the reactor. The bio-oil was collected in three numbered plastic bottles fitted with a stopper and connected together in sequence. The product recovery set up was buried in ice cubes contained in an ice

chest. The following data are expressed as the averages of the values that were obtained from replicate measurements. At least three runs were conducted for each experimental condition and at least triplicate measurements were taken for each of the responses. The yields of bio-oil and biochar at different pyrolysis temperatures were shown in Figures 20 and 21. The graphs represents the yield of bio-oil and biochar on the vertical axis and pyrolysis temperature on the horizontal axis. The yields of volatiles or bio-oil that were condensed and collected at the pyrolysis temperature of 300°C were 12.0 wt%, 16.3 wt% and 19.73 wt % ( wet basis) for textile, paper and wood respectively. The maximum yields of bio-oil were 52.5wt% (wb) for textile obtained at 700°C, 57.4 wt% (wb) for paper obtained at of 600°C and 64.9 wt % ( wb) for wood obtained at temperature of 500°C. From the ANOVA analysis, at 95% confidence interval, the pyrolysis operating temperature within the range of 300°C to 700°C plays a significant role ( p-value =0.002) role in the bio-oil production from the MSW components under study.

**6.3.1 Effect of temperature.** Bio-oil and biochar yields on wet basis versus temperature are illustrated in Figure 20 and Figure 21 respectively. For the pyrolysis temperature from 300°C to 800°C, the oil yields (on a wet basis) were from 16.3% to 64.9% for wood, 19.7% to 57.4% for paper and 12% to 52.8% for textile, respectively. The yield of bio-oil from the pyrolysis of paper continuously increased with the temperature up to 600°C and then decreased with the the further increase of temperature to 800°C, while the yield of bio-oil from the wood pyrolysis increased steadily over the temperature range between 300°C and 500°C, and sharply declined with the further increase in temperature up to 600°C and then increased steadily again to 800°C. Textile showed yield characteristics similar to wood , however, it increased from 300oC to 400oC and declined at 500oC and then increased slightly from 600oC to 700oC with the

optimum yield of oil 700°C. The results indicated that optimum oil yield from the MSW components were recorded at temperatures between 500°C and 700°C

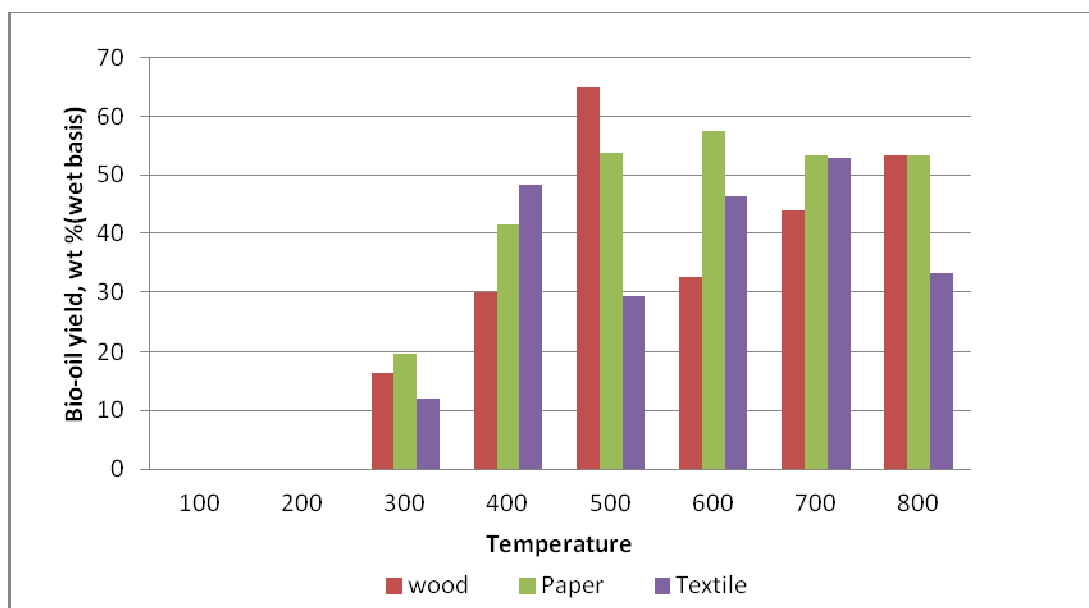


*Figure 22.* Effect of temperature on oil yield for three MSW components

Biochar yields for MSW components under study versus pyrolysis temperature are presented in Figure 21. The char yields generally decreased with increasing temperature because increased quantities of volatiles from the samples were converted to oil and non condensable gases (NCG). The char yields for all three MSW components were marked by slight variations over all temperatures. For the pyrolysis temperature from 300°C to 800°C, the char yields were between 21.8 and 72.2 wt% ( wet basis) for wood, 23.3 and 68.2 wt% ( wet basis) for paper and 22.6 and 74.2 wt % (wet basis) for textile, respectively

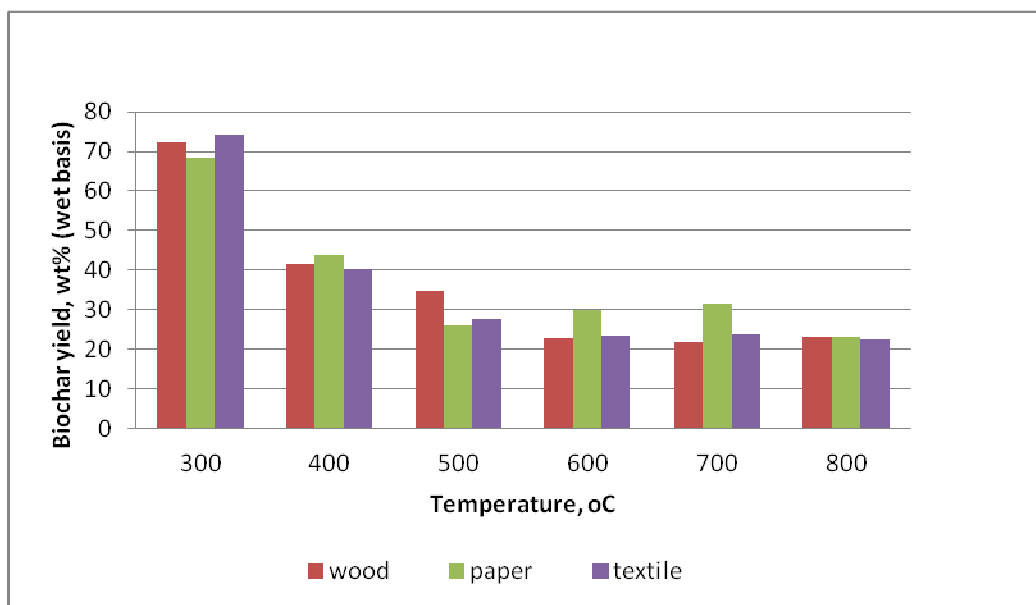


Figure 23. Effect of temperature on biochar yield for MSW samples

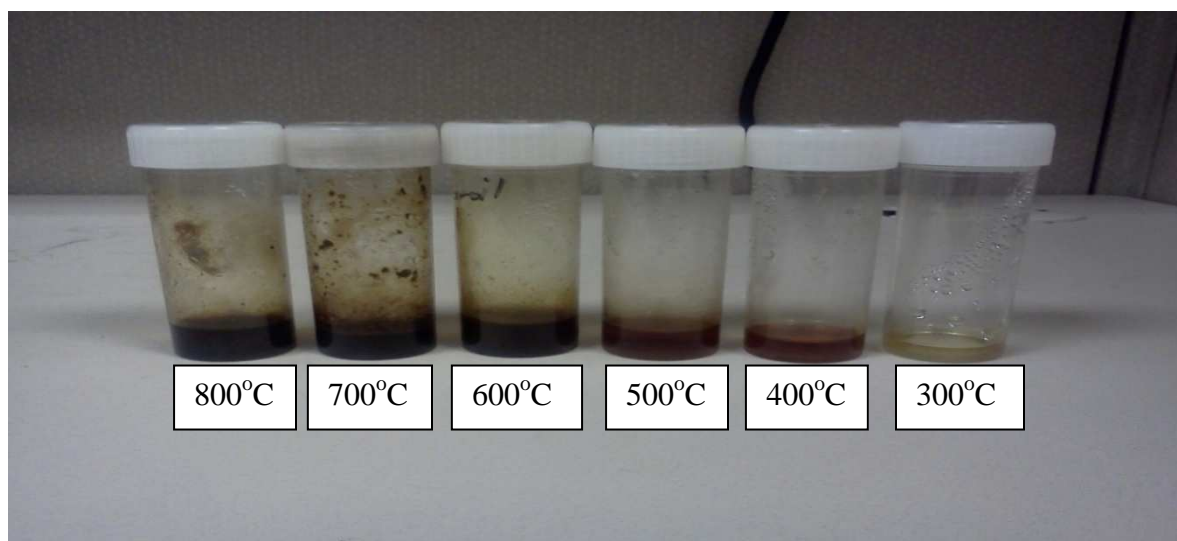
#### 6.4 Product Analysis

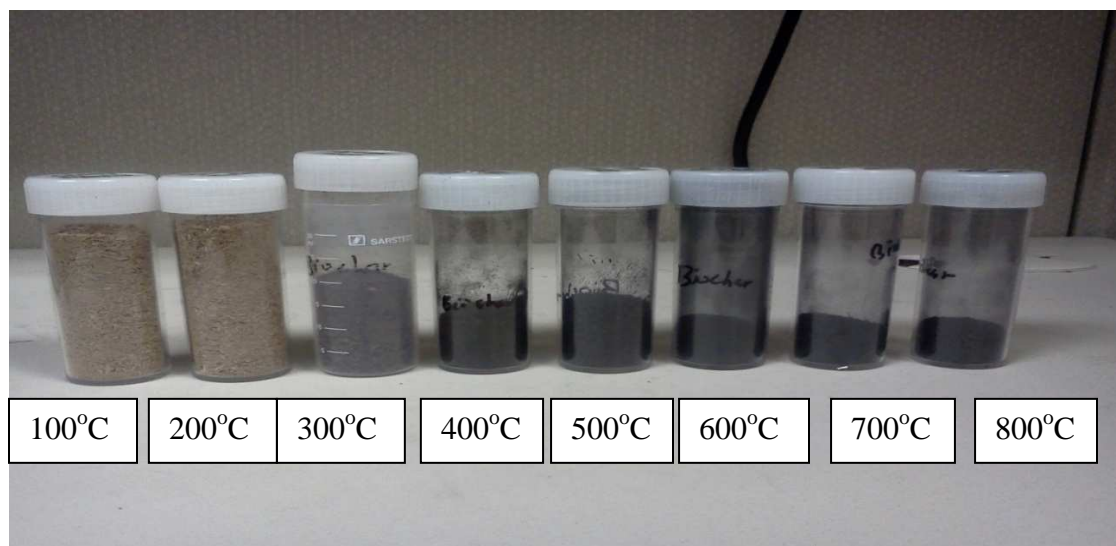
Various physical and chemical properties of the biochar and bio-oil samples that were collected at each pyrolysis temperature from 300°C to 800°C were characterized to analyze the effects of the pyrolysis temperature on the properties of biochar and bio-oil. The appearance and color of bio-oil representing pyrolysis temperature from 800°C to 300°C are shown in Figures 22. Additionally, the colors of oil collected at a temperature from 600°C to 800°C were darker and viscous than oil collected at 500°C and 400°C. The bio-oil has two parts of light aqueous and heavy oil fractions. At lower temperatures (300°C), the oil is mostly the light fraction with approximately 73.3 wt%, 77 wt% and 74.8 wt.% overall aqueous content for textile, paper and wood respectively. With the increase of pyrolysis temperatures, the proportion of heavy oil fraction increased. The phase composition of bio-oil is shown in Table 3. A sample of biochar collected at all the pyrolysis temperatures are shown in Figure 20. The physical appearance of biochar samples collected at different pyrolysis temperature shows the differences in texture and color.

Table 2

*Phase composition of bio-oil and water content*

Temperature	Phase (wt.%) Paper		Water (wt.%)	Phase (wt.%) Wood		Water (wt.%)	Phase (wt.%) Textile		Water ( wt.%)
	Aqueous	Tar		Aqueous	Tar		Aqueous	Tar	
300	77.06	22.94	72.2	74.81	25.19	68.2	73.30	26.7	68.5
400	72.32	27.68	64.4	74.56	25.44	62.4	73.10	26.9	60.3
500	64.64	35.36	54.1	56.72	43.28	62.6	70.15	29.85	60.1
600	65.11	34.89	52.9	43.86	56.14	52.3	67.43	32.57	61.1
700	66.03	33.97	49.3	60.80	39.2	49.0	71.78	28.22	45.8
800	70.21	29.79	50.3	63.68	36.32	48.7	71.88	28.12	40.1

*Figure 24. Samples of bio-oil obtained at different temperatures*



*Figure 25.* Samples of biochar of MSW at different temperatures

**6.4.1 High Heating Value (HHV)** The values of biochar obtained for all MSW components increased steadily with temperature. The HHVs were from 17.7MJ/kg at 100oC to 31.2 MJ/kg at 800oC for wood, 15.2MJ/kg at 100oC to 21.3MJ/kg at 800oC for paper and 15.8MJ/kg at 300oC to 27.2 MJ/kg at 800oC for textile. It is noted that textile was not pyrolyzed at 100oC and 200oC because of difficulty in collecting the biochar from the tubular reactor at these temperatures. Wood component had higher calorific values at all temperatures than paper and textile, which was consistent with the volatile matter content for the MSW components.

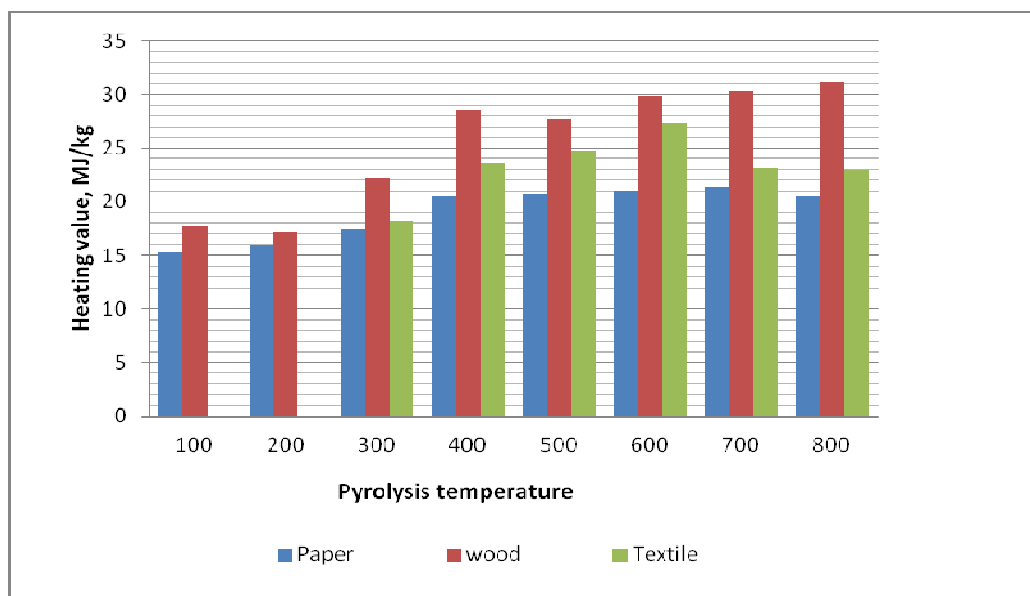


*Figure 26.* Heating value of biochar from MSW components from fixed bed pyrolysis at different temperatures

**6.4.2 Moisture content.** Moisture content of raw MSW components and biochar from fixed bed pyrolysis were determined in oven by heating at 105°C for 24 h and was compared with the moisture content obtained from pyrolysis in TGA analyzer. The average values of moisture content of MSW obtained on wet basis for paper, wood and textile were 9.3 wt.%, 7.2 wt.% and 4.5 wt.%, respectively. The average values obtained from biochar samples collected at different temperatures ranged from 3.3 wt.% (wb) to 5.2 wt.%(wb) for paper, 0.5 wt.%(wb) to 4.3wt.%(wb) for textile and 3.8 wt.%(wb) to 5.0 wt.% for wood

**6.4.3 Volatile matter (VM).** During the process of heating of the biomass, the further increase of temperature after the removal of moisture leads to the progressive release of pyrolytic products. These volatiles are produced from thermal cleavage of chemical bonds which are cellulose, hemicelluloses and lignin. The values of volatile content obtained from biochar from pyrolysis of MSW components increased with temperature from 300°C to 800°C.

Table 3

*Proximate analysis of MSW biochar from fixed bed pyrolysis at different temperatures*

	Pyrolysis temperature (°C)					
	300	400	500	600	700	800
<b>Moisture content (wt%)</b>						
Paper	5.2	4.8	5.0	4.4	3.3	4.4
Wood	4.0	5.0	5.0	4.5	3.8	4.3
Textile	0.9	4.3	3.6	0.5	1.3	1.5
<b>Volatile Matter (VM) (wt.%)</b>						
Paper	75.1	50.7	31.6	22.0	17.4	17.5
Wood	83.7	40.4	39.2	26.5	22.1	21.8
Textile	85.6	46.9	18.9	10.6	10.3	11.52
<b>Fixed carbon (FC)</b>						
Paper	15.7	27.4	43.5	55.7	61.3	60.8
Wood	12.3	50.8	52.0	72.5	85.4	83.1
Textile	11.1	44.0	70.8	74.3	76.5	74.7

Table 4

*Proximate and Ultimate analysis of raw MSW components before pyrolysis*

Item	Paper	Textile	Wood
<b>Proximate analysis</b>			
Moisture	6.29	4.25	6.57
Volatile	65.62	69.75	73.43
Fixed carbon	21.83	7.12	17.81
Ash	6.26	18.88	2.11
<b>Ultimate analysis</b>			
Carbon	46.0	43.8	45.9
Hydrogen	6.60	6.10	6.67
Nitrogen	1.20	3.5	3.63
Oxygen *	45.89	46.2	43.53
Sulfur	0.31	0.30	0.60

\* calculated from the difference

## **6.5 Elemental Composition of Biochar and Bio-oil from MSW Pyrolysis at different temperatures**

**6.5.1 Biochar.** Carbon, hydrogen and nitrogen were determined from an elemental analyzer operated in the CHN mode. Results obtained for biochar generated from MSW components generally showed an increase in carbon and hydrogen content with the increase in pyrolysis temperature while oxygen and nitrogen decreased with the temperature. Paper increased in carbon content from 41.7 wt.% (wb) at 100°C to 58.8 wt.% (wb) at 700°C with hydrogen decreasing from 6.1 wt.% (wb) at 100°C to 0.20 wt.% (wb) at 700°C and oxygen

decreased from 53.57 wt.% (wb) at 200oC to 40.03 wt.% (wb) at 700oC as shown in Figure 25. Wood biochar increased in carbon content from 45.4 wt.% (wb) at 100°C to 84.4 wt.% (wb) at 700°C, hydrogen content decreased from 5.4 wt.% (wb) to 0.8 wt.% (wb), oxygen decreased from 49.43 wt.% (wb) at 200oC to 13.73 wt.% (wb) at 700oC and nitrogen increased from 0.4 wt.% (wb) to 1.0 wt.% (wb) as shown in Figure 27. Textile showed relatively high nitrogen content which increased from 2.6 wt.%(wb) at 300°C to 4.3 wt.% (wb) at 800°C. Carbon content increased from 60.5 wt.% (wb) at 300°C to 74.2 wt.% (wb) at 800°C while hydrogen content decreased from 3.9 wt.% (wb) at 300°C to 0.12 wt.% (wb) at 800°C and oxygen content decreased from 32.83 wt.% (wb) to 25.1 wt.% (wb) as shown in Figure 26

Table 5

*Elemental composition of biochar from paper pyrolysis at different temperatures*

	T-100	T-200	T-300	T-400	T-500	T-600	T-700	T-800
Carbon	41.71	40.83	43.22	53.65	55.94	56.75	58.86	54.04
Hydrogen	6.10	5.12	4.97	4.17	2.51	0.88	0.19	0.62
Nitrogen	0.50	0.48	0.55	0.65	0.72	0.91	0.92	0.59
Oxygen	51.69	53.57	51.26	41.53	40.83	41.46	40.03	55.25

Table 6

*Elemental composition of biochar from wood pyrolysis at different temperatures*

	T-100	T-200	T-300	T-400	T-500	T-600	T-700	T-800
Carbon	45.48	44.67	50.96	65.28	66.19	78.74	84.42	83.09
Hydrogen	5.37	5.45	4.35	3.07	3.23	1.49	0.82	1.09
Nitrogen	0.41	0.45	0.73	0.83	0.47	0.54	1.03	0.90
Oxygen	48.74	49.43	43.96	30.82	30.11	19.23	13.73	14.92

Table 7

*Elemental composition of biochar from textile pyrolysis at different temperatures*

	T-300	T-400	T-500	T-600	T-700	T-800
Carbon	60.55	62.82	70.47	75.90	70.50	74.20
Hydrogen	3.95	3.27	2.54	0.43	0.13	0.12
Nitrogen	2.67	3.93	7.13	5.80	4.27	4.29
Oxygen	32.83	29.98	19.86	17.87	25.1	21.39

Note: Textile was not pyrolyzed at 100oC and 200oC

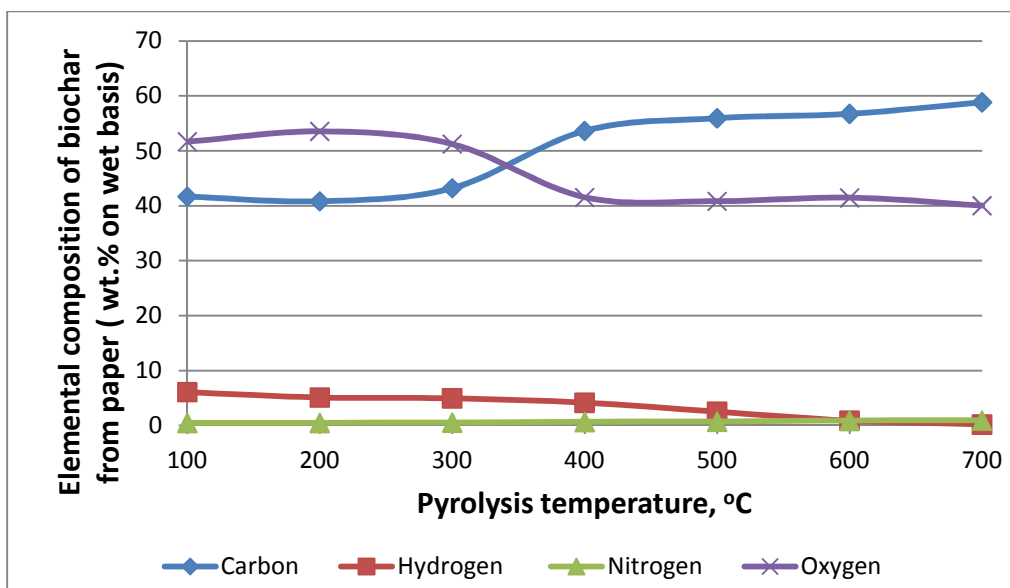


Figure 27. Elemental composition of biochar fraction of paper pyrolysis

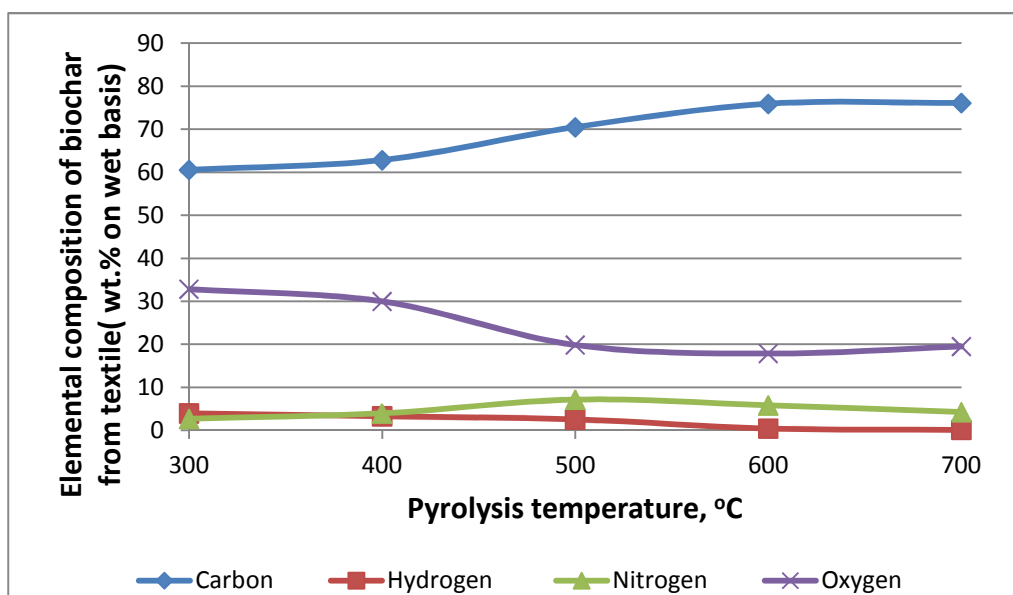


Figure 28. Elemental composition of biochar fraction from textile pyrolysis

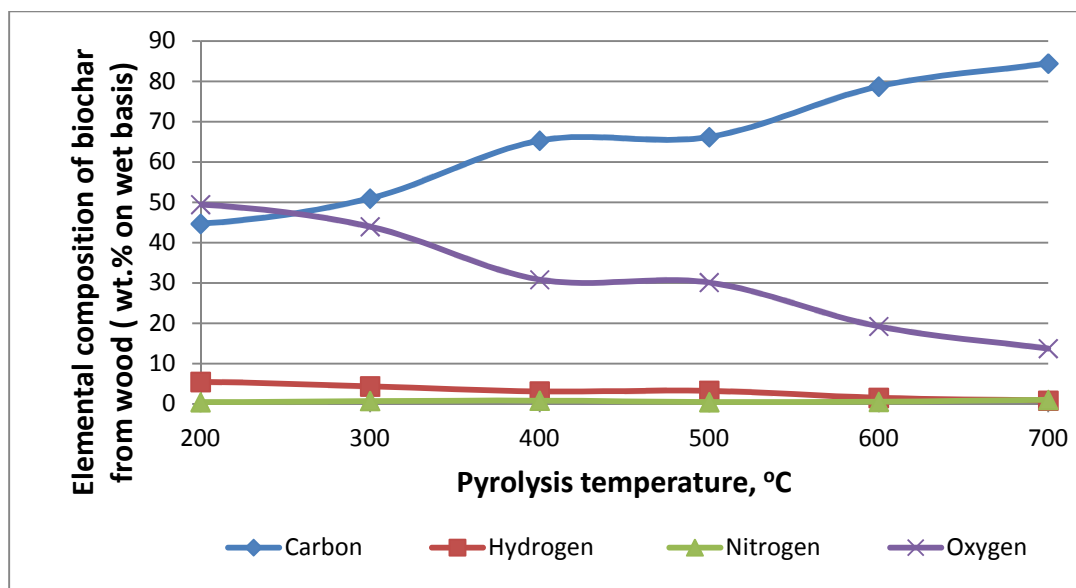


Figure 29. Elemental composition of biochar fraction from wood pyrolysis

**6.5.2 Bio-oil.** carbon content of bio-oil for MSW components were generally low and this is as a result of the high water content in the bio-oil produced. The values for carbon content for all MSW components pyrolyzed ranged from 4.7 wt. % (wb) to 18.7 wt. % (wb). The elemental composition for the MSW component at different pyrolysis temperatures are given in Tables 9 to 11.

Table 8

*Elemental composition of bio-oil from textile pyrolysis at different temperatures*

	T-300	T-400	T-500	T-600	T-700	T-800
Carbon	6.26	8.03	11.31	12.21	15.31	10.87
Hydrogen	4.56	3.90	6.33	5.63	5.74	6.41
Nitrogen	1.52	0.88	1.72	1.44	1.07	1.15
Oxygen	87.66	87.19	80.64	80.98	77.88	81.57

Table 9

*Elemental composition of bio-oil from paper pyrolysis at different temperatures*

	T-300	T-400	T-500	T-600	T-700	T-800
Carbon	4.71	5.13	8.89	10.25	15.01	8.91
Hydrogen	2.84	2.59	1.99	0.18	4.61	4.36
Nitrogen	0.26	0.26	0.43	0.11	0.38	0.26
Oxygen	92.19	92.02	88.69	89.46	80.00	86.47

Table 10

*Elemental composition of bio-oil from wood pyrolysis at different temperatures*

	T-300	T-400	T-500	T-600	T-700	T-800
Carbon	10.30	11.30	15.54	18.71	12.68	11.91
Hydrogen	4.59	5.59	6.99	5.42	5.0	4.76
Nitrogen	0.22	0.34	0.49	0.32	0.27	0.16
Oxygen	84.89	82.77	76.98	75.55	82.05	83.17

### **6.6 Kinetic Studies of MSW Components Pyrolysis from TGA Experiments**

Modeling to predict the yield and composition of products from the pyrolysis requires the knowledge of reaction kinetics and its parameters. This is done by thermogravimetric and differential scanning calorimetric methods and has been reported by several authors [77, 96]. The temperature-dependent kinetic parameters were determined using the Arrhenius equation and applying the first order equation as given by [93]

$$\frac{dX(t)}{dt} = k (X_p - X(t)) \quad (27)$$

$$X(t) = \frac{m_o - m(t)}{m_o} \quad (28)$$

$$X_p = \frac{m_o - m_\infty}{m_o} \quad (29)$$

with  $m_o$  being the initial weight of MSW sample at time  $t = 0$ , (mg),  $m_\infty$  as residual weight of MSW sample after the reaction (mg),  $m(t)$  as the weight of MSW sample at time  $t$  during the experiment (mg). The reaction rate constant,  $k$ , is a function of temperature and was calculated at each time from the weight change- time-temperature generated in excel from the universal analysis data software. From Arrhenius equation (equation No) , a plot of  $\ln k$  versus  $1/T$  was generated for each sample to determine the activation energy,  $E$  and pre-exponential factor,  $A$  from the slope and intercept respectively.

$$k = A \exp(-E_a/RT) \quad (30)$$

**6.6.1 Pyrolysis in nitrogen atmosphere.** It is observed from the TGA plots given in Figure 25 that pyrolysis in nitrogen gas for all MSW samples was characterized by three distinct stages of weight change corresponding to range of temperatures during the process. Similar results were reported by other authors [9,79, 93]. The first stage is the dehydration stage which occurred between 25°C to around 110°C for paper, wood and textile. Plastic (HDPE) however, did not show a significant loss within this temperature range because plastic (HDPE) has very low moisture content. The second stage of weight loss, which is the active pyrolysis, was observed from 220°C to 380°C for paper, wood and textile with only one peak in this region as shown in the derivative plot on the second axis (DTG). The TGA plot from plastics (HDPE) shows a weight loss for temperature range between 380°C and 480°C for the second stage of

active pyrolysis and the DTG plot shows an observable peak with a maximum of over 80 wt% per min. Table 11 gives the results of weight changes at increasing heating rate (20°C/min, 40°C/min and 60°C/min) for all MSW components performed in the TGA. The plots for standard component ( cellulose, hemicelluloses and lignin) are provided in Figure 31

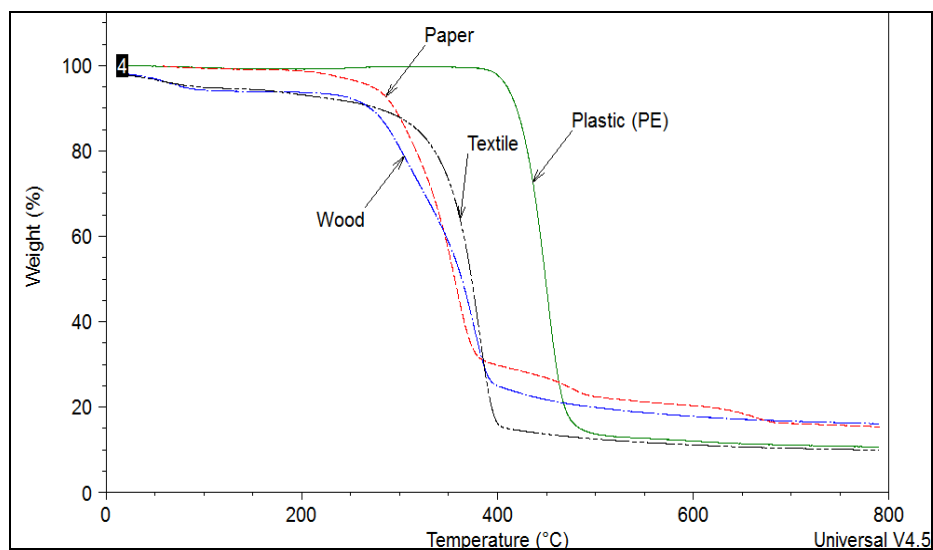


Figure 30. Thermal degradation profile of different MSW with increasing temperature

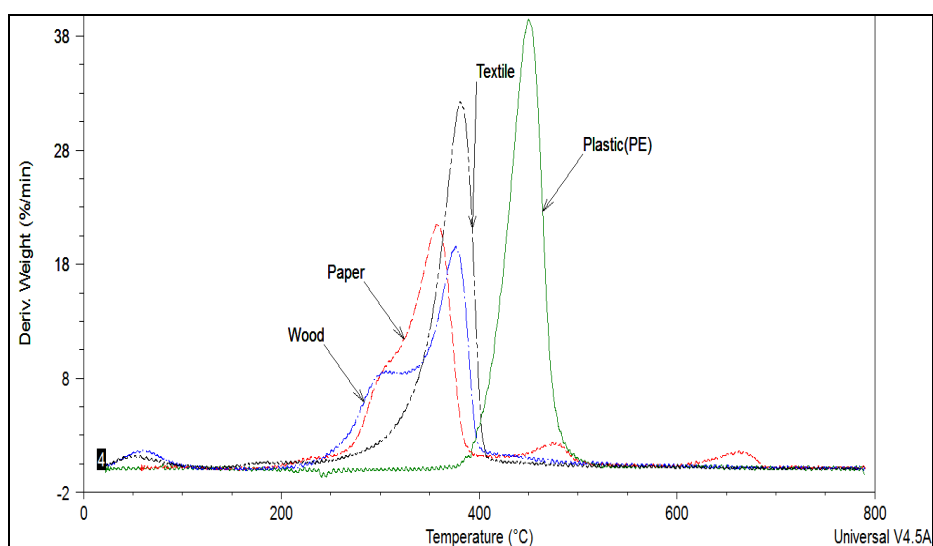


Figure 31. DTG curve for different MSW components at increasing temperature

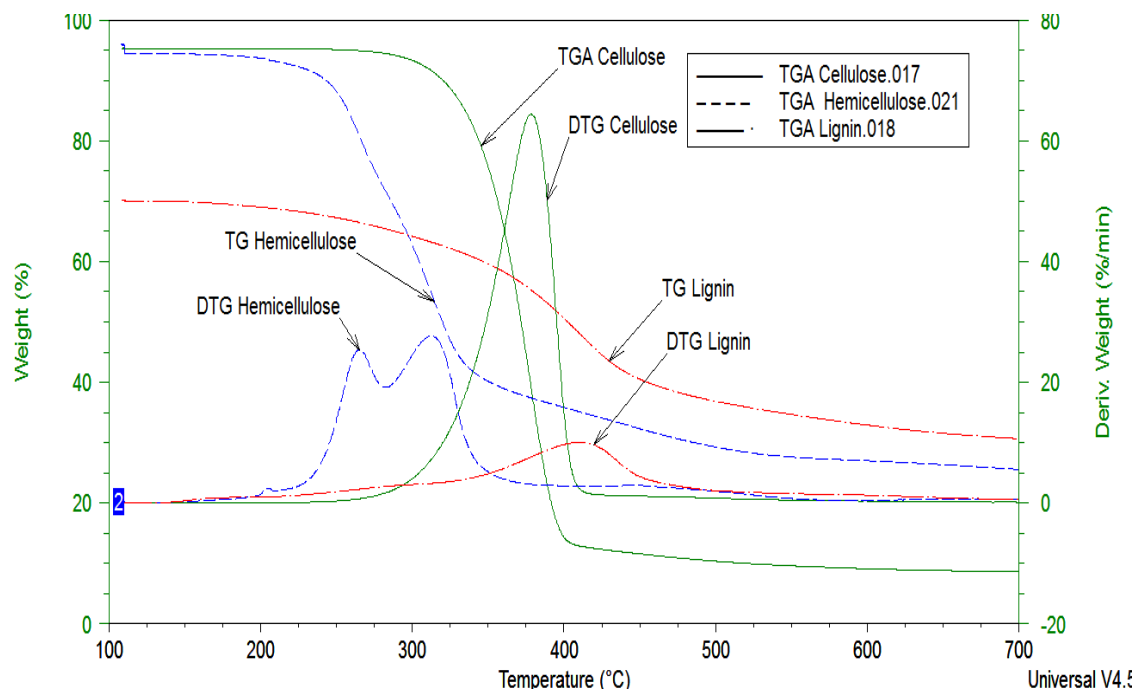


Figure 32. TG and DTG curve for cellulose, hemicelluloses and lignin standard components

Table 11

*Temperature range and weight loss of MSW components at different heating rates in nitrogen atmosphere*

	MSW sample	20°C/min		40°C/min		60°C/min	
		Temperature, °C	Weight %	Temperature(°C)	Weight %	Temperature,°C	Weight, %
Stage I	Paper	25	100	25	100	25	100
		120	99.19	130	97.52	200	98.85
	Wood	25	100	25	100	25	100
		120	94.04	270	90.32	290	85.26
	Textile	25	100	25	100	25	100
		120	94.67	140	95	130	95.36
	Plastic	25	100	25	100	25	100
		110	99.43	110	99.64	110	99.91
Stage II	Paper	220	98.19	280	94.1	290	94.6
		420	28.68	400	28.43	440	31.26
	Wood	240	92.92	280	88.89	290	84.71
		400	25.01	420	24.41	450	21.14
	Textile	290	88.93	270	90.19	270	89
		450	13.67	440	30.78	460	24.78
	Plastic	380	99.38	390	98.95	390	98.79
		480	15.67	490	14.37	510	9.79
Stage III	Paper	420	28.68	400	28.43	440	31.26
		550	21.24	550	21.84	600	23.68
	Wood	400	25.01	420	24.41	450	21.14
		500	19.94	490	20.71	510	18.8
	Textile	450	13.67	440	30.78	460	24.78
		520	14.61	530	24.98	500	22.64
	Plastic	480	15.67	490	18.62	490	19.7
		580	12.32	600	13.57	610	7.08
Fixed carbon + Ash	Paper	790	15.39	800	17.13	790	19.06
	Wood	800	12.04	800	12.78	770	15.41
	Textile	770	10.02	790	19.75	770	13.94
	Plastic	780	10.72	800	12.07	770	5.83

**6.6.1.1 Reaction kinetics parameters for pyrolysis in nitrogen atmosphere.** The reaction kinetics determined for standard components (cellulose, hemicelluloses and lignin) in nitrogen atmosphere with r-squared values greater than 0.90 were in the temperature range from 200°C to 380°C. The parameters for MSW recorded r-squared value ( $R^2 = 0.610$ ) for paper in the temperature range 250°C to 420°C; wood recorded r-squared value ( $R^2 = 0.830$ ) within temperature range of 250°C to 420°C; plastic (HDPE) recorded r-squared value ( $R^2 = 0.996$ ) within temperature range of 390°C to 480°C; textile residue recorded r-squared value ( $R^2=0.790$ ) within temperature range of 250°C to 400°C. The activation energy and pre exponential factors were determined for heating rates 20°C, 40°C and 60°C in nitrogen atmosphere and provided in Table 12

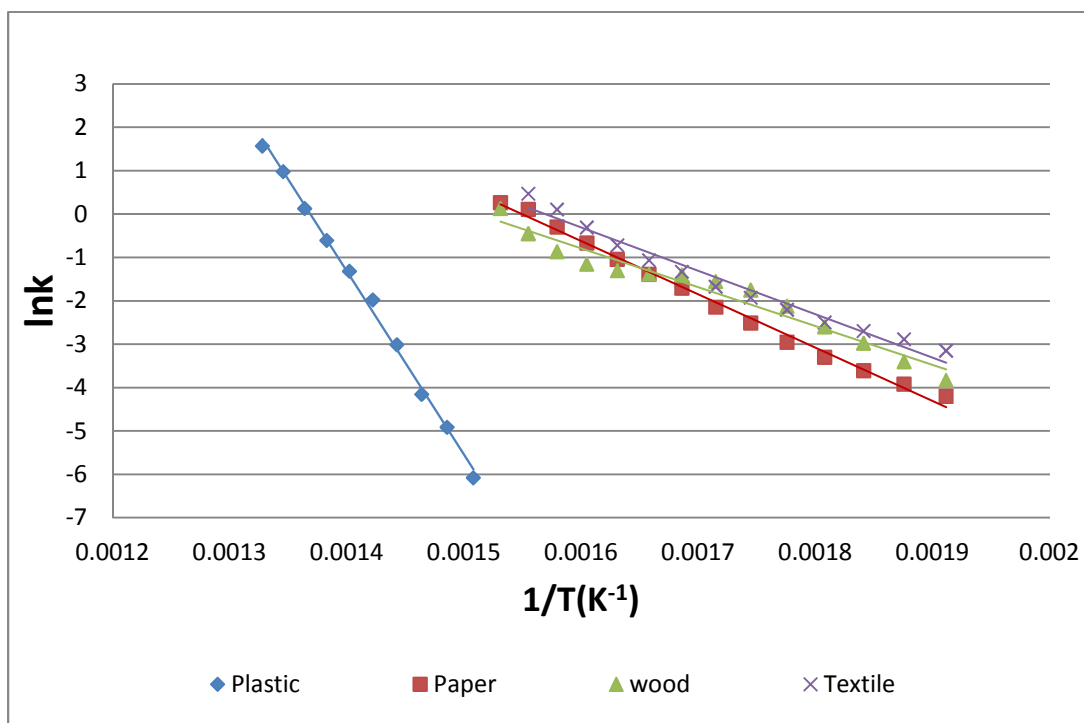


Figure 33. Temperature dependency of the rate constant of MSW pyrolysis at a heating rate of 40 °C/min for plastic, wood, paper and textile

Table 12

*Comparison of activation energy and pre-exponential factors for MSW components in nitrogen atmosphere*

MSW	Temperature range(°C)	Heating rate( °C/min)	A(s <sup>-1</sup> )	Ea( KJmol <sup>-1</sup> )
Wood	250 - 420	20	$2.78 \times 10^2$	36.61
	250 - 420	40	$1.93 \times 10^4$	57.46
	250 - 420	60	$1.50 \times 10^5$	66.32
Textile residue	200 - 420	20	1.74	12.17
	200 - 420	40	$1.56 \times 10^3$	44.6
	200 - 420	60	$1.69 \times 10^3$	43.43
Paper	250 - 420	20	$1.87 \times 10^2$	36.61
	250 - 420	40	$2.21 \times 10^3$	46.36
	250 - 420	60	$9.57 \times 10^2$	51.82
plastic (PE)	380 - 480	20	$6.37 \times 10^7$	113.2
	380 - 480	40	$1.74 \times 10^{13}$	185.2
	380 - 480	60	$4.22 \times 10^{23}$	313.93

**6.6.1.2 Effect of heating rate.** Heating rate affected the plots for MSW samples by increasing the temperature range for active pyrolysis. The activation energy (Ea) increased for each MSW studied when heating rate was increased. For example the activation energy for paper, plastic (HDPE), and wood increased from 47.8, 253.7, 58.3 KJ/mol at heating rate of 20°C/min to activation energy of 62.5, 351.6, 64.8 KJ/mol at heating rate of 40°C/min respectively. Textile recorded a decrease in activation energy from 110.2KJ/mol at heating rate of 20°C/min to 63.1 KJ/mol at 40°C/min heating rate. The increment in activation energy recorded in the samples when heating rate was increased may be due to heat transfer limitation which resulted from longer time required for purge gas to come into equilibrium with the actual sample temperature.

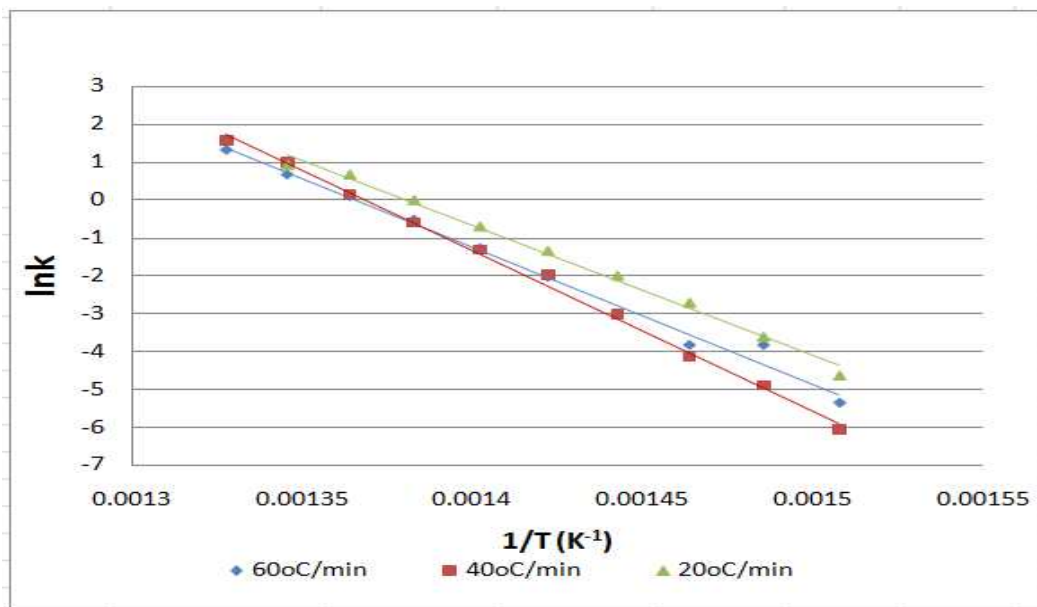


Figure 34. Temperature dependency of the reaction rate of the pyrolysis of plastic (PE) at different heating rate

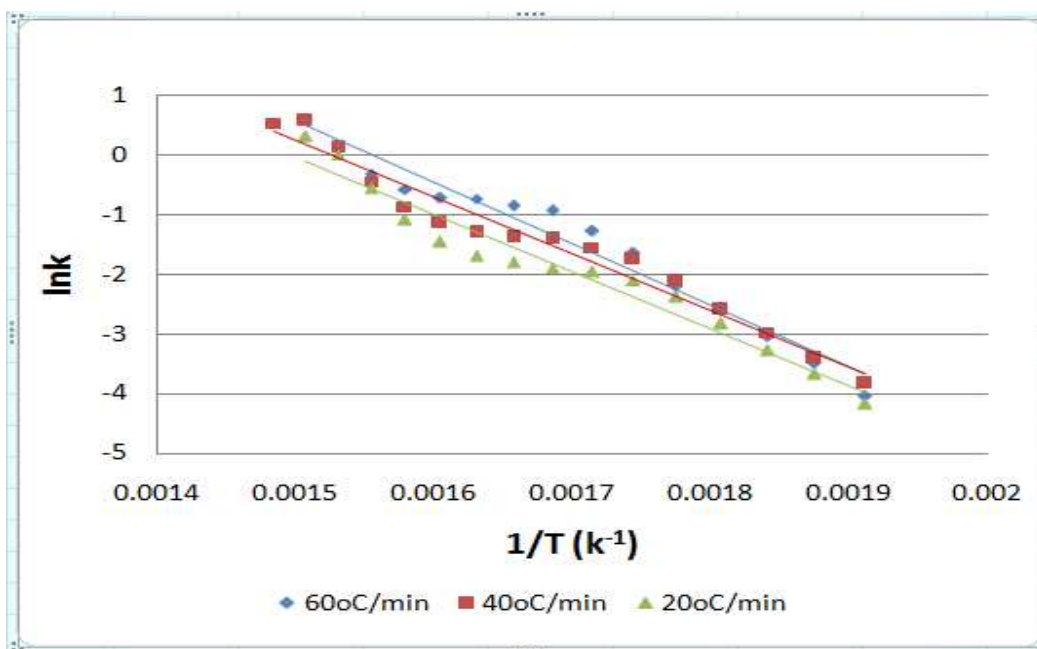


Figure 35. Temperature dependency of the reaction rate of the pyrolysis of wood at different heating rate

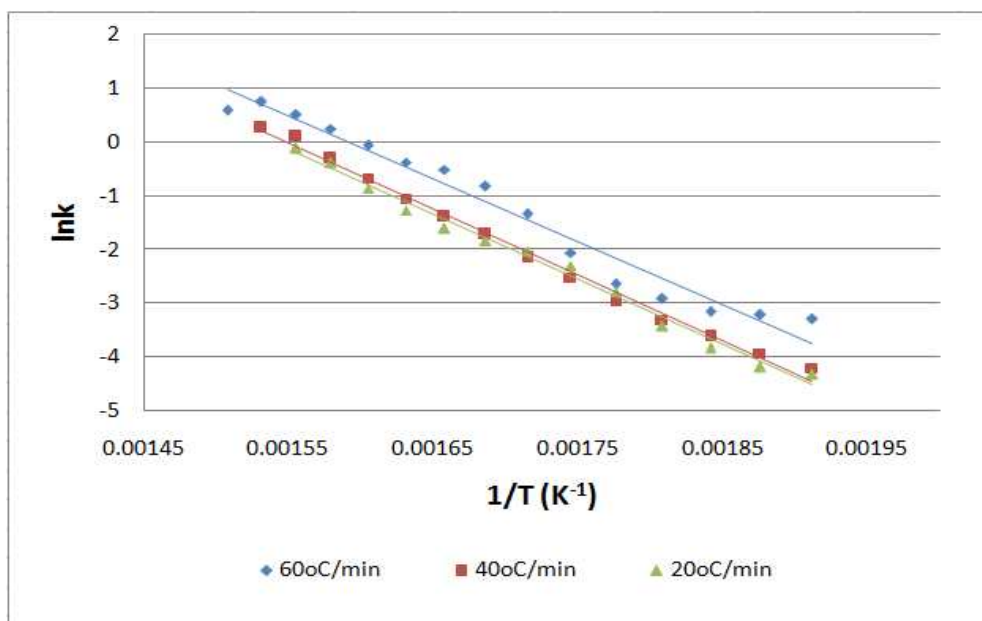


Figure 36. Temperature dependency of the reaction rate of the pyrolysis of paper at different heating rate

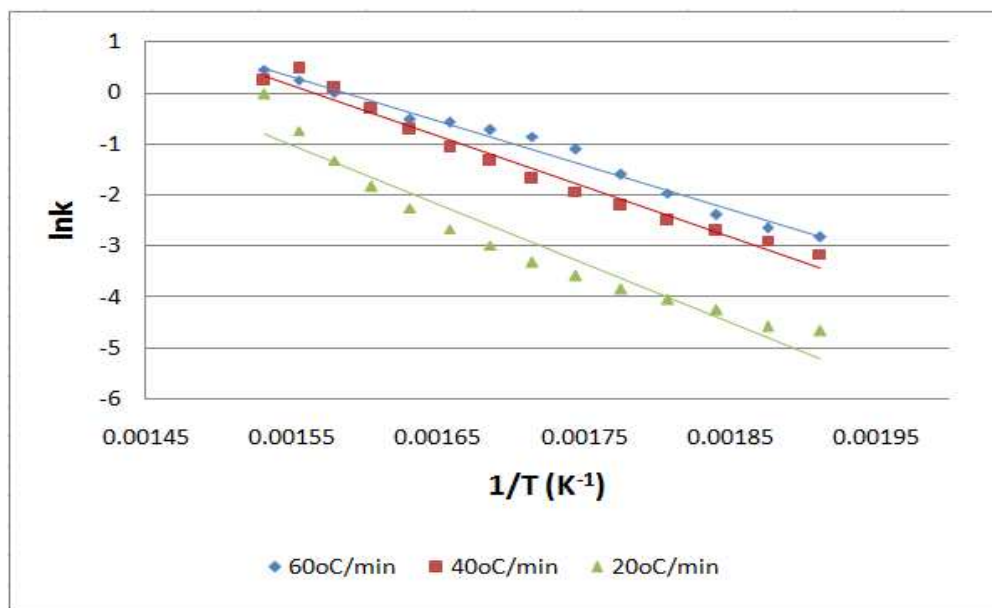


Figure 37. Temperature dependency of the reaction rate of the pyrolysis of textile at different heating rate

**6.6.2 Pyrolysis in CO<sub>2</sub> atmosphere.** From the profiles obtained from the pyrolysis of MSW compounds in CO<sub>2</sub>, the TGA plots suggested that there were three stages of weight loss characterized by dehydration and volatilization of light gases, volatilization of heavy hydrocarbons and the final stage being char decomposition. Plastic (HDPE) decomposition at the second stage ranged from 360oC to 490oC with a large weight loss (~89%) at a rate of less (<2% /oC) compared to a weight loss of (~86%) in nitrogen atmosphere at the same rate of less (<2%/oC) in the same temperature range.

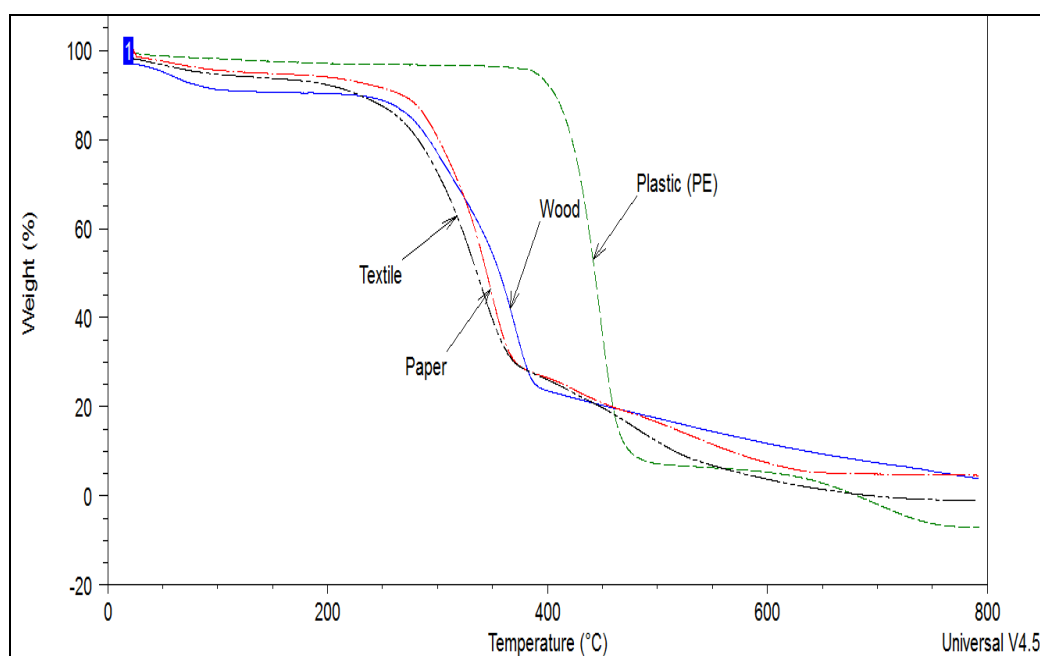


Figure 38. TGA profile of MSW in CO<sub>2</sub> atmosphere

**6.6.2.1 Parameters of reaction kinetics for pyrolysis in CO<sub>2</sub> atmosphere.** The kinetics in CO<sub>2</sub> atmosphere are similar to kinetics obtained in the nitrogen atmosphere. However, the magnitude of the parameters as shown in Table 14 is generally lower in CO<sub>2</sub> atmosphere compared to nitrogen atmosphere.

Table 13

*Comparison of activation energy and pre-exponential factors for MSW components in CO<sub>2</sub> atmosphere*

<b>MSW</b>	<b>Temperature range(°C)</b>	<b>Heating rate( °C/min)</b>	<b>A(s<sup>-1</sup>)</b>	<b>Ea( KJmol<sup>-1</sup>)</b>
Wood	250 - 420	20	$2.96 \times 10^2$	39.27
	250 - 420	40	$8.57 \times 10^3$	53.36
	250 - 420	60	$2.85 \times 10^4$	57.69
Textile residue	200 - 420	20	$4.7 \times 10^1$	29.28
	200 - 420	40	$4.21 \times 10^4$	57.79
	200 - 420	60	$2.45 \times 10^5$	66.37
Paper	250 - 420	20	$1.81 \times 10^2$	37.06
	250 - 420	40	$1.33 \times 10^4$	54.84
	250 - 420	60	$3.52 \times 10^4$	58.89
plastic (PE)	380 - 480	20	$5.18 \times 10^{13}$	192.76
	380 - 480	40	$1.33 \times 10^{19}$	264.42
	380 - 480	60	$4.8 \times 10^{18}$	261.31

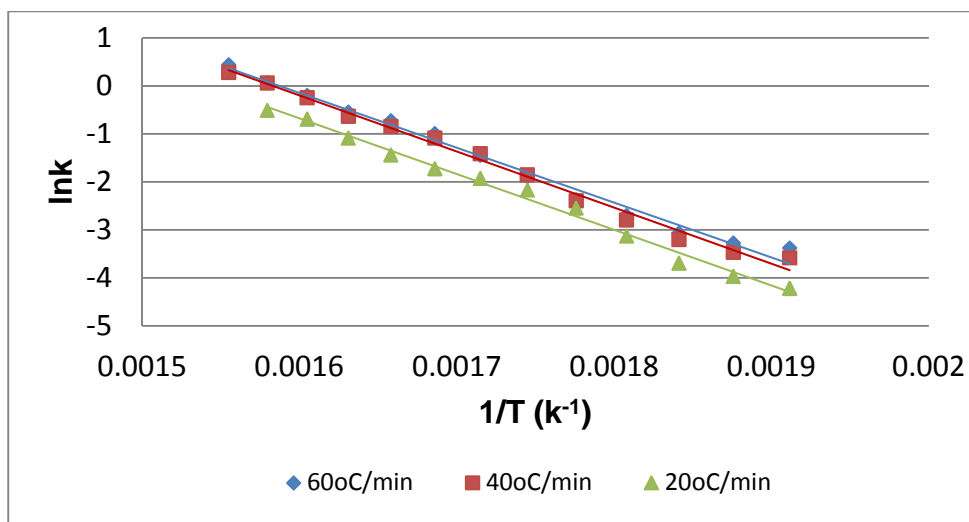


Figure 39. Temperature dependency of the reaction rate of the pyrolysis of paper at different heating rate

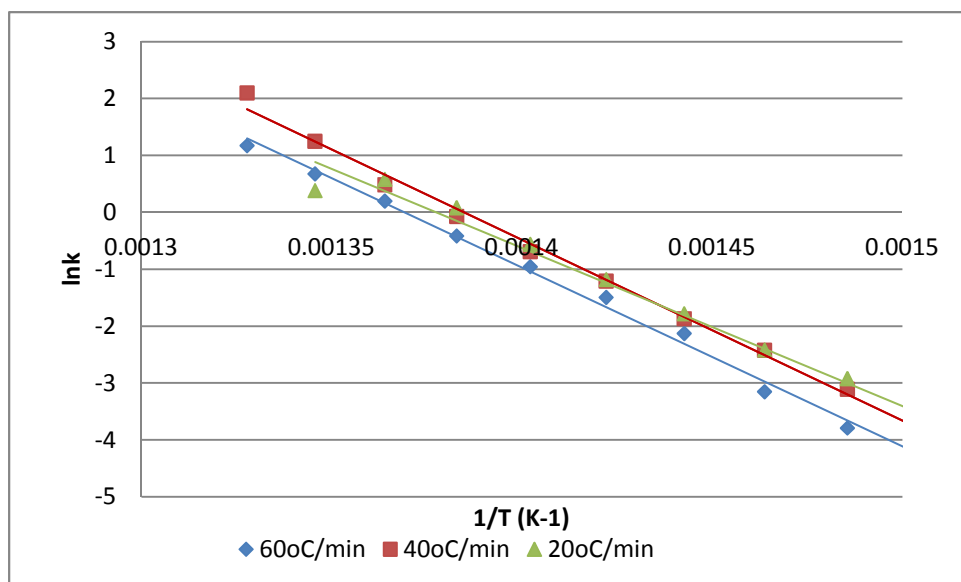


Figure 40. Temperature dependency of the reaction rate of the pyrolysis of plastic (PE) at different heating rate

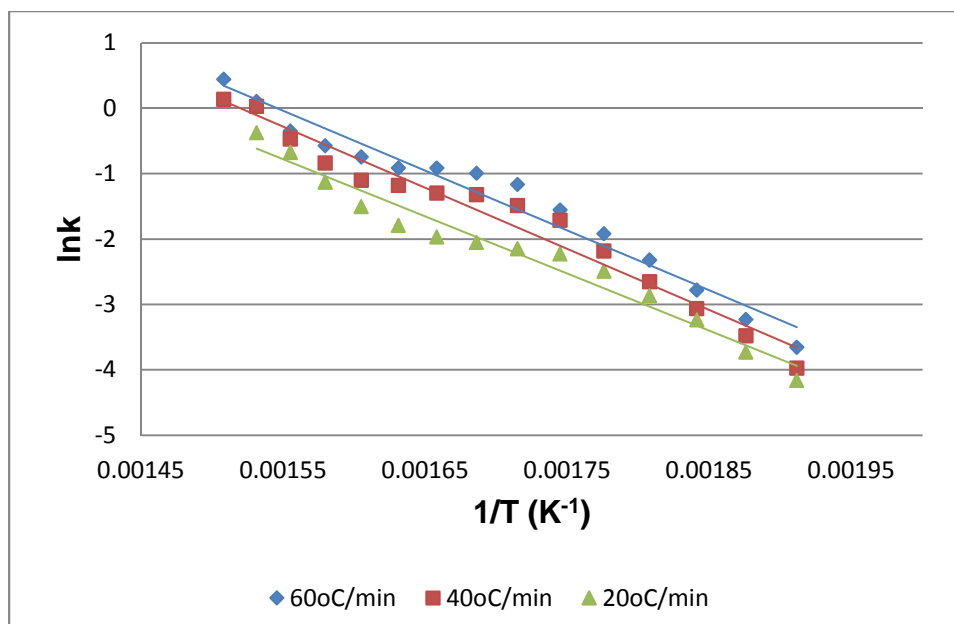


Figure 41. Temperature dependency of the reaction rate of the pyrolysis of wood at different heating rate

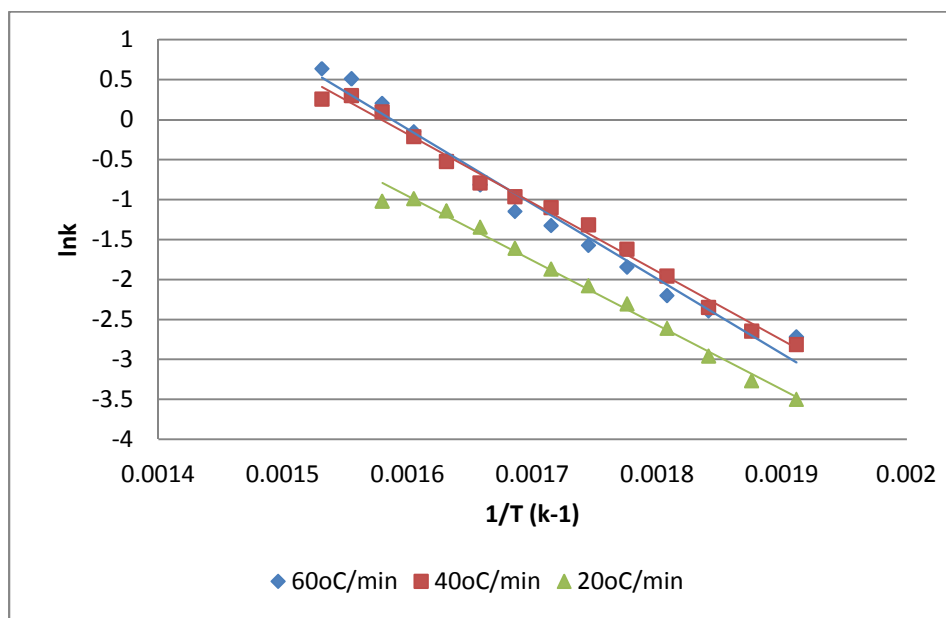


Figure 42. Temperature dependency of the reaction rate of the pyrolysis of textile at different heating rate

## 6.7 Differential Scanning Calorimetry (DSC) of the Pyrolysis of MSW Components

The DSC curve allows the calculation of the flow of energy by integrating the surfaces of the positive or negative peaks for exothermic and endothermic processes, respectively. The total caloric requirement consists of the heat required to dry biomass, heating of biomass, degradation of biomass and aggregation of char.

In the drying stage of MSW components, the DSC curve in Figure 29 shows that there are corresponding peaks of the drying process for paper, wood, textile and plastic below 150°C with corresponding small weight change of 1.3%, 6.4%, 6.8% and 0.8%, respectively. The caloric requirement in this stage is the energy to heat the sample and to vaporize water from the sample. It is difficult to accurately measure the caloric requirement due to the unstable segment at the beginning of each run.

Between 150°C and 250°C, paper, wood and textile were heated without any significant change in weight as shown in Figure 36 and there were no obvious peaks in the DSC curve as shown in Figure 41. The increase in the heat flow at the temperature from 150°C to 250°C was as a result of sensible heat to increase the temperature of the sample to the temperature before pyrolysis. However, plastic showed a slight endothermic peak within this temperature range which may indicate the glass transition of plastics at a temperature of 250°C. The DSC curve changes from 3.8 W/g to 3.9W/g for plastic, 3.1W/g to 4.2W/g for paper, 2.5W/g to 3.6W/g for wood and 1.8W/g to 2.5W/g for textile, respectively, within 150°C to 250°C.

When the samples were further heated from 250°C, the degradation reaction started for paper, wood, and textile while the plastic started to degrade at 380°C. The DTG curves in Figure 25 showed an apparent peak which indicated a significant mass loss rate during pyrolysis. The mass loss in this stage was 66.8% (from 96.7% to 29.84%) for paper, 67.3% (from 92.3% to

25.0%) for wood, and 75.2% (from 91.4% to 16.2%) for textile, respectively. The mass loss of plastic was 85.6% (from 99.3% to 13.7%) within the temperature range from 380°C to 500°C. It is noted that the value of the heat flow varied greatly within these temperature ranges and the DSC curves are complex. The energy absorption is calculated from the integration of the endothermic peaks that occur within these temperature stages.

The final stage is the heating of the residual char and the aggregation of the char which started at 400°C for paper, wood and textile whereas plastic start at 500°C. The caloric requirement at this stage was the heat needed to heat the char after subtracting the heat due to aggregation.

In conclusion, the heat requirement of the pyrolysis process is the sum of heat needed to heat the sample and the heat of reactions. Thus the calorific requirement of the MSW component can be calculated by integrating the DSC curve in Figure 29 using Equation 18 as given below [97]:

$$\frac{Q}{m_{s,0}} = \int_0^t \frac{\left( m_s C_{p,s} \frac{dT}{dt} + m_s H \right)}{m_{s,0}} dt \quad (31)$$

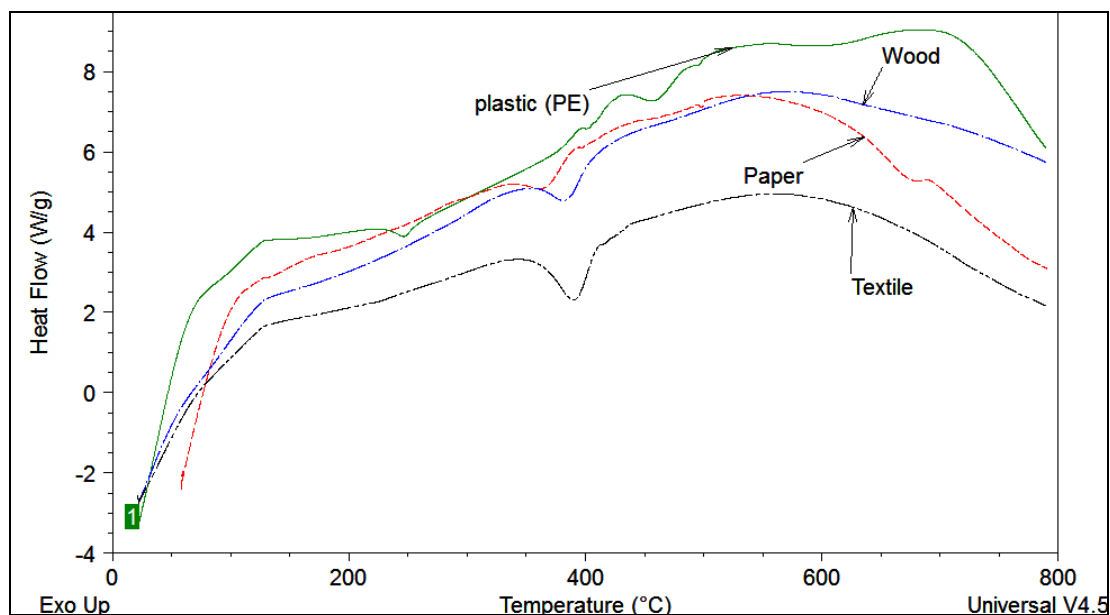


Figure 43. DSC profile of different MSW components with increasing temperature in nitrogen atmosphere at heating rate of 20°C/min

Table 14

*Relationship of calorific value and mass residue of plastic with temperature*

Final temperature(°C)	200	250	300	350	400	450	500	550	600
Mass residue (%)	99.1	99.5	99.6	99.6	97.7	48.2	13.7	12.7	12.1
Caloric requirement(J/g)	990.3	1596.7	2266.0	3047.7	3957.5	5030.1	6192.8	7483.5	8784.2

Table 15

*Relationship of calorific value and mass residue of textile with temperature*

Final temperature(°C)	200	250	300	350	400	450	500	550	600
Mass residue (%)	93.1	91.4	87.8	73.2	16.2	13.7	12.5	11.7	11.4
Caloric requirement(J/g)	16.1	359.9	774.1	1258.4	1685.1	2260.8	2937.7	3668.1	4406.1

Table 16

*Relationship of calorific value and mass residue of paper with temperature*

Final temperature(°C)	200	250	300	350	400	450	500	550	600
Mass residue (%)	98.7	96.7	87.9	56.6	29.8	26.8	22.4	21.2	20.3
Caloric requirement(J/g)	585.6	1173.5	1857.2	2622.6	3451.8	4431.9	5482.7	6587.3	7673

Table 17

*Relationship of calorific value and mass residue of wood with temperature*

Final temperature(°C)	200	250	300	350	400	450	500	550	600
Mass residue (%)	93.7	92.3	80.8	58.6	25.0	21.7	19.9	18.7	17.8
Caloric requirement(J/g)	305.6	805.6	1413.5	2142.0	2896.6	3827.5	4853.4	5946.7	7073.1

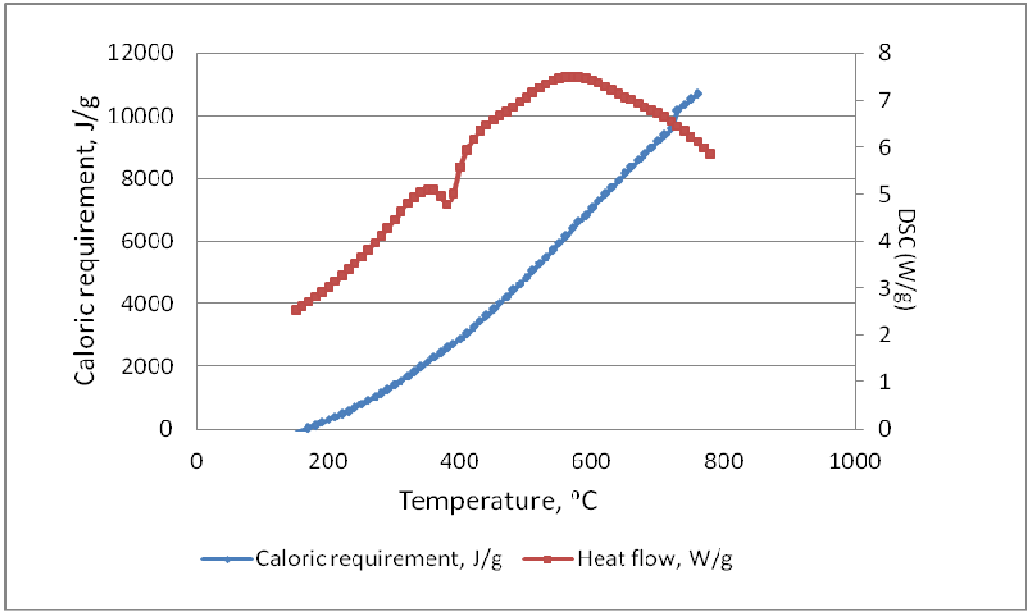


Figure 44. DSC curve and caloric requirement by integrating DSC curve of wood

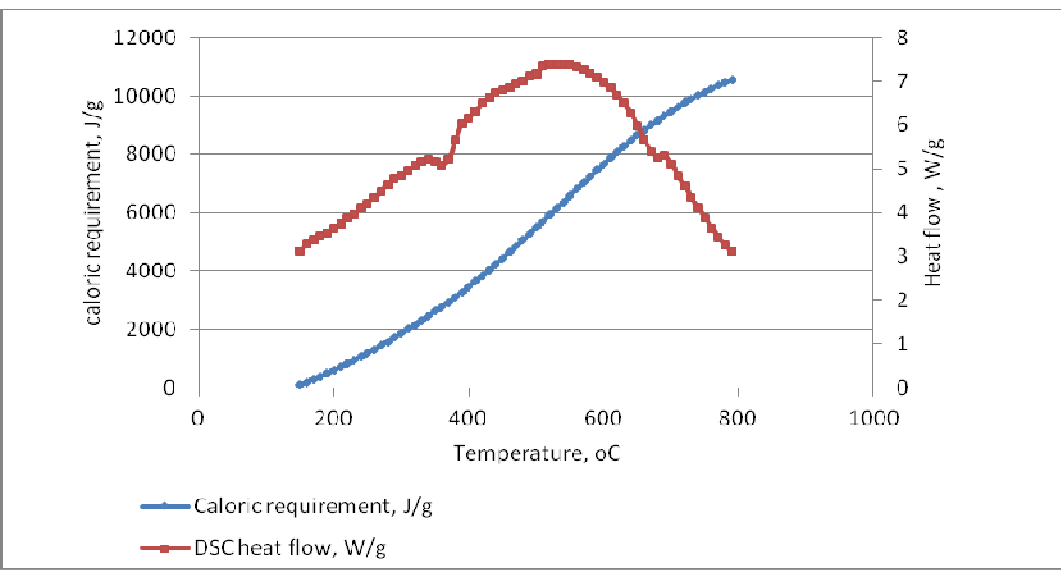


Figure 45. DSC curve and caloric requirement by integrating DSC curve of paper

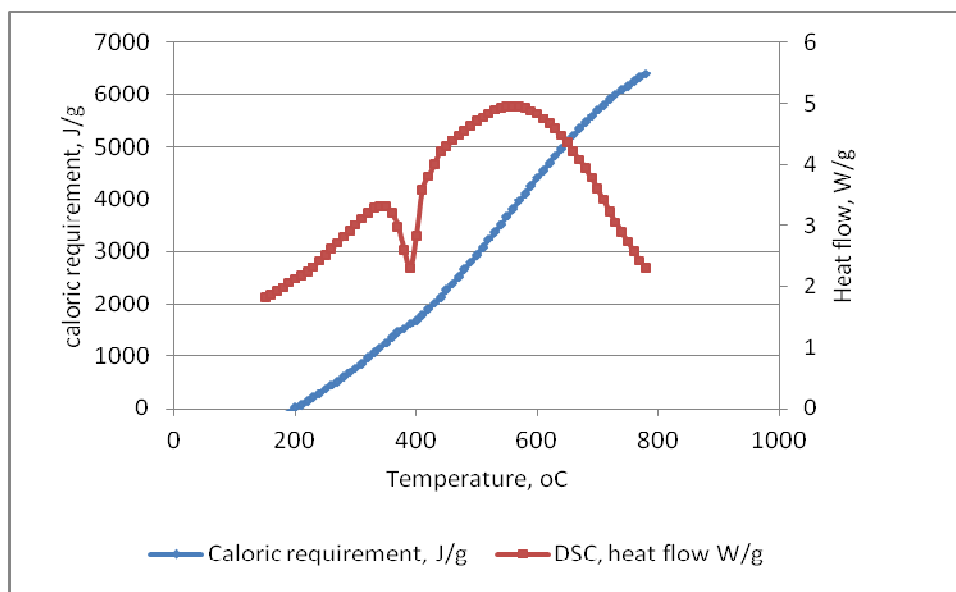


Figure 46. DSC curve and caloric requirement by integrating DSC curve of textile

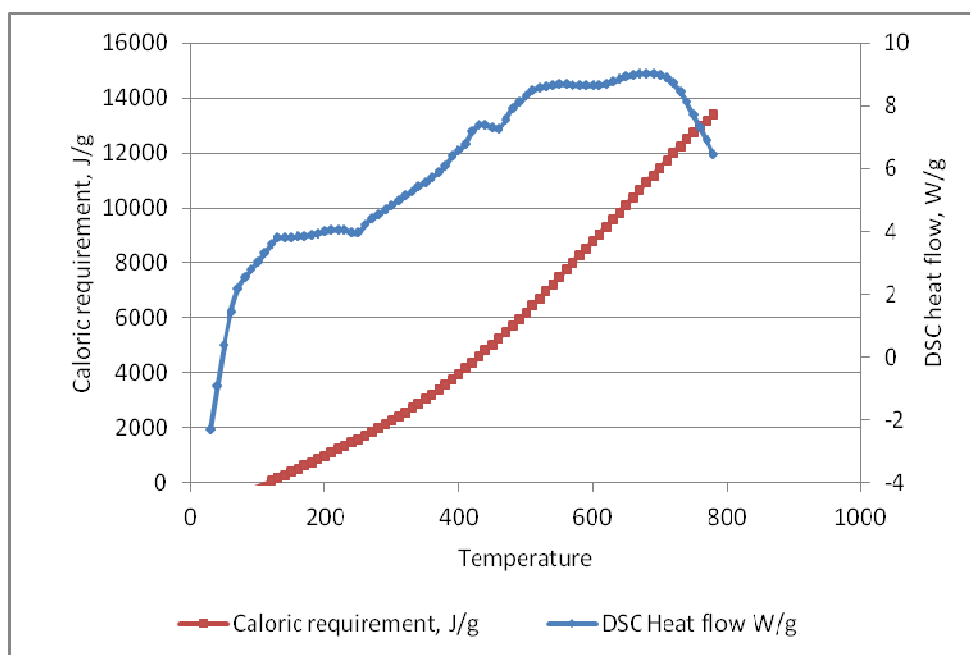


Figure 47. DSC curve and caloric requirement by integrating DSC curve of plastic

## 6.8 Mass Spectrometry of the gas evolved from the Pyrolysis of MSW Components

This section shows the analysis of gas products distribution corresponding to decomposition of MSW samples studied in the two purging gases used in the experiment. The TGA-MS technique is an important method of simultaneously measuring the decomposition and gas product distribution of biomass samples from the pyrolysis of standard biomass components (cellulose, hemicellulose and lignin) and major organic components of MSW in the TGA.

**6.8.1 Gas analysis from the pyrolysis of MSW in nitrogen atmosphere.** Mass spectrometric profiles of the gases generated from the pyrolysis of wood, textile, plastic (PE) and paper in nitrogen atmosphere are shown in Figures 30 to 33. As seen from the profiles for wood, textile and paper, the pyrolysis process occurred in a relatively narrow range of temperature (200°C to 500°C) which is consistent with most of the gases detected in that temperature range. Similarly plastic (PE) showed a mass spectrometric profile within a narrow but higher temperature range of 380°C to 500°C which also showed the consistency with the thermal degradation profile from the TGA. The gases detected in all pyrolysis were based on their relative intensities and relevancy and in the present study a peak jump method for gases from H<sub>2</sub>, CO<sub>2</sub>, H<sub>2</sub>O, CH<sub>4</sub>, OH, -CH<sub>3</sub>, O<sub>2</sub>, N<sub>2</sub> corresponding to ion/mass intensities of 2, 44, 18, 16, 17, 15, 32, 28 respectively were used. Among the gases detected, CO<sub>2</sub>, H<sub>2</sub>O, CH<sub>4</sub> and -CH<sub>3</sub> were common to all MSW (paper, wood, textile, plastic) pyrolysis with each component evolving these gases within different temperature ranges.

Textile released most of gases at start temperature of 280°C and ended at 500°C which was consistent with its thermal degradation curve. It is interesting to note that at temperature between 30°C to 110°C, water was released as the only gas which is shown as the peaks corresponding to ions (m/z) of 18 and 17. The m/z of 17 only confirms the source of hydroxyl

ion ( $\text{OH}^-$ ) could only be water since it tracks very well with  $m/z$  of 18. This water is the moisture content of the textile while as the second peak within the temperature range  $320^\circ\text{C}$  and  $500^\circ\text{C}$  is indicated the water generated from reactions. It was observed that oxygen ( $\text{O}_2$ ) declined with increasing temperature, while carbon ( $\text{C}$ ) increased from  $220^\circ\text{C}$  to  $420^\circ\text{C}$  and then decreased from  $420^\circ\text{C}$  to  $470^\circ\text{C}$  and remained fairly constant from temperature of  $500^\circ\text{C}$  and above.

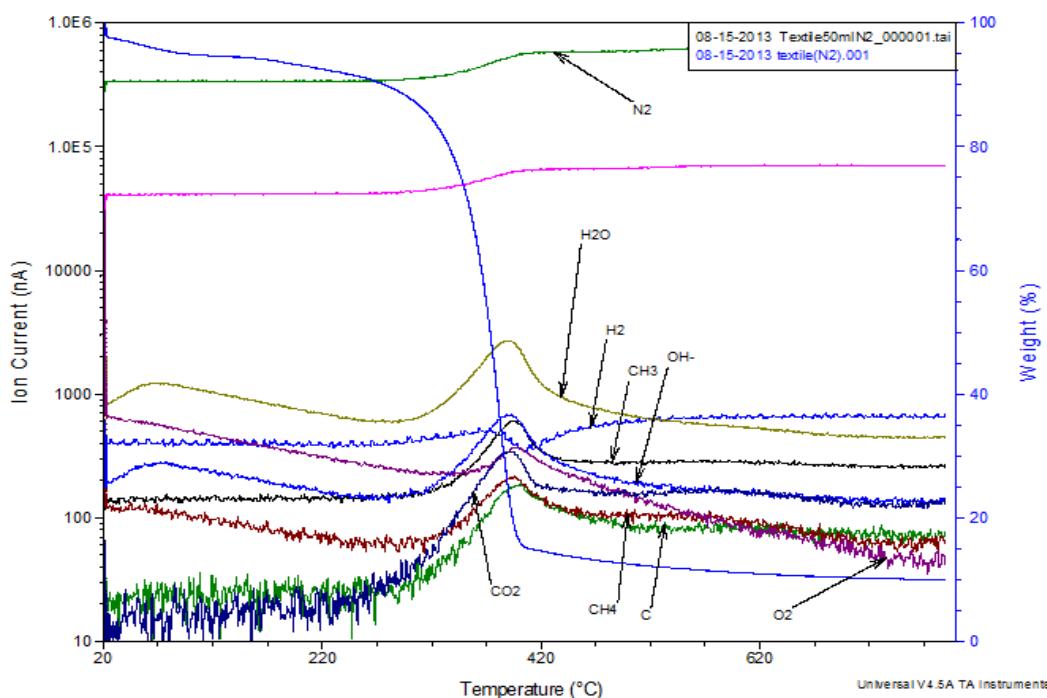


Figure 48. Mass spectra corresponding to the pyrolysis of textile

The spectra from wood pyrolysis are similar to that obtained from textile. Wood pyrolysis is characterized by a first shoulder peak (as a result of hemicelluloses decomposition) and the active pyrolysis (decomposition of cellulosic fraction). The two decomposition process has an overlapping temperature range. Carbon dioxide ( $\text{CO}_2$ ), water ( $\text{H}_2\text{O}$ ), methyl group ( $-\text{CH}_3$ ) and methane ( $\text{CH}_4$ ) were all detected between  $330^\circ\text{C}$  to  $400^\circ\text{C}$  during hemicellulose decomposition and more intense peaks were detected between  $430^\circ\text{C}$  and  $500^\circ\text{C}$  corresponding to the active pyrolysis. It is observed that hydrogen ( $\text{H}_2$ ) gas start to increase at  $500^\circ\text{C}$  and above during the

time when methane ( $\text{CH}_4$ ) and methyl groups ( $-\text{CH}_3$ ) are consumed in the pyrolysis process. Hydrogen ( $\text{H}_2$ ) production is attributed to secondary reaction as steam reforming of methane and/or tar cracking[76]

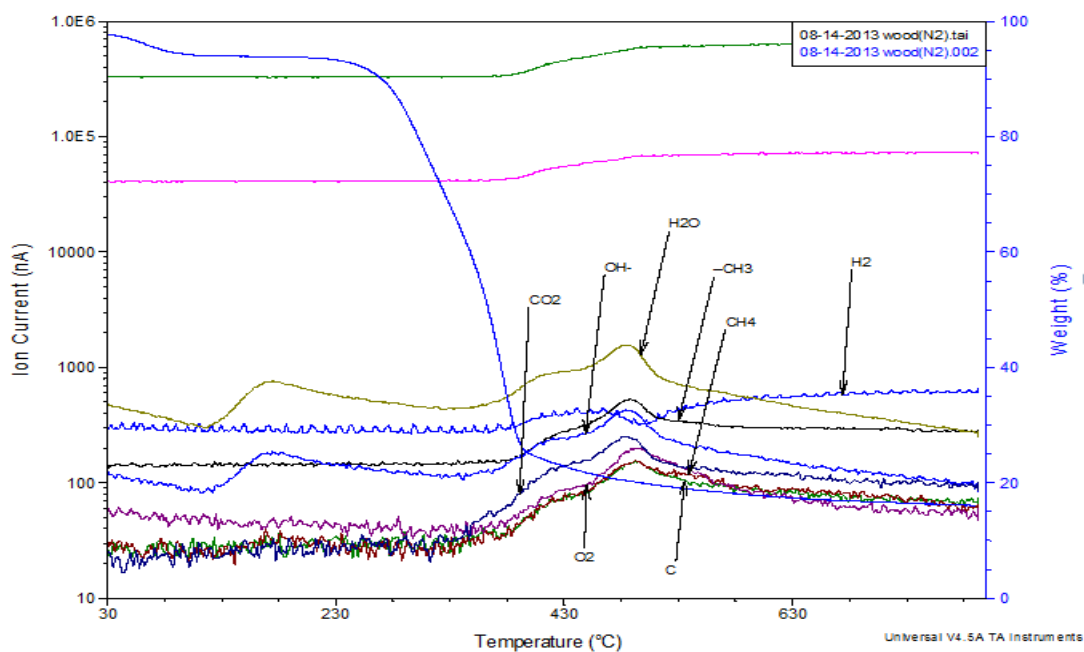


Figure 49. Mass spectra corresponding to the pyrolysis of wood

Mass spectra of pyrolysis of plastic (PE) (Figure 32) was characterized by detection of gases within a narrow temperature range ( $380^{\circ}\text{C}$  to  $500^{\circ}\text{C}$ ). Gases such as carbon dioxide ( $\text{CO}_2$ ), methyl groups ( $-\text{CH}_3$ ) and methane ( $\text{CH}_4$ ) formed the dominant gases detected within the temperature range. The detection of water ( $\text{H}_2\text{O}$ ) was very low as can be seen in the profile and that is consistent with the highly viscous bio-oil product obtained from plastic pyrolysis as reported in literature.

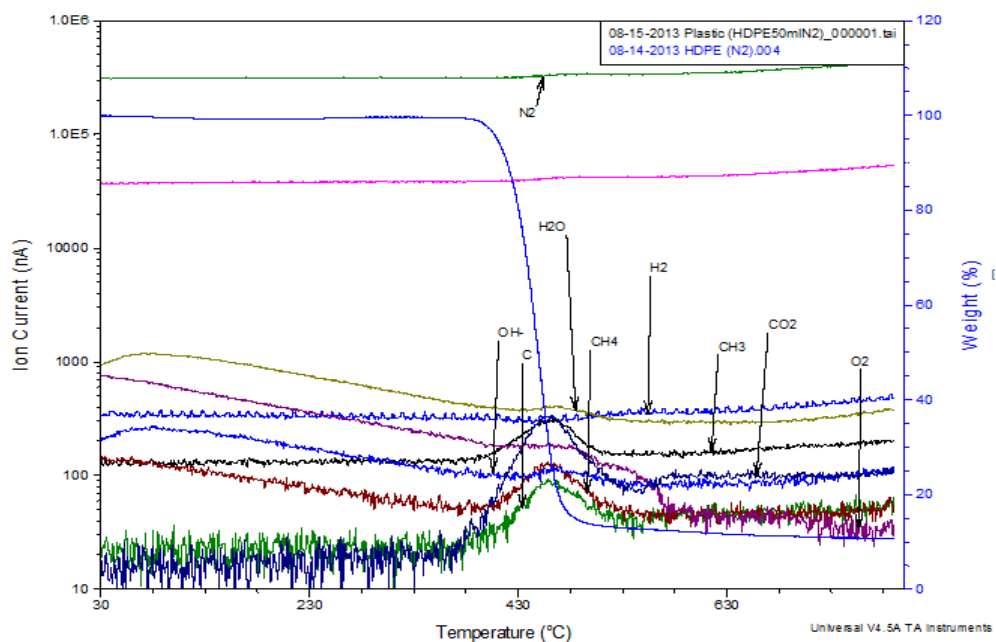


Figure 50. Mass spectra corresponding to the pyrolysis of plastic (PE)

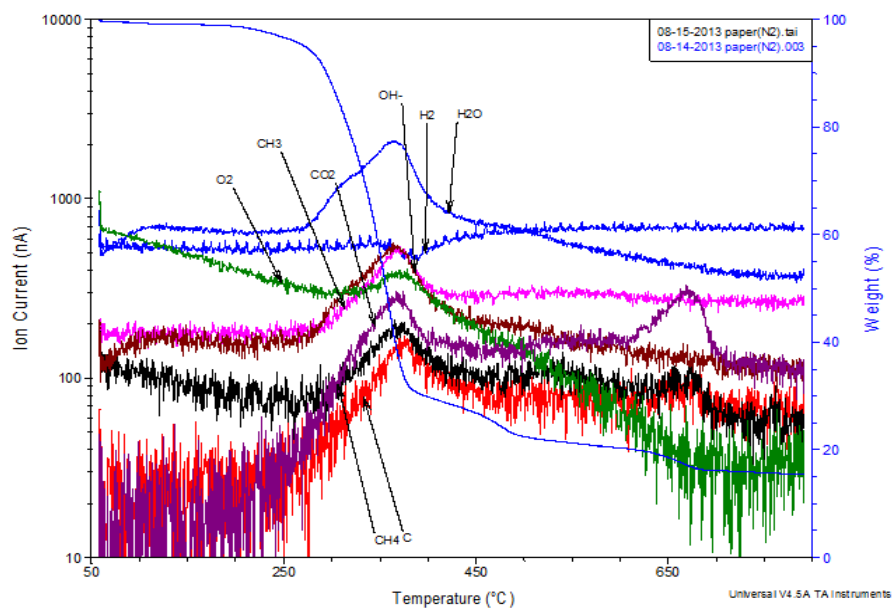


Figure 51. Mass spectra corresponding to the pyrolysis of paper

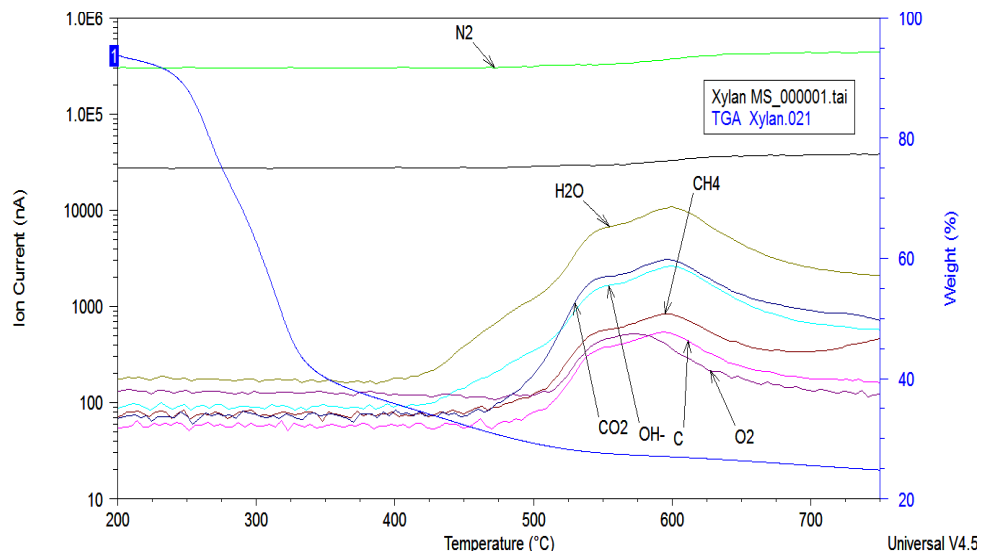


Figure 52. Mass spectra of hemicellulose pyrolysis

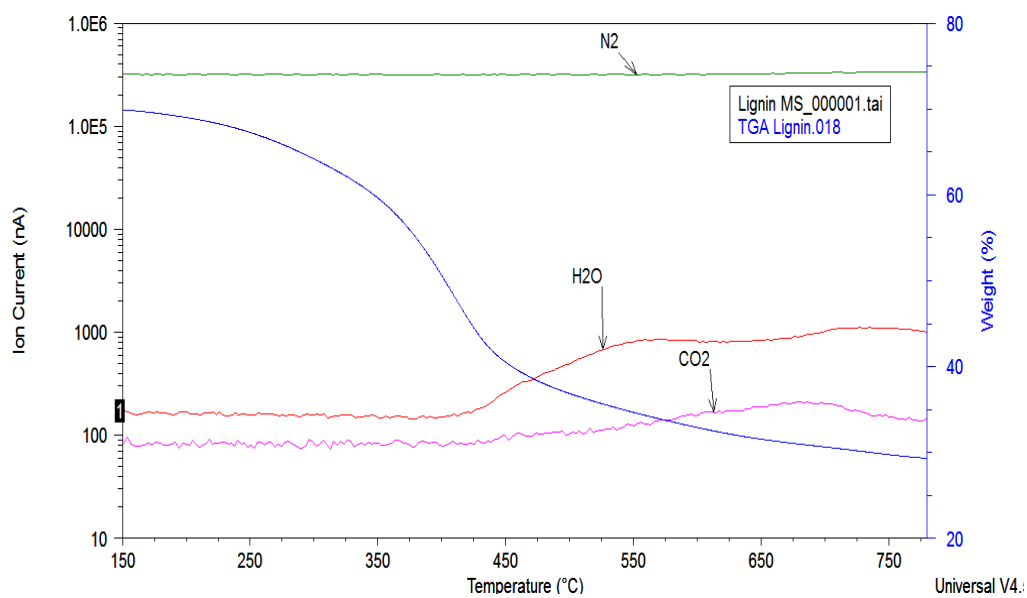


Figure 53. Mass spectra of lignin pyrolysis

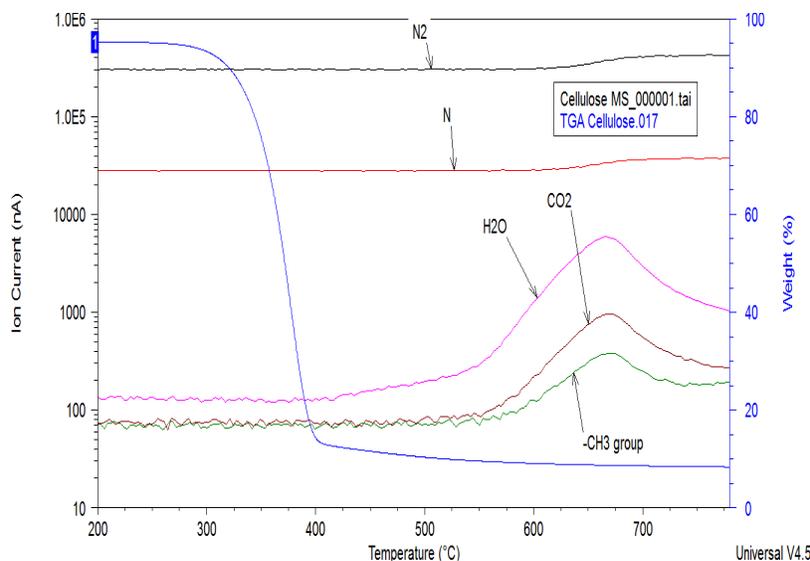


Figure 54. Mass spectra of cellulose pyrolysis

## 6.9 Aspen Simulation Results

The yield of tar oil from the ASPEN simulation increased from 63.58 wt% at 375°C to maximum at 67.12 wt. % at 600°C and start to decline at that temperature to 67.05 wt. % at 700°C. The char yield increases slightly from 24.39 wt. % at 375°C to 26.2 wt % at 525°C and significantly start to decrease from 26.20wt. % at 525°C to 23.59 wt. % at 700°C. The yield of non-condensable gas increased from 7.10 wt. % at 575°C to 8.87 wt. % at 700°C.

The compositions of pyrolysis products predicted from the ASPEN based simulations are given in Table 19. It was found that CO<sub>2</sub> in the non-condensable gases decreased from 62.34 (v %) at 450°C to 51.65 (v%) at 600°C and the CO content in the gas increased from 21.26 (v%) at 450°C to 23.94 (v%) at 600°C. The H<sub>2</sub> in the non-condensable gas increased from 2.98 (v %) at 450°C to 6.22 (v %) at 600°C.

Table 18

*Yield of pyrolysis product at varying reactor temperature*

Temperature (°C)	Yield ( %wt/ wt of MSW )		
	OIL	CHAR	NCG
375	63.58	24.39	12.02
400	64.36	25.03	10.6
425	65	25.5	9.48
450	65.54	25.84	8.61
475	65.93	26.05	8.00
500	66.23	26.17	7.58
525	66.48	26.2	7.31
550	66.68	26.15	7.15
575	66.84	26.04	7.10
600	66.97	25.87	7.15
625	67.06	25.65	7.27
650	67.12	25.39	7.45
700	67.05	23.59	8.87

Table 19

*Composition of pyrolysis products at pyrolysis temperature (400oC to 500°C)*

Volatiles	400		425		450		475		500	
	NCG(v%)	OILS(w%)								
H <sub>2</sub>	2.37		2.65		2.98		3.35		3.78	
CO <sub>2</sub>	65.95		64.10		62.34		60.25		58.17	
CO	19.14		20.25		21.26		22.01		22.60	
H <sub>2</sub> O	0	50.09	0	49.70	0.00	49.40	0.00	49.20	0.00	49.07
CH <sub>4</sub>	7.11	-	7.64	-	8.13	-	8.51	-	8.84	-
C <sub>2</sub> H <sub>6</sub>	3.54	-	3.24	-	2.95	-	2.66	-	2.37	-
C <sub>2</sub> H <sub>4</sub>	-	-	-	-	-	-	0.70	-	1.57	-
C <sub>2</sub> H <sub>2</sub>	-	-	-	-	-	-	-	-	-	-
C <sub>6</sub> H <sub>6</sub>	-	9.98	-	10.06	-	10.12	-	10.16	-	10.19
C <sub>10</sub> H <sub>12</sub> O <sub>4</sub> (TAR)	-	39.93	-	40.24	-	40.48	-	40.64	-	40.74

Table 20

Composition of pyrolysis products at pyrolysis temperature (525°C to 700°C)

Volatiles	525		550		575		600	
	NCG(v%)	OILS(w%)	NCG(v%)	OILS(w%)	NCG(v%)	OILS(w%)	NCG(v%)	OILS(w%)
H <sub>2</sub>	4.27		4.83		5.48		6.22	
CO <sub>2</sub>	56.29		54.58		53.05		51.65	
CO	23.09		23.48		23.77		23.94	
H <sub>2</sub> O	0.00	48.98	0.00	48.93	0.00	48.90	0.00	48.91
CH <sub>4</sub>	9.13	-	9.37	-	9.58	-	9.74	-
C <sub>2</sub> H <sub>6</sub>	2.10	-	1.85	-	1.62	-	1.40	-
C <sub>2</sub> H <sub>4</sub>	2.35	-	3.03	-	3.62	-	4.11	-
C <sub>2</sub> H <sub>2</sub>	-	-	-	-	0.01	-	0.09	-
C <sub>6</sub> H <sub>6</sub>	-	10.20	-	10.21	-	10.22	-	10.22
C <sub>10</sub> H <sub>12</sub> O <sub>4</sub> (TAR)	-	40.81	-	40.86	-	40.88	-	40.87

Table 21

Composition of pyrolysis products at pyrolysis temperature (625°C to 700°C)

Volatiles	625		650		675		700	
	NCG(v%)	OILS(w%)	NCG(v%)	OILS(w%)	NCG(v%)	OILS(w%)	NCG(v%)	OILS(w%)
H <sub>2</sub>	7.06		7.01		7.00		6.58	
CO <sub>2</sub>	50.42		46.40		43.21		40.04	
CO	24.00		24.87		25.03		25.98	
H <sub>2</sub> O	0.00	48.01	0.00	47.87	0.00	47.62	0.00	47.43
CH <sub>4</sub>	9.86	-	9.87	-	9.98	-	9.97	-
C <sub>2</sub> H <sub>6</sub>	1.19	-	0.34	-	1.40	-	1.41	-
C <sub>2</sub> H <sub>4</sub>	4.50	-	4.78	-	4.11	-	4.04	-
C <sub>2</sub> H <sub>2</sub>	0.16	-	0.42	-	0.09	-	0.08	-
C <sub>6</sub> H <sub>6</sub>	-	10.21	-	10.16	-	10.22	-	10.21
C <sub>10</sub> H <sub>12</sub> O <sub>4</sub> (TAR)	-	40.89	-	40.94	-	50.01	-	50.23

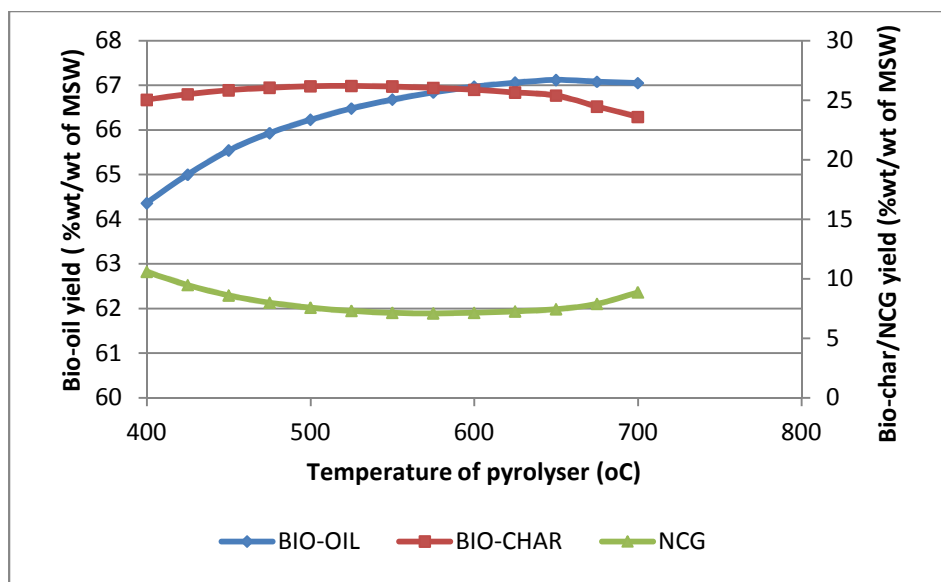


Figure 55. Effect of temperature of pyrolyser on the yields of pyrolysis products

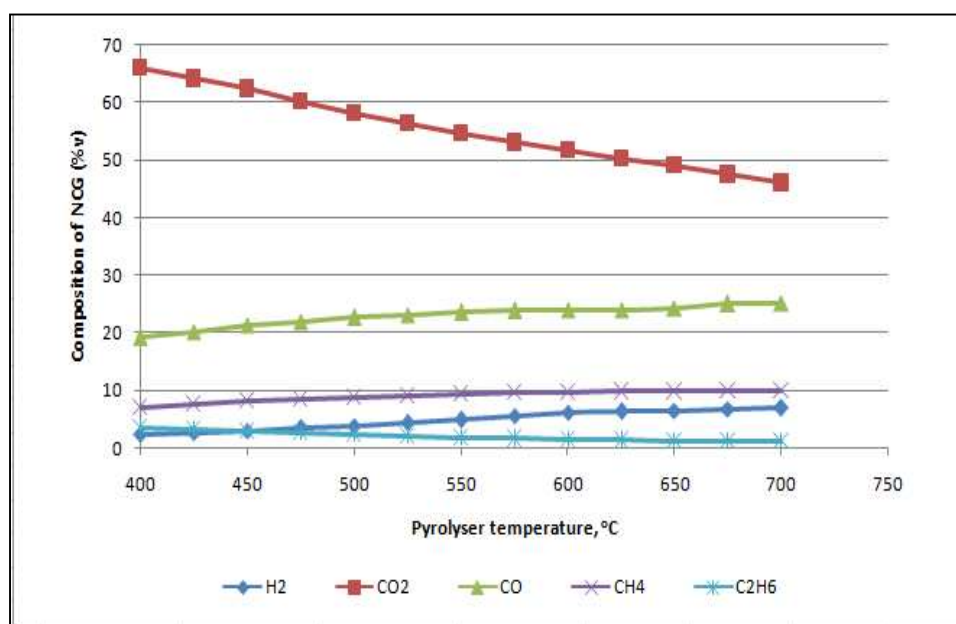


Figure 56. Composition of components in non condensable gas varying with pyrolyser temperature

## 6.10 Results of Economic Assessment of MSW Pyrolysis

All cost are adjusted to 2013 dollars. Capital cost included the purchase of equipment and facility preparation and construction. This cost was amortized using a 20-year design basis and a 10% interest rate for all parts of the facility. Data of costs were provided by sales literature, equipment manufacturers and literature as referenced. The analysis provided in Table 22 assumed a 100 MT production capacity of MSW with 70% combustibles and an initial moisture content of 44%. The conversion of bio-oil was 65 wt.% at 600°C. The total working days per year was assumed at 300 with 65 days of downtime for maintenance. The total amount of raw MSW processed per year was estimated to be 35,000 MT/year and the amount of bio-oil produced per year was calculated as 9,555 MT/year.

The unit cost of electricity was assumed at 0.15\$/KWh and the unit cost of natural gas at 27.8 \$/GJ

Table 22

*Economic assessment results of MSW pyrolysis process plant at a loading capacity of 100 MT*

*MSW/day*

<b>Equipment/process</b>	<b>Rate</b>	<b>Units</b>	<b>Cost</b>	<b>Unit</b>
<b>1. Utility cost</b>				
<b>Sorting</b>				
<i>Combustible</i>	70	%		
<i>Non combustible</i>	30	%		
<i>Total amount of wet combustible</i>	70	MT/day		
<i>Unit operating cost</i> <i>( trommel screening used to separate organic fraction)</i>	3.36	\$/gal. of diesel		
<i>Equipment consumption of diesel</i>	100	Gal/day	336	\$/day
<b>Drying</b>				
<i>Initial moisture content</i>	44.3	% wt		
<i>Final moisture content</i>	7	% wt		
<i>Total of dried MSW combustibles</i>	41.9	MT/day		
<i>Total amount of heat required for drying</i>	123.43	GJ/day		
<i>Total amount of electricity required for drying</i>	3427.78	KWh/day		
<i>Total cost of heat supply</i>	3431.48	\$/day		
<i>Total cost of electricity supply</i>	514.16	\$/day		
<i>Total operating cost for drying</i>			3945.65	\$/day

Table 23

*Economic assessment results of MSW pyrolysis process plant*

Equipment/process	Rate	Units	Cost	Unit
<b>Size reduction ( employed hammer mill)</b>				
<i>Total amount of dried MSW combustibles</i>	41.9	MT/day		
<i>Unit operating cost</i>	11	\$/MT		
<i>Total operating cost for sizing reduction</i>			461.17	\$/day
<b>Pyrolysis</b>				
<i>Total of dried MSW combustibles</i>	41.9	MT/day		
<i>MSW to bio-oil conversion efficiency</i>	65.0	% wt.		
<i>Total amount of bio-oil produced</i>	27.3	MT/day		
<i>Total amount of heat required for pyrolysis</i>	40.87	GJ/day		
<i>Total amount of electricity required for pyrolysis</i>	1135.15	KWh/day		
<i>Total cost of heat supply</i>	1136.37	\$/day		
<i>Total cost of electricity supply</i>	170.27	\$/day		
<i>Total operating cost for pyrolysis</i>			1306.65	\$/day
<b>Other operating cost</b>				
<i>Total operating cost for cyclone operation ( electricity)</i>	11	\$/MT	461.17	\$/day
<i>Total operating cost for Bio-oil collection and storage (electricity and water)</i>	5	\$/MT	136.50	\$/day
<b>Total utility cost</b>			6646.90	\$/day
<b>Total utility cost per year ( 300 days)</b>			<b>1,994,072.08</b>	<b>\$/year</b>

Table 24

*Economic assessment results of MSW pyrolysis process plant (continuation)*

<b>2. Capital cost</b>				
<i>Total plant capital cost</i> ( based on regression curve for 100MT)			9,893,495.48	<b>\$/year</b>
<i>Life of the plant</i>	20	years		
<i>Interest</i>	10	%		
<i>Annualized capital cost</i>			1,162,086,267.00	
<b>3. Personnel</b>				
<i>Three shifts at \$100,000 /each/year</i>			300,000.00	<b>\$/year</b>
<b>4. Maintenance</b>				
<i>Rate ( 1.5% of the total capital costs)</i>	1.5	%/year		
<i>Maintenance cost per year</i>			148,402.43	<b>\$/year</b>
<b>5. Feedstock</b>				
<i>Unit cost of feedstock</i>	-20	\$/MT		
<i>Total cost of feedstock per year</i>			-600,000	<b>\$/year</b>
<b>Total production costs/year</b>			3,004,560.79	<b>\$/year</b>
<b>Cost per kg of MSW processed</b>			<b>0.10</b>	<b>\$/Kg MSW</b>
<b>Cost per kg of bio-oil produced</b>			<b>0.37</b>	<b>\$/kg of Bio-oil</b>

Table 25

*Cost of MSW pyrolysis plant at different scales*

	<b>Production capacity, MT/day</b>				
	<b>100</b>	<b>150</b>	<b>200</b>	<b>250</b>	<b>300</b>
Utility cost, M\$/year	1.994	2.940	3.887	4.834	5.780
Annualized Capital cost, M\$/year	1.162	1.379	1.533	1.653	1.751
Personel cost, M\$/year	0.300	0.300	0.300	0.300	0.300
Maintenance cost, M\$/year	0.148	0.176	0.196	0.211	0.223
Feedstock cost, M\$/year	-0.600	-0.900	-1.200	-1.500	-1.800
Total production cost , M\$/year	3.004	3.896	4.717	5.498	6.255
Cost per kg of MSW processed, \$/kg MSW	0.100	0.086	0.078	0.073	0.069
Cost per kg of Bio-oil produced, \$/kg Bio-oil	0.367	0.317	0.288	0.269	0.255
Cost per litre of Bio-oil Produced ( assuming density of bio-oil is 0.9kg/l), \$/L bio-oil	0.330	0.285	0.259	0.242	0.229

As seen from Table 25, the total cost will amount to \$ 0.100 to process one kg of raw MSW for a plant which can process 100 MT of raw MSW per day. It will require \$ 0.330 to produce each liter of bio-oil from MSW. The production cost will decrease with the increase of production size. It only cost \$0.069 to process one kg of raw MSW if the plant production capacity increases from 100 MT/day to 300 MT/day. In this case, the production cost of the bio-oil will reduce to \$ 0.229/liter.

## CHAPTER 7

### Conclusions and Recommendations

This section summarizes the experimental analysis, results from laboratory-scale fixed bed pyrolysis, the TGA-DSC and MS profiles and the model simulation by Aspen plus of MSW components pyrolysis conducted throughout the span of the project work. In the study, four components of MSW consisting of paper, wood, textile residue and plastic were investigated at different temperatures varying between 300°C to 800°C for the fixed bed pyrolysis, from ambient to 700°C in the TGA-DSC-MS analysis and between 450°C to 700°C for the Aspen plus simulations. Additionally, the economic assessment of pyrolysis of MSW to bio-oil was performed to show the viability of the process. These conclusions and future recommendations are discussed.

#### 7.1 Conclusion

MSW components (paper, wood and textile) were successfully pyrolysed in 100 ml tubular reactor at different temperatures and the yield of products were determined from the average of three runs for each component and temperature. The maximum bio-oil yields for paper, wood and textile in the MSW were 57 wt.% , 64.9 wt% and 52.8 wt.%, respectively. The yield of biochar from the pyrolysis was found to decrease with increasing temperature.

The heating values of bio-oil and biochar were analyzed using a oxygen bomb calorimeter. The results indicated the heating value of biochar obtained from the pyrolysis increased for all MSW components at increasing temperature. The heating values of biochar obtained from different MSW components at a high temperature were close. The moisture content of the bio-oil was determined to be quite high in the range of (68% - 72% ) at lower

pyrolysis temperatures (300°C) and then decreased with increasing temperature to between 40% to 50% at 700°C.

The experimental results studied on a micro level with TGA-DSC-MS indicated that the yields of the evolved volatile gases for paper, wood, textile and plastic at a heating rate of 20°C/min were 69.5 wt%, 67.9 wt%, 75.3 wt% and 83.7 wt%, respectively. The yields of the volatile gases were found to decrease to 63.4 wt%, 63.6 wt% and 64.3 wt% for paper, wood and textile respectively when the heating rate was increased to 60°C/min. The yield of the volatile gases generated from plastic, however, increased from 83.7 wt% obtained at 20°C/min to 89 wt% at 60°C/min. These were found to be consistent with the fact that when the heating rate increased, heat might not be able to be transferred into the inside of the sample instantaneously due to heat transfer limitations, which would result in an increase in activation energy for the pyrolysis reactions. The DSC curves also revealed the caloric requirement for MSW components increased with increasing temperature and becomes almost constant at the charring stage. The mass spectra profiles obtained from the pyrolysis of MSW components showed that CO<sub>2</sub>, H<sub>2</sub>O, CH<sub>4</sub> and H<sub>2</sub> formed the main components in the non-condensable gas stream.

The results obtained from Aspen plus simulation indicated that the model can predict the variations in pyrolysis products with increasing pyrolysis temperature when correlation equations from experimental results were modeled in the Aspen RYIELD reactor block and the char obtained from the pyrolysis can be combusted to supply the energy for drying of the MSW feed.

Finally, the economic analysis shows that for a pyrolysis plant at a scale of 100 MT/day, it costs \$0.10 to process 1 kg of raw MSW and the corresponding production cost of the bio-oil is \$0.36/l bio-oil. The production cost will decrease with the increase of production size and at a plant capacity of 300MT/day the unit cost of bio-oil is \$0.255/l.

## **7.2 Recommendations for Future Work**

Future work should be done to improve the efficiency of the process and increase the yield of products. Since MSW exists in nature as a heterogeneous feedstock and varies in its composition, a mixture of simulated waste in different proportions can be pyrolysed to determine the variations in product yields as a function of MSW composition.

In the design of a fixed bed reactor, a well constructed system with multiple stage condensation can significantly increase the yield of products. The effect of different reactor types and configuration on the yield and quality of products can be evaluated for the MSW pyrolysis process.

Additionally, analysis of bio-oil and non-condensable gases using a GC-MS will help determine most of the compounds in the bio-oil and non-condensable gases which will result in representative model equations to be used in Aspen plus software.

## References

1. Puy, N., et al., *Valorisation of forestry waste by pyrolysis in an auger reactor*. Waste Management, 2011. **31**(6): p. 1339-1349.
2. Velghe, I., et al., *Study of the pyrolysis of municipal solid waste for the production of valuable products*. Journal of Analytical and Applied Pyrolysis, 2011. **92**(2): p. 366-375.
3. Zhou, C., et al., *A study of the pyrolysis behaviors of pelletized recovered municipal solid waste fuels*. Applied Energy, 2013. **107**(0): p. 173-182.
4. He, M., et al., *Syngas production from pyrolysis of municipal solid waste (MSW) with dolomite as downstream catalysts*. Journal of Analytical and Applied Pyrolysis, 2010. **87**(2): p. 181-187.
5. Cheng, H. and Y. Hu, *Municipal solid waste (MSW) as a renewable source of energy: Current and future practices in China*. Bioresource Technology, 2010. **101**(11): p. 3816-3824.
6. Abu-Qudais, M.d. and H.A. Abu-Qdais, *Energy content of municipal solid waste in Jordan and its potential utilization*. Energy Conversion and Management, 2000. **41**(9): p. 983-991.
7. Bosmans, A., et al., *The crucial role of Waste-to-Energy technologies in enhanced landfill mining: a technology review*. Journal of Cleaner Production, (0).
8. Zheng, J., et al., *Pyrolysis characteristics of organic components of municipal solid waste at high heating rates*. Waste Management, 2009. **29**(3): p. 1089-1094.
9. Sørum, L., M.G. Grønli, and J.E. Hustad, *Pyrolysis characteristics and kinetics of municipal solid wastes*. Fuel, 2001. **80**(9): p. 1217-1227.

10. Ryu, C., et al., *Combustion of textile residues in a packed bed*. Experimental Thermal and Fluid Science, 2007. **31**(8): p. 887-895.
11. Ryu, C., et al., *Co-combustion of textile residues with cardboard and waste wood in a packed bed*. Experimental Thermal and Fluid Science, 2007. **32**(2): p. 450-458.
12. Li, Y., H. Liu, and O. Zhang, *High-pressure compaction of municipal solid waste to form densified fuel*. Fuel Processing Technology, 2001. **74**(2): p. 81-91.
13. Buah, W.K., A.M. Cunliffe, and P.T. Williams, *Characterization of Products from the Pyrolysis of Municipal Solid Waste*. Process Safety and Environmental Protection, 2007. **85**(5): p. 450-457.
14. Baggio, P., et al., *Energy and environmental analysis of an innovative system based on municipal solid waste (MSW) pyrolysis and combined cycle*. Applied Thermal Engineering, 2008. **28**(2-3): p. 136-144.
15. Fruergaard, T. and T. Astrup, *Optimal utilization of waste-to-energy in an LCA perspective*. Waste Management, 2011. **31**(3): p. 572-582.
16. Cozzani, V., L. Petarca, and L. Tognotti, *Devolatilization and pyrolysis of refuse derived fuels: characterization and kinetic modelling by a thermogravimetric and calorimetric approach*. Fuel, 1995. **74**(6): p. 903-912.
17. Psomopoulos, C.S., A. Bourka, and N.J. Themelis, *Waste-to-energy: A review of the status and benefits in USA*. Waste Management, 2009. **29**(5): p. 1718-1724.
18. Stehlík, P., *Contribution to advances in waste-to-energy technologies*. Journal of Cleaner Production, 2009. **17**(10): p. 919-931.

19. Abnisa, F., W.M.A. Wan Daud, and J.N. Sahu, *Optimization and characterization studies on bio-oil production from palm shell by pyrolysis using response surface methodology*. Biomass and Bioenergy, 2011. **35**(8): p. 3604-3616.
20. Zhong, Z.W., B. Song, and M.B.M. Zaki, *Life-cycle assessment of flash pyrolysis of wood waste*. Journal of Cleaner Production, 2010. **18**(12): p. 1177-1183.
21. Peng, J.H., et al., *Torrefaction and densification of different species of softwood residues*. Fuel, (0).
22. Uslu, A., A.P.C. Faaij, and P.C.A. Bergman, *Pre-treatment technologies, and their effect on international bioenergy supply chain logistics. Techno-economic evaluation of torrefaction, fast pyrolysis and pelletisation*. Energy, 2008. **33**(8): p. 1206-1223.
23. Chew, J.J. and V. Doshi, *Recent advances in biomass pretreatment – Torrefaction fundamentals and technology*. Renewable and Sustainable Energy Reviews, 2011. **15**(8): p. 4212-4222.
24. van der Stelt, M.J.C., et al., *Biomass upgrading by torrefaction for the production of biofuels: A review*. Biomass and Bioenergy, 2011. **35**(9): p. 3748-3762.
25. Stelte, W., et al., *Fuel pellets from biomass: The importance of the pelletizing pressure and its dependency on the processing conditions*. Fuel, 2011. **90**(11): p. 3285-3290.
26. Demirbaş, A., *Yields of oil products from thermochemical biomass conversion processes*. Energy Conversion and Management, 1998. **39**(7): p. 685-690.
27. Agirre, I., et al., *Production of charcoal as an alternative reducing agent from agricultural residues using a semi-continuous semi-pilot scale pyrolysis screw reactor*. Fuel Processing Technology, (0).

28. Bridgwater, A.V., *Review of fast pyrolysis of biomass and product upgrading*. Biomass and Bioenergy, 2012. **38**(0): p. 68-94.
29. Ertaş, M. and M. Hakkı Alma, *Pyrolysis of laurel (Laurus nobilis L.) extraction residues in a fixed-bed reactor: Characterization of bio-oil and bio-char*. Journal of Analytical and Applied Pyrolysis, 2010. **88**(1): p. 22-29.
30. Bellomare, F. and M. Rokni, *Integration of a municipal solid waste gasification plant with solid oxide fuel cell and gas turbine*. Renewable Energy, 2013. **55**(0): p. 490-500.
31. Li, J., et al., *Experimental study on catalytic steam gasification of municipal solid waste for bioenergy production in a combined fixed bed reactor*. Biomass and Bioenergy, 2012. **46**(0): p. 174-180.
32. Furusawa, T., et al., *Hydrogen production from the gasification of lignin with nickel catalysts in supercritical water*. International Journal of Hydrogen Energy, 2007. **32**(6): p. 699-704.
33. Phan, A.N., et al., *Characterisation of slow pyrolysis products from segregated wastes for energy production*. Journal of Analytical and Applied Pyrolysis, 2008. **81**(1): p. 65-71.
34. Tabasová, A., et al., *Waste-to-energy technologies: Impact on environment*. Energy, 2012. **44**(1): p. 146-155.
35. Singh, R.P., et al., *An overview for exploring the possibilities of energy generation from municipal solid waste (MSW) in Indian scenario*. Renewable and Sustainable Energy Reviews, 2011. **15**(9): p. 4797-4808.

36. Demirbas, A., *The influence of temperature on the yields of compounds existing in bio-oils obtained from biomass samples via pyrolysis*. Fuel Processing Technology, 2007. **88**(6): p. 591-597.
37. Day, M., Z. Shen, and J.D. Cooney, *Pyrolysis of auto shredder residue: experiments with a laboratory screw kiln reactor*. Journal of Analytical and Applied Pyrolysis, 1999. **51**(1–2): p. 181-200.
38. Aho, A., et al., *Catalytic pyrolysis of woody biomass in a fluidized bed reactor: Influence of the zeolite structure*. Fuel, 2008. **87**(12): p. 2493-2501.
39. Hammond, J., et al., *Prospective life cycle carbon abatement for pyrolysis biochar systems in the UK*. Energy Policy, 2011. **39**(5): p. 2646-2655.
40. Önal, E.P., B.B. Uzun, and A.E. Pütün, *Steam pyrolysis of an industrial waste for bio-oil production*. Fuel Processing Technology, 2011. **92**(5): p. 879-885.
41. He, P.-w., et al., *Gasification of biomass char with air-steam in a cyclone furnace*. Renewable Energy, 2012. **37**(1): p. 398-402.
42. Balat, M., et al., *Main routes for the thermo-conversion of biomass into fuels and chemicals. Part 1: Pyrolysis systems*. Energy Conversion and Management, 2009. **50**(12): p. 3147-3157.
43. Iribarren, D., J.F. Peters, and J. Dufour, *Life cycle assessment of transportation fuels from biomass pyrolysis*. Fuel, 2012. **97**(0): p. 812-821.
44. Bahng, M.-K., et al., *Current technologies for analysis of biomass thermochemical processing: A review*. Analytica Chimica Acta, 2009. **651**(2): p. 117-138.

45. Butler, E., et al., *A review of recent laboratory research and commercial developments in fast pyrolysis and upgrading*. Renewable and Sustainable Energy Reviews, 2011. **15**(8): p. 4171-4186.
46. Brown, J.N. and R.C. Brown, *Process optimization of an auger pyrolyzer with heat carrier using response surface methodology*. Bioresource Technology, 2012. **103**(1): p. 405-414.
47. Mesa-Perez, J.M., et al., *Unidimensional heat transfer analysis of elephant grass and sugar cane bagasse slow pyrolysis in a fixed bed reactor*. Fuel Processing Technology, 2005. **86**(5): p. 565-575.
48. Pather, T.S. and W.A. Al-Masry, *The influence of bed depth on secondary reactions during slow pyrolysis of coal*. Journal of Analytical and Applied Pyrolysis, 1996. **37**(1): p. 83-94.
49. Islam, M.R., M. Parveen, and H. Haniu, *Properties of sugarcane waste-derived bio-oils obtained by fixed-bed fire-tube heating pyrolysis*. Bioresource Technology, 2010. **101**(11): p. 4162-4168.
50. Lim, X.Y. and J.M. Andrésen, *Pyro-catalytic deoxygenated bio-oil from palm oil empty fruit bunch and fronds with boric oxide in a fixed-bed reactor*. Fuel Processing Technology, 2011. **92**(9): p. 1796-1804.
51. Ferdous, D., et al., *Production of H<sub>2</sub> and medium Btu gas via pyrolysis of lignins in a fixed-bed reactor*. Fuel Processing Technology, 2001. **70**(1): p. 9-26.
52. Hoekstra, E., et al., *Fast pyrolysis in a novel wire-mesh reactor: Design and initial results*. Chemical Engineering Journal, 2012. **191**(0): p. 45-58.

53. Sipilä, K., et al., *Characterization of biomass-based flash pyrolysis oils*. Biomass and Bioenergy, 1998. **14**(2): p. 103-113.
54. Akhtar, J. and N. Saidina Amin, *A review on operating parameters for optimum liquid oil yield in biomass pyrolysis*. Renewable and Sustainable Energy Reviews, 2012. **16**(7): p. 5101-5109.
55. Papadikis, K., S. Gu, and A.V. Bridgwater, *CFD modelling of the fast pyrolysis of biomass in fluidised bed reactors. Part B: Heat, momentum and mass transport in bubbling fluidised beds*. Chemical Engineering Science, 2009. **64**(5): p. 1036-1045.
56. Isahak, W.N.R.W., et al., *A review on bio-oil production from biomass by using pyrolysis method*. Renewable and Sustainable Energy Reviews, 2012. **16**(8): p. 5910-5923.
57. Zhang, H., et al., *Comparison of non-catalytic and catalytic fast pyrolysis of corncob in a fluidized bed reactor*. Bioresource Technology, 2009. **100**(3): p. 1428-1434.
58. Berruti, F.M., et al., *Pyrolysis of cohesive meat and bone meal in a bubbling fluidized bed with an intermittent solid slug feeder*. Journal of Analytical and Applied Pyrolysis, 2012. **94**(0): p. 153-162.
59. Peacocke, G.V.C. and A.V. Bridgwater, *Ablative plate pyrolysis of biomass for liquids*. Biomass and Bioenergy, 1994. **7**(1-6): p. 147-154.
60. Lédé, J., *Comparison of contact and radiant ablative pyrolysis of biomass*. Journal of Analytical and Applied Pyrolysis, 2003. **70**(2): p. 601-618.
61. Liaw, S.-S., et al., *Effect of pyrolysis temperature on the yield and properties of bio-oils obtained from the auger pyrolysis of Douglas Fir wood*. Journal of Analytical and Applied Pyrolysis, 2012. **93**(0): p. 52-62.

62. Janse, A.M.C., et al., *Heat transfer coefficients in the rotating cone reactor*. Powder Technology, 1999. **106**(3): p. 168-175.
63. Guoxin, H., et al., *Experimental studies on flow and pyrolysis of coal with solid heat carrier in a modified rotating cone reactor*. Chemical Engineering and Processing: Process Intensification, 2008. **47**(9–10): p. 1777-1785.
64. Sirijanusorn, S., K. Sriateep, and A. Pattiya, *Pyrolysis of cassava rhizome in a counter-rotating twin screw reactor unit*. Bioresource Technology, (0).
65. Luo, S., et al., *Effect of particle size on pyrolysis of single-component municipal solid waste in fixed bed reactor*. International Journal of Hydrogen Energy, 2010. **35**(1): p. 93-97.
66. Amutio, M., et al., *Influence of temperature on biomass pyrolysis in a conical spouted bed reactor*. Resources, Conservation and Recycling, 2012. **59**(0): p. 23-31.
67. Guillain, M., et al., *Attrition-free pyrolysis to produce bio-oil and char*. Bioresource Technology, 2009. **100**(23): p. 6069-6075.
68. Fassinou, W.F., et al., *Pyrolysis of Pinus pinaster in a two-stage gasifier: Influence of processing parameters and thermal cracking of tar*. Fuel Processing Technology, 2009. **90**(1): p. 75-90.
69. Haykiri-Acma, H., *The role of particle size in the non-isothermal pyrolysis of hazelnut shell*. Journal of Analytical and Applied Pyrolysis, 2006. **75**(2): p. 211-216.
70. Shen, J., et al., *Effects of particle size on the fast pyrolysis of oil mallee woody biomass*. Fuel, 2009. **88**(10): p. 1810-1817.

71. Asadullah, M., S. Zhang, and C.-Z. Li, *Evaluation of structural features of chars from pyrolysis of biomass of different particle sizes*. *Fuel Processing Technology*, 2010. **91**(8): p. 877-881.
72. Chen, G., et al., *Biomass pyrolysis/gasification for product gas production: the overall investigation of parametric effects*. *Energy Conversion and Management*, 2003. **44**(11): p. 1875-1884.
73. Pütün, E., B.B. Uzun, and A.E. Pütün, *Fixed-bed catalytic pyrolysis of cotton-seed cake: Effects of pyrolysis temperature, natural zeolite content and sweeping gas flow rate*. *Bioresource Technology*, 2006. **97**(5): p. 701-710.
74. Mohamed, A.R., et al., *The Effects of Holding Time and the Sweeping Nitrogen Gas Flowrates on the Pyrolysis of EFB using a Fixed-Bed Reactor*. *Procedia Engineering*, 2013. **53**(0): p. 185-191.
75. Özbay, N., et al., *Comparative analysis of pyrolysis oils and its subfractions under different atmospheric conditions*. *Fuel Processing Technology*, 2006. **87**(11): p. 1013-1019.
76. Sanchez-Silva, L., et al., *Thermogravimetric–mass spectrometric analysis of lignocellulosic and marine biomass pyrolysis*. *Bioresource Technology*, 2012. **109**(0): p. 163-172.
77. Sun, L., et al., *Kinetics modeling of dynamic pyrolysis of bagasse fibers*. *Bioresource Technology*, 2011. **102**(2): p. 1951-1958.
78. White, J.E., W.J. Catallo, and B.L. Legendre, *Biomass pyrolysis kinetics: A comparative critical review with relevant agricultural residue case studies*. *Journal of Analytical and Applied Pyrolysis*, 2011. **91**(1): p. 1-33.

79. García, A.N., A. Marcilla, and R. Font, *Thermogravimetric kinetic study of the pyrolysis of municipal solid waste*. *Thermochimica Acta*, 1995. **254**(0): p. 277-304.
80. Vargas-Moreno, J.M., et al., *A review of the mathematical models for predicting the heating value of biomass materials*. *Renewable and Sustainable Energy Reviews*, 2012. **16**(5): p. 3065-3083.
81. Telmo, C. and J. Lousada, *Heating values of wood pellets from different species*. *Biomass and Bioenergy*, 2011. **35**(7): p. 2634-2639.
82. Dupont, C., et al., *Heat capacity measurements of various biomass types and pyrolysis residues*. *Fuel*, (0).
83. Eric, A., et al., *Experimental determination thermo physical characteristics of balled biomass*. *Energy*, 2012. **45**(1): p. 350-357.
84. Carrier, M., et al., *Thermogravimetric analysis as a new method to determine the lignocellulosic composition of biomass*. *Biomass and Bioenergy*, 2011. **35**(1): p. 298-307.
85. Tsai, W.-T., et al., *Textural and chemical properties of swine-manure-derived biochar pertinent to its potential use as a soil amendment*. *Chemosphere*, 2012. **89**(2): p. 198-203.
86. Nikoo, M.B. and N. Mahinpey, *Simulation of biomass gasification in fluidized bed reactor using ASPEN PLUS*. *Biomass and Bioenergy*, 2008. **32**(12): p. 1245-1254.
87. Yuehong, Z., W. Hao, and X. Zhihong, *Conceptual design and simulation study of a co-gasification technology*. *Energy Conversion and Management*, 2006. **47**(11–12): p. 1416-1428.
88. Zheng, H., N. Kaliyan, and R.V. Morey, *Aspen Plus simulation of biomass integrated gasification combined cycle systems at corn ethanol plants*. *Biomass and Bioenergy*, 2013. **56**(0): p. 197-210.

89. Ramzan, N., et al., *Simulation of hybrid biomass gasification using Aspen plus: A comparative performance analysis for food, municipal solid and poultry waste*. Biomass and Bioenergy, 2011. **35**(9): p. 3962-3969.
90. Rogers, J.G. and J.G. Brammer, *Estimation of the production cost of fast pyrolysis bio-oil*. Biomass and Bioenergy, 2012. **36**(0): p. 208-217.
91. Kim, Y. and W. Parker, *A technical and economic evaluation of the pyrolysis of sewage sludge for the production of bio-oil*. Bioresource Technology, 2008. **99**(5): p. 1409-1416.
92. Kumar, A. and S. Sokhansanj, *Switchgrass (*Panicum virgatum*, L.) delivery to a biorefinery using integrated biomass supply analysis and logistics (IBSAL) model*. Bioresource Technology, 2007. **98**(5): p. 1033-1044.
93. Van de Velden, M., et al., *Fundamentals, kinetics and endothermicity of the biomass pyrolysis reaction*. Renewable Energy, 2010. **35**(1): p. 232-242.
94. Bridgwater, A.V., A.J. Toft, and J.G. Brammer, *A techno-economic comparison of power production by biomass fast pyrolysis with gasification and combustion*. Renewable and Sustainable Energy Reviews, 2002. **6**(3): p. 181-246.
95. Kuppens, T., et al., *Economic assessment of flash co-pyrolysis of short rotation coppice and biopolymer waste streams*. Journal of Environmental Management, 2010. **91**(12): p. 2736-2747.
96. Skreiberg, A., et al., *TGA and macro-TGA characterisation of biomass fuels and fuel mixtures*. Fuel, 2011. **90**(6): p. 2182-2197.
97. He, F., W. Yi, and X. Bai, *Investigation on caloric requirement of biomass pyrolysis using TG–DSC analyzer*. Energy Conversion and Management, 2006. **47**(15–16): p. 2461-2469.